

2017

Numerical Analysis Of Unprotected And Fire Protected Circular Hollow Structural Steel Column Sections In Fire

Abdul Fahim Rustamy
Lehigh University

Follow this and additional works at: <https://preserve.lehigh.edu/etd>



Part of the [Structural Engineering Commons](#)

Recommended Citation

Rustamy, Abdul Fahim, "Numerical Analysis Of Unprotected And Fire Protected Circular Hollow Structural Steel Column Sections In Fire" (2017). *Theses and Dissertations*. 2965.
<https://preserve.lehigh.edu/etd/2965>

This Thesis is brought to you for free and open access by Lehigh Preserve. It has been accepted for inclusion in Theses and Dissertations by an authorized administrator of Lehigh Preserve. For more information, please contact preserve@lehigh.edu.

**NUMERICAL ANALYSIS OF UNPROTECTED AND
FIRE PROTECTED CIRCULAR HOLLOW STRUCTURAL STEEL COLUMN
SECTIONS IN FIRE**

by

Fahim Rustamy

A Thesis

Presented to the Graduate and Research Committee

of Lehigh University

in Candidacy for the Degree of

Master of Science

in

Structural Engineering

Lehigh University

June 2017

This thesis is accepted and approved in partial fulfillment of the requirements for the
Master of Science.

Date

Professor Stephen Pessiki
(Thesis Advisor)

Professor Panayiotis Diplas
(Department Chair)

ACKNOWLEDGEMENTS

The author would like to sincerely thank Dr. Stephen Pessiki, his advisor, for his continued guidance throughout this study. Working under his supervision was a great honor and immense pleasure for the author. The author also thanks his family for their support, encouragement and patients during his study.

The author specially thanks the US Department of State, and the Fulbright Foreign Scholarship Board (FFSB) for funding his graduate studies at Lehigh University. Without their support and sponsorship, it was not possible for him to attend graduate school and conduct this research.

The findings and conclusions presented in this study are those of the author, and may not represent the views of the sponsors and acknowledged people above.

TABLE OF CONTENTS

LIST OF TABLES	vii
LIST OF FIGURES	viii
ABSTRACT	1
CHAPTER 1: INTRODUCTION	2
1.1 Introduction	2
1.2 Objectives	3
1.3 Summary of Approach.....	3
1.4 Summary of Findings	4
1.5 Outline of Report.....	5
1.6 Notation	6
1.7 Unit Conversions	8
CHAPTER 2: BACKGROUND INFORMATION	9
2.1 Introduction	9
2.2 Heat Transfer.....	9
2.2.1 Conduction.....	9
2.2.2 Convection	10
2.2.3 Radiation.....	11
2.3 Fire Loads	12
2.3.1 ASTM E119 Fire.....	13
2.3.2 Real Fires	13
2.4 Properties of Steel at Elevated Temperatures	14
2.4.1 Thermal Conductivity of Steel.....	15
2.4.2 Specific Heat of Steel	15
2.4.3 Steel Stress-Strain Curves.....	15
2.4.4 Density of Steel.....	16
2.5 Properties of Intumescent Paint at Elevated Temperatures	16
2.5.1 Intumescent Paint Thermal Conductivity and Specific Heat	17
2.6 Sprayed Fire Resistant Material (SFRM)	18
2.6.1 SFRM Thickness Calculation	18
2.6.2 Behavior of SFRM at Elevated Temperatures	20
2.7 Properties of Concrete at Elevated Temperatures	20

2.7.1	Thermal Conductivity and Specific Heat of Concrete	21
2.7.2	Compressive Strength of Concrete.....	21
2.7.3	Density of Concrete.....	22
2.8	Heat Transfer Finite Element	22
CHAPTER 3: ANALYSIS MODELS AND METHODS		32
3.1	Introduction.....	32
3.2	Analytical Models	32
3.3	Analytical Matrix	33
3.4	Analytical Tool.....	34
3.4.1	Convection and Radiation Heat Transfer Modeling	35
3.4.2	Cavity Radiation Modeling.....	36
3.5	Summary	37
CHAPTER 4: THERMAL ANALYSIS RESULTS		44
4.1	Introduction.....	44
4.2	Unprotected Columns with Various Section Sizes in E119 Fire Exposure (Case 1).....	44
4.3	Unprotected 8xx Section in Real Fire Exposures (Case 2).....	46
4.4	SFRM as Thermal Insulation (Case 3)	47
4.4.1	1-h Fire Rating SFRM	47
4.4.2	2-h Fire Rating SFRM	47
4.5	Intumescent Paint as Thermal Insulation (Case 4).....	48
4.6	Concrete-Filled Columns (Case 5).....	49
4.7	Summary	50
CHAPTER 5: STRENGTH ANALYSIS RESULTS.....		62
5.1	Introduction.....	62
5.2	Strength Analysis of Unprotected Steel Columns in E119 Fire Exposure (Case 1).....	62
5.3	Strength of Unprotected 8xx Section in Real Fire Exposures (Case 2)	63
5.4	Strength of Columns with SFRM as Thermal Insulation (Case 3)	64
5.4.1	1-h Fire Rating Thick SFRM	64
5.4.2	2-h Fire Rating Thick SFRM	65
5.5	Strength of Intumescent Paint Insulated Columns (Case 4)	65
5.6	Strength of Concrete-Filled Models (Case 5)	66

5.7	Summary	67
CHAPTER 6: RESULTS COMPARSION AND DISCUSSION.....		77
6.1	Introduction.....	77
6.2	Effects of Increasing Size of the Cross Section	77
6.2.1	Heat Transfer.....	77
6.2.2	Strength.....	78
6.3	Effects of Using SFRM	79
6.3.1	Heat Transfer.....	79
6.3.1	Strength.....	80
6.4	Effect of Using Intumescent Paint as Thermal Insulation	81
6.4.1	Heat Transfer.....	81
6.4.2	Strength.....	81
6.5	Effect of Concrete-Filled Sections	82
6.5.1	Heat Transfer.....	82
6.5.2	Strength.....	83
6.6	Additional Comparison.....	84
6.6.1	Change in Strength after the First 20 and 30 Minutes.....	84
6.7	Summary	85
CHAPTER 7: SUMMARY, CONCLUSIONS AND FUTURE WORK.....		103
7.1	Introduction.....	103
7.2	Summary	103
7.2.1	Heat Transfer Analysis	104
7.2.2	Strength Analysis	105
7.2.3	Additional Summary and Remarks	106
7.3	Conclusions.....	107
7.4	Future Work.....	108
REFERENCES.....		109
VITA.....		112
APENDIX		113

LIST OF TABLES

CHAPTER 2

Table 2-1 Reduction in yield strength and modulus of elasticity of steel at elevated temperatures (EC3, 2001).....24

Table 2-2 Emissivity of steel taken from different sources. (Note: this table is copied from Keller (2012). References of the sources Keller used are included in reference list of this report).24

Table 2-3 Intumescent paint parameters based on Chen and Shen (2011).....25

Table 2-4 Coefficients of C_1 and C_2 for common SFRM manufacturers (based on AISC Design Guide 19 (2003))25

CHAPTER 3

Table 3-1 Analytical matrix for the models considered for analysis.....38

CHAPTER 6

Table 6-1 Maximum temperature, the minimum yield strength and minimum modulus of elasticity as well as the time they occur for the all analyzed models.....87

LIST OF FIGURES

CHAPTER 2

Figure 2-1 Heat conduction mechanism through a material of thickness L (Wang, 2002).....	26
Figure 2-2 Surface configuration factor for radiating and receiving surfaces (Drysdale, 1998).....	26
Figure 2-3 Temperature-time profile for the E119 fire taken from ASTM E119.....	27
Figure 2-4 Temperature-time profile for the small compartment Cardington fire (digitized from British steel, 1999).....	27
Figure 2-5 Temperature-time profile for the large compartment Cardington fire (digitized from British Steel, 1999).....	27
Figure 2-6 Thermal conductivity of steel as a function of temperature (EC3, 2001).....	28
Figure 2-7 Specific heat of steel as a function of temperature (EC3, 2001).....	28
Figure 2-8 Stress-strain curves for steel at higher temperatures (SFPE, 1998).....	28
Figure 2-9 Effective yield strength proposed by Kirby and Preston (1988).....	29
Figure 2-10 Reduction in yield strength and modulus of elasticity at elevated temperatures (EC3, 2001).....	29
Figure 2-11 Reaction process of intumescent paint at elevated temperatures (Bradley and Sizemore, 2014).....	29
Figure 2-12 Thermal conductivity of intumescent paint as a function of temperature based on Chen and Shen (2011).....	30
Figure 2-13 Thermal conductivity of Blaze Shield II SFRM as a function of temperature based on NIST (2005).....	30

Figure 2-14 Specific heat of Blaze Shield II as a function of temperature based on NIST (2005).....	30
Figure 2-15 Concrete thermal conductivity as a function of temperature (Buchanan, 2002).....	31
Figure 2-16 Variation in compressive strength of concrete at elevated temperatures (Kodur, 2014)	31
Figure 2-17 Concrete stress and strain curves at elevated temperatures (Kodur, 2014).....	31

CHAPTER 3

Figure 3-1 Unprotected circular steel section with different wall thicknesses used in this study: (a) 8x1.5; (b) 8x1; (c) 8xx; (d) 8x0.5	39
Figure 3-2 Protected 8xx tube section with different types of insulations applied :(a) 8xx with 2-h thick insulation; (b) 8xx with 1-h thick insulation; (c) 8xx with one layer of intumescent paint; (d) concrete fill 8xx	40
Figure 3-3 Heat transfer analysis with and without considering cavity radiation for 8x1.5 tube column under E119 fire exposure. ‘c’ means cavity radiation has been included.	41
Figure 3-4 Results of cavity radiation analysis on 8x1.5 steel tube when half of the column surface is under E119 fire exposure. ‘c’ means with cavity radiation. (a) location of each nodes where data is extracted; (b) temperature-time profile for node 1; (c) node 2; (d) node 3; (e) node 4; (f) node 5; (g) node 6.....	42

Figure 3-5 Mesh arrangements for the 8xx steel tube created for the study in
this report: (a) Bare steel; (b) with one layer of intumescent paint;
(c) with 1-h thick SFRM; (d) with 2-h thick SFRM; (e) concrete-filled43

CHAPTER 4

Figure 4-1 Variation in temperature for Nodes 1, 2 and 3 as a function of
time for the analysis BS-8X1.5-E119.....51

Figure 4-2 Temperature difference between exterior and interior surface of
the column for the analysis BS-8X1.5-E119.....51

Figure 4-3 Variation in temperature for Nodes 1, 2 and 3 as a function of
time for the analysis BS-8X1-E119.....52

Figure 4-4 Temperature difference between exterior and interior surface of
the column for the analysis BS-8X1-E11952

Figure 4-5 Variation in temperature for Nodes 1, 2 and 3 as a function of
time for the analysis BS-8X0.5-E119.....53

Figure 4-6 Temperature difference between exterior and interior surface of
the column for the analysis BS-8X0.5-E119.....53

Figure 4-7 Variation in temperature for Nodes 1, 2 and 3 as a function of
time for the analysis BS-8xx-E119.....54

Figure 4-8 Temperature difference between exterior and interior surface of
the column for the analysis BS-8xx-E11954

Figure 4-9 Variation in temperature for Nodes 1, 2 and 3 as a function of time
for the analysis BS-8xx-LC.....55

Figure 4-10 Variation in temperature for Nodes 1, 2 and 3 as a function of time for the analysis BS-8xx-SC	55
Figure 4-11 Variation in temperature for Nodes 1, 2 and 3 as a function of time for the analysis SFRM1h-8xx-E119	56
Figure 4-12 Variation in temperature for Nodes 1, 2 and 3 as a function of time for the analysis SFRM1h-8xx-LC	56
Figure 4-13 Variation in temperature for Nodes 1, 2 and 3 as a function of time for the analysis SFRM1h-8xx-SC.....	57
Figure 4-14 Variation in temperature for Nodes 1, 2 and 3 as a function of time for the analysis SFRM2h-8xx-E119	57
Figure 4-15 Variation in temperature for Nodes 1, 2 and 3 as a function of time for the analysis SFRM1h-8xx-LC	58
Figure 4-16 Variation in temperature for Nodes 1, 2 and 3 as a function of time for the analysis SFRM1h-8xx-SC.....	58
Figure 4-17 Variation in temperature for Nodes 1, 2 and 3 as a function of time for the analysis IP-8xx-E119.....	59
Figure 4-18 Variation in temperature for Nodes 1, 2 and 3 as a function of time for the analysis IP-8xx-LC	59
Figure 4-19 Variation in temperature for Nodes 1, 2 and 3 as a function of time for the analysis IP-8xx-SC	60
Figure 4-20 Variation in temperature for Nodes 1, 2 and 3 as a function of time for the analysis CF-8xx-E119.....	60

Figure 4-21 Variation in temperature for Nodes 1, 2 and 3 as a function of time for the analysis CF-8xx-LC.....	61
Figure 4-22 Variation in temperature for Nodes 1, 2 and 3 as a function of time for the analysis CF-8xx-SC.....	61

CHAPTER 5

Figure 5-1 Variation in yield strength and modulus of elasticity for the model BS-8X1.5-E119.....	68
Figure 5-2 Variation in yield strength and modulus of elasticity for the model BS-8X1-E119.....	68
Figure 5-3 Variation in yield strength and modulus of elasticity for the model BS-8xx-E119.....	69
Figure 5-4 Variation in yield strength and modulus of elasticity for the model BS-8X0.5-E119.....	69
Figure 5-5 Variation in yield strength and modulus of elasticity for the model BS-8xx-LC.....	70
Figure 5-6 Variation in yield strength and modulus of elasticity for the model BS-8xx-SC.....	70
Figure 5-7 Variation in yield strength and modulus of elasticity for the model SFRM1h-8xx-E119.....	71
Figure 5-8 Variation in yield strength and modulus of elasticity for the model SFRM1h-8xx-LC.....	71

Figure 5-9 Variation in yield strength and modulus of elasticity for the model	
SFRM1h-8xx-SC.....	72
Figure 5-10 Variation in yield strength and modulus of elasticity for the model	
SFRM2h-8xx-E119.....	72
Figure 5-11 Variation in yield strength and modulus of elasticity for the model	
SFRM2h-8xx-LC.....	73
Figure 5-12 Variation in yield strength and modulus of elasticity for the model	
SFRM2h-8xx-SC.....	73
Figure 5-13 Variation in yield strength and modulus of elasticity for the model	
IP-8xx-E119	74
Figure 5-14 Variation in yield strength and modulus of elasticity for the model	
IP-8xx-LC	74
Figure 5-15 Variation in yield strength and modulus of elasticity for the model	
IP-8xx-SC.....	75
Figure 5-16 Variation in yield strength and modulus of elasticity for the model	
CF-8xx-E119.....	75
Figure 5-17 Variation in yield strength and modulus of elasticity for the model	
CF-8xx-LC	76
Figure 5-18 Variation in yield strength and modulus of elasticity for the model	
CF-8xx-SC	76

CHAPTER 6

Figure 6-1 Temperature-time profile for unprotected 8x1.5, 8x1, 8xx, 8x0.5 tube sections under E119 fire exposure. Plotted curves are for mid-section temperatures.	88
Figure 6-2 Variation in temperature difference between exterior and interior wall surface (Nodes 1 and 3) of unprotected 8x1.5, 8x1, 8xx, 8x0.5 tube sections under E119 fire exposure.....	88
Figure 6-3 Variation in yield strength of unprotected 8x1.5, 8x1, 8xx, 8x0.5 tube sections under the E119 fire exposure.....	89
Figure 6-4 Variation in modulus of elasticity of unprotected 8x1.5, 8x1, 8xx, 8x0.5 tube sections under the E119 fire exposure.	89
Figure 6-5 Variation in axial force resistance of unprotected 8x1.5, 8x1, 8xx, 8x0.5 tube sections under the E119 fire exposure.	90
Figure 6-6 Effects of adding SFRM on temperature of 8xx section under the E119 fire exposure.	90
Figure 6-7 Effects of adding SFRM on strength of the 8xx section under the E119 fire exposure.	91
Figure 6-8 Effects of adding SFRM on temperature of 8xx section under the large compartment fire exposure.	91
Figure 6-9 Effect of adding SFRM on strength of the section under the large compartment fire exposure.....	92
Figure 6-10 Effect of adding SFRM on temperature of 8xx section under the small compartment fire exposure.	92

Figure 6-11 Effect of adding SFRM on strength of the section under the small compartment fire exposure.	93
Figure 6-12 Effect of adding intumescent paint to the column surface on temperature of the section under the E119 fire exposure.....	93
Figure 6-14 Effect of adding intumescent paint to the column surface on temperature of the section under the small compartment fire exposure.	94
Figure 6-15 Effect of adding intumescent paint to the column surface on strength of the section under the E119 fire exposure.	95
Figure 6-16 Effect of adding intumescent paint to the column surface on strength of the section under the exposure of large compartment fire.	95
Figure 6-17 Effect of adding intumescent paint to the column surface on temperature of the section under the small compartment fire exposure.	96
Figure 6-18 Effect of filling the column with concrete on temperature of the section under the E119 fire exposure.....	96
Figure 6-19 Effect of filling the column with concrete on temperature of the section under the large compartment fire exposure.....	97
Figure 6-20 Effect of filling the column with concrete on temperature of the section under the small compartment fire exposure.	97
Figure 6-21 Effect of filling the column with concrete on strength of the section under the E119 fire exposure.....	98
Figure 6-22 Effect of filling the column with concrete on strength of the section under the large compartment fire exposure.	98

Figure 6-23 Effect of filling the column with concrete on strength of the section under Small compartment fire exposure.....	99
Figure 6-24 Variation of temperature as a function of time with different insulation types for an 8xx steel tube column under E119 fire exposure.	99
Figure 6-25 Variation of temperature as a function of time for an 8xx steel tube column with different insulation types under large compartment fire exposure.....	100
Figure 6-26 Variation of temperature as a function of time for and 8xx steel tube section with different insulation types under small compartment fire exposure.....	100
Figure 6-27 Variation of temperature as a function of time for the unprotected 8x1.5, 8x1, 8xx, 8x0.5 and concrete filled 8xx tube sections	101
Figure 6-28 Normalized strength of each analyzed model with respect to the strength of unprotected 8xx steel tube section after 20 and 30 minutes of standard and real fire exposures	102

ABSTRACT

This report examines different fire protection measures to increase the fire resistance of circular hollow structural steel column sections while maintaining their appealing architectural appearance. The question of whether increasing size of the cross section can provide enough fire resistance to these members is asked. Also, the efficiency of adding intumescent paint, or filling the column with concrete on the fire resistance of the steel members is examined.

Eighteen unprotected and fire protected circular structural hollow steel section models are analyzed with Abaqus software for heat transfer and strength calculations. Intumescent paint and concrete-filled column sections are studied among the fire protection methods that does not harm surface appearance of the structural steel members. These fire protection measures are then compared with the SFRM applied column models to evaluate their fire resistance efficiency.

It was found that increasing size of the cross section in unprotected columns helps reduce the temperature of steel and delay the reduction in its strength during a fire. This can be used to increase fire resistance of unprotected steel columns when the required fire rating is below 30 minutes. Intumescent paint provided a good amount of fire resistance to the column when the fire exposure was not severe, because intumescent paint degrades at temperatures above 800 °C. For the concrete filled section, however, if the concrete is used only as heat sink, it was shown that it cannot provide considerable fire resistance. Lastly, of the fire protection methods studied, SFRM proved to be the most efficient fire protection method when the surface appearance of steel member is of no importance.

CHAPTER 1

INTRODUCTION

1.1 Introduction

Architects occasionally desire to keep the appearance of the exposed structural steel in their architectural designs. Since the strength of steel components decrease at higher temperatures, these structural members should be safe and operate within their serviceability limit state during a fire exposure. This may be accomplished by using several fire protection methods such as, using unprotected steel members with increased cross section size, intumescent paint, concrete-filled section and sprayed fire resistance material (SFRM). The focus of this thesis is to investigate ways to provide acceptable fire performance of structural steel column members while preserving the nice aesthetic appearance of the original steel cross-section.

The prototype column considered for this study is hollow circular steel column section, which was inspired by an actual project. One way of using unprotected column section proposed in this study is increasing size of the cross section. This delays the temperature increase in the member and provides extra load bearing surface when the strength of steel decrease at higher temperatures. The cost associated with using heavier section can be compensated with having an aesthetically appealing surface and eliminating the extra fire protection cost. The two methods of fire protection that do not harm the appearance of steel members proposed in this study are filling the column with concrete and applying intumescent paint to the column surface. Concrete inside functions as heat sink absorbing heat energy from its steel casing. The benefit of using intumescent paint is that it provides thermal resistance when the fire occurs and is inert at normal temperatures.

An additional way of demonstrating adequate performance of a steel structure in fire design is examining the response of the structure to a more realistic, often less intense fire. The code specified fire load E119 considers a severe fire case for all environments and conditions. However, by the growing trend of performance based designs permitted by the IBC Code Section 104.11, real fire curves can be generated by considering the size of the fire compartment and the ventilation size. This study investigates both the code specified fire and real fires with large and small compartment sizes on the steel column.

This thesis studies the possibility of using unprotected circular hollow steel column sections in a building, and investigate the ways to thermally protect these members in standard and real fire exposures without harming their appealing architectural appearance.

1.2 Objectives

The objective of this study is to examine the methods to protect circular hollow structural steel column members in fire exposures without harming the aesthetic appearance of the original steel section. The following are the main objectives for this study.

- Examine the behavior of unprotected steel columns under the exposure of code specified and real fires, and investigate if an increase in size of the column cross section provides adequate fire resistance without using any type of fire protection.
- Study methods of fire protection that do not change the appealing surface appearance of the steel member in normal condition and can provide adequate fire protection for the structure to be safe in a fire situation.

1.3 Summary of Approach

The following four tasks are developed to attain the objectives of this study.

1. Create two-dimensional finite element heat transfer models for the cross section of the column with a finite element analysis software. Generate models of unprotected, intumescent painted, concrete filled and SFRM applied columns.
2. Conduct heat transfer analysis for the unprotected and fire protected models and generate temperature-time profile of the cross section for the duration of the fire exposure.
3. Conduct strength analysis of these column models by using the heat transfer analysis data obtained from step three and generate strength-time profile of the column cross section for the duration of fire exposure for each model.
4. Compare the results obtained from heat transfer and strength analysis in tasks 3 and 4 for the created models.

1.4 Summary of Findings

1. It was found that unprotected steel column sections cannot endure long durations of fire exposures. 60% of the column strength was reduced in the first 15 minutes. Increasing size of the cross section had small effect on the reduction in column's strength and cannot be considered as the only means of fire protection. However, increasing size of the cross section can delay the reduction in strength and can be used to increase fire resistance of the column when the required fire ratings is small.
2. It was found that adding intumescent paint to the column surface reduces the section's temperature and slows the reduction in strength of the column in fire exposures. Intumescent paint protected column performed satisfactory in real fires

and at the beginning of the standard fire, but it behaved like unprotected column sections as intumescent paint started to degrade at temperatures above 800 °C.

3. Using concrete solely as heat sink to absorb heat energy from the column had a minor effect on fire resistance of the column.
4. Among the fire-resistant material analyzed in this study, SFRM provides the most efficient fire protection to steel member.

1.5 Outline of Report

The report is organized into seven chapters as follows:

Chapter 2 contains background information related to this study. Topics such as heat transfer mechanisms, fire curves, material properties at elevated temperatures and use of finite element for heat transfer calculations are discussed in this chapter.

Chapter 3 discusses the analysis models and methods used in this study. The type and characteristics of the analysis models and how they are implemented with Abaqus software are discussed in this chapter. The chapter also includes the organization of analysis matrix for this study.

Chapter 4 presents the results of heat transfer analysis for the unprotected and fire protected models created for this study. Temperature-time profiles for the three nodes across the section are presented under the exposure of E119 and real fires.

Chapter 5 presents the results of strength analysis for the analytical models considered for this study. Included in this chapter are the plots, and tables for the variation in yield strength, yield force and modulus of elasticity of these column sections during the fire exposure time.

Chapter 6 presents the discussion and comparison of the heat transfer and strength analysis results obtained in Chapters 4 and 5. Effects of increasing size of the cross section, adding SFRM and intumescent paint to the column surface as well as filling the column section with concrete on temperature distribution and variation of strength in these sections are discussed in this chapter.

Chapter 7 presents the summary and conclusion drawn from analysis in this report. The chapter ends by discussing the potential future work to extend the knowledge around this topic.

1.6 Notation

A	Surface area (m^2)
c_p	Specific heat ($J/kg-K$)
C_1	SFRM material dependent constant
C_2	SFRM material dependent constant
$^{\circ}C$	Temperature in degree Celsius ($^{\circ}C$)
E	Modulus of elasticity at elevated temperatures (N/m^2)
E_0	Modulus of elasticity at normal temperature (N/m^2)
F	Yield strength at elevated temperatures (N/m^2)
f_y	Yield strength at normal temperature (N/m^2)
h	Convection heat transfer coefficient (w/m^2K)
k	Thermal conductivity coefficient ($W/m-K$)

$[K_T]$	Thermal conductivity matrix (W/m-K)
n	Vector normal to the surface area
$\{Q\}$	Matrix of thermal loads (W)
q_x	Components of heat flow in a unit area in x direction (W/m ²)
q_y	Components of heat flow in a unit area in y direction (W/m ²)
q_z	Components of heat flow in a unit area in z direction (W/m ²)
q_r	The incident radiant heat flow per unit surface area (W/m ²)
q''	Heat flow per unit area (W/m ²)
R	Fire resistance rating (hours)
T_e	Absolute temperature of the radiation emitting surface (K)
T_r	Absolute temperature of the radiation receiving surface (K)
$\{T\}$	Nodal temperature matrix (K)
1-h	One hour fire rating
2-h	Two hour fire rating
ΔT	Temperature difference between two system (C or K)
φ	Configuration factor for calculation of heat radiation
ε	Resultant emissivity of the radiation emitting and receiving surfaces
ρ	Density (kg/m ³)

ϵ_r	Emissivity of the receiving surface
ϵ_e	Emissivity of the emitting surface
σ	Stefan-Boltzmann constant, equal to $5.67 \times 10^{-8} \text{ W}/(\text{m}^2\text{-K}^4)$
α	Surface absorption coefficient
$\frac{\partial T}{\partial t}$	Time rate of temperature change (K/s)
$\frac{\partial q_x}{\partial x}, \frac{\partial q_y}{\partial y}, \frac{\partial q_z}{\partial z}$	Material temperature gradient in x, y and z directions

1.7 Unit Conversions

SI units are used in most part of this report. Some dimensions for the column cross-section are presented in US customary units and the following factors can be used for unit conversions:

$$1 \text{ J} = 9.48 \times 10^{-4} \text{ BTU}$$

$$1 \text{ kg/m}^3 = 6.24 \times 10^{-2} \text{ lb/ft}^3$$

$$1 \text{ mm} = 25.4 \text{ in}$$

$$1 \text{ N} = 2.25 \times 10^{-1} \text{ lbf}$$

$$1 \text{ Pa} = 2.09 \times 10^{-2} \text{ psf}$$

$$1 \text{ W} = 3.41 \text{ BTU/hr}$$

CHAPTER 2

BACKGROUND INFORMATION

2.1 Introduction

This chapter presents background information relevant to this study. Included in this chapter is a discussion of heat transfer mechanisms, followed by background information on fire properties and the fire loads. The next half of this chapter presents properties of the materials used in this study at elevated temperatures. This includes information about mechanical and thermal properties of steel, intumescent paint, concrete and sprayed fire resistance material (SFRM).

2.2 Heat Transfer

Heat transfer is the exchange of heat between systems. The rate at which heat flows depends on properties of the heated objects and the medium that heat flows through. The three major heat transfer mechanisms are conduction, convection, and radiation. In most practical problems, the three mechanisms of heat transfer occur at the same time. Each of these heat transfer mechanisms are briefly reviewed in the following sections.

2.2.1 Conduction

Heat conduction is the mechanism of heat movement through solid objects, which is done by the movements of electrons within the object. Conduction occurs when there is temperature gradient between two points in a body. When one part of the body is heated, the particles gain more energy and vibrate rapidly (AISC Design Guide 19, 2003). This vibration of particles, transfers heat from elevated temperature regions to lower temperature regions. Equation 2.1 is the general equation for one-dimensional conduction heat transfer rate calculations.

$$Q = -k \cdot A \cdot \frac{dT}{dx} \quad (\text{Equation 2.1})$$

In this equation, k is the thermal conductivity of material (W/m-K), A is the area through which heat flows (m^2), and $\frac{dT}{dx}$ is the temperature gradient across the thickness of the section (K/m), shown in Figure 2-1. The negative sign indicates the direction of heat flow, because heat energy moves from high temperature regions towards lower temperature regions.

In general, materials that are effective electrical conductors are usually good conductors of heat, and those that are poor conductor of electricity have lower conductivity. To perform heat transfer analysis involving the conduction mechanism, information about material properties, such as density, specific heat, and thermal conductivity are needed. These properties are discussed later in this chapter.

In the case of unprotected steel, heat from a fire source reaches the exterior surface of the column through convection and radiation heat transfer mechanisms. After it reaches the exterior surface, it moves across the section by conduction mechanism. If intumescent paint or SFRM is applied on the surface of the column, heat would reach the insulation first. Then, the heat moves through the insulation and steel by the conduction heat transfer mechanism.

2.2.2 Convection

Convection heat transfer is the transfer of heat from one place to another place by the movement of fluids (liquid or gas). In fire applications, convective heat transfer is usually performed between moving fluid and a solid body. The amount of convective heat

transfer between two bodies is directly proportional to their temperature difference and is interpreted as in Equation 2.2 (Buchanan 2002).

$$q'' = h \cdot \Delta T \quad (\text{Equation 2.2})$$

where, h is the convective heat transfer coefficient ($\text{w/m}^2\text{K}$), ΔT is the temperature difference between the surface of the solid and the fluid (C or K), and q'' is heat flow per unit area (w/m^2). The parameter h depends on the nature and velocity of the fluid as well as surface regularity of the solid body.

A typical value for convective heat transfer coefficient proposed by EC3 (2001) for heat transfer analysis in fire is $25 \text{ w/m}^2\text{K}$ and is used in this study. However, different values have been used in various sources. Lee (2006) performed sensitivity analysis by considering 6.5, 15 and 25 W/m^2 values for h . These different values of h had small impact on heat transfer analysis results, because radiation heat transfer mechanism is dominant mechanism for the heat transfer in fires. Therefore, the value of 25 W/m^2 used in this report yields reliable results.

2.2.3 Radiation

Radiation is a major mechanism of heat transfer in fire situations. Heat transfer via transmission of electromagnetic waves is identified as thermal radiation. All bodies radiate energy in form of photons emitting from their surfaces. When these photons reach another surface, they are either absorbed, reflected or transmitted. For radiation heat transfer mechanism, and intervening medium is not required, as heat can travel through the vacuum. The heat flux through radiation is calculated with the Equation 2.3 (Buchanan 2002).

$$q'' = \varphi \varepsilon \sigma (T_e^4 - T_r^4) \quad (\text{Equation 2.3})$$

T_r is the absolute temperature of receiving surface (K), T_e is the absolute temperature of the emitting surface (K), and φ is the configuration factor, and can be calculated with Equation 2.4.

$$\varphi = \int^{A_1} \frac{\cos\Theta_1 \cos\Theta_2}{\pi r^2} \quad (\text{Equation 2.4})$$

σ is the proportionality constant, referred to as the Stefan-Boltzmann constant, equal to $5.67 \times 10^{-8} \text{ W}/(\text{m}^2\text{-K}^4)$. The values of Θ_1 and Θ_2 are displayed in Figure 2-2.

The resultant emissivity ε of the emitting and receiving surfaces, given by Equation 2.5.

$$\varepsilon = \frac{1}{\frac{1}{\varepsilon_e} + \frac{1}{\varepsilon_r} - 1} \quad (\text{Equation 2.5})$$

where ε_r is emissivity of the receiving surface and ε_e is emissivity of the emitting surface.

Emissivity of fire (in this case the emitting surface) is usually considered 0.8 (Lee and Pessiki, 2006). Emissivity of receiving surface depends on the type of material and the receiving surface conditions. For instance, values as low as 0.625 in EC3 and as high as 0.9 in ASCE SFP has been used for emissivity of steel. Table 2-2 shows various values of emissivity for steel that have been proposed from different sources. Sensitivity analysis performed by Lee and Pessiki (2006) explains that heat transfer analysis is highly dependent on emissivity value and the temperature increases as equivalent emissivity value rises. Careful parametric studies shall be conducted while selecting the value of emissivity in heat transfer analysis in fires.

2.3 Fire Loads

In order to evaluate performance of structural steel column in a fire exposure, a standard pre-defined fire load will be applied to them. This thesis considers two types of fires: Code specified fire (ASTM E119) and real fires. In performance based design methods, it is allowed by the code to create the specific fire curves considering the size of

the compartment under consideration and its ventilation size and should satisfy all the safety requirement set by the code. These fires, sometimes called real fires, will be studied for small and large compartments sizes in this study. These fire types are briefly explained in the following subsections.

2.3.1 ASTM E119 Fire

ASTM E119 (Figure 2-3) is the fire load specified by the design codes. ASTM E119 fire provides temperature-time profile of the fire as a function of time in the furnace. To calculate the fire rating of a product, manufacturers place it under this standardized fire test and find the time in which the material can retain their structural integrity. This standard is used to measure and describe the response of materials, products, or assemblies to heat and flame under controlled conditions. Application of these results predict the performance of actual building construction materials under the standard fire. While performing the test, temperature-time values shown in Figure 2-3 are controlled inside the furnace.

In this study, E119 fire temperature is applied on each column section for 2 hours.

2.3.2 Real Fires

Building Research Establishment (BRE) built an 8-storey composite steel and lightweight concrete building frame at their large-scale test facility at Cardington, UK. They subjected the building to six full-scale fire tests in different floor levels and sections. Large amount of useful data was found during these fire tests, which brought significant changes to the design guides. One of their findings was that the temperature profile was different in each compartment and it depends on the size of the compartment and the size of the ventilation. (British Steel 1999).

Large Compartment Fires

In the BRE Test 2, a large compartment fire simulation with floor area of 340m² and a fuel load of 40kg/m² was considered (British Steel 1999). Temperature-time profile observed for this fire is shown in Figure 2-4 (regenerated from British Steel (1999) for this study).

Small Compartment Fires (Office fire)

In the British Steel Test 4, an office simulation in the corner compartment of the second floor with an area of 136m² and an equivalent wood fuel load of 46kg/m² was used. Temperature-time profile observed for this fire is shown in Figure 2-5 (regenerated from British Steel (1999) for this study).

In large compartment fires (Figure 2-4), the temperatures do not reach as high as small compartments fire, but the elevated temperature exists for longer durations. This is due to the small ratio of ventilation to compartment size. This small ventilation size contains most of the fire inside the room, and allows smaller heat loss through the openings (Kirby 1999). This slow burning, causes a long decay period of large compartment fires. However, in small compartment fires (Figure 2-5), the ratio of ventilation size to size of the compartment is small and the heat energy escape at a high rate through the openings. This leads to faster decay in temperature-time profile in the small compartment fire.

2.4 Properties of Steel at Elevated Temperatures

As the temperature in steel increases, it begins to behave differently and its material properties starts to change. This section discusses thermal and mechanical properties of steel at elevated temperatures, which are used for heat transfer calculation in later chapters.

2.4.1 Thermal Conductivity of Steel

Thermal conductivity is the amount of heat transferred in a unit thickness of material normal to the surface of a unit area due to temperature difference in steady state conditions. For heat transfer calculations, thermal conductivity of steel and its change as a function of temperature is an important parameter. As shown in Figure 2-5 taken from EC3 (2001), the thermal conductivity of steel varies linearly with respect to temperature up to 800°C. After the temperature reaches 800°C, it remains constant.

2.4.2 Specific Heat of Steel

Specific heat is the amount of heat required per unit mass to rise the temperature of a material by one degree Celsius. In heat transfer analysis, specific heat is an important parameter. For steel, in simple calculations, a specific heat value of 600 J/kg K can be used. However, for more accurate and detailed calculation, the specific heat curve of steel shown in Figure 2-7 taken from EC3 (2001) is used. As can be seen in Figure 2-7, the peak in specific heat value at 735°C is due to metallurgical changes in in molecular structure of steel. The following equations taken from EC3 (2001) can also be used to find specific heat of steel as a function of temperature.

$$cp = 425 + 0.773 T - 1.69 \times 10^{-3} T^2 + 2.22 \times 10^{-6} T^3 \quad 20^\circ\text{C} \leq T \leq 600^\circ\text{C}$$

$$cp = 666 + 13002/(738 - T) \quad 600^\circ\text{C} \leq T \leq 735^\circ\text{C}$$

$$cp = 545 + 17820/(T - 731) \quad 735^\circ\text{C} \leq T \leq 900^\circ\text{C}$$

$$cp = 650 \quad 900^\circ\text{C} \leq T \leq 1200^\circ\text{C}$$

2.4.3 Steel Stress-Strain Curves

Stress-strain relationships in steel are important material properties to predict the mechanical behavior of a steel member. Both yield stress and modulus of elasticity

decreases as temperatures rises. As shown in Figure 2-8, steel has a well-defined stress-strain relationship at low temperatures, but as the temperature escalates, transition from elastic to plastic region becomes smooth. For design purposes, knowing the yield strength value of steel is an important parameter, but as is shown in Figure 2-8, this value is not clear at higher temperatures. As shown in Figure 2-9, 1% offset value as an effective yield strength which is recommended by Kirby and Preston (1988) can be used in engineering calculations.

Table 2-1 and Figure 2-10, which are taken from EC3 (2001) shows the reduction in yield strength and modulus of elasticity of steel as a function of temperature. As the temperature of steel increases, its modulus of elasticity and yield strength decreases. This table is used for strength analysis in Chapter 5 of this study and interpolation will be performed for the values in between.

2.4.4 Density of Steel

Density is the mass of material that occupies a unit volume. The density of steel varies based on its alloying constituents but usually ranges between 7,750 and 8,050 kg/m³. As the temperature increases, materials expand. However, the change is not significant to influence the density. Because density has small effect on heat transfer calculations, a constant value of 7860 kg/m³ will be used for the analysis in this study.

2.5 Properties of Intumescent Paint at Elevated Temperatures

Intumescent paints are thin chemical films, which comprise a mixture of binders, ceramics, resins and refractory fillers. When temperature rises, these films expand and gases within the film tends to escape. It forms a durable, adherent and fire resisting foam (AISC Design guide 19). Intumescent paint is applied directly to steel members by means

of spray-applied adhesion. Intumescent paint expands significantly when exposed to hot temperatures. The key feature is that the paint is inert at low temperatures, but provides insulation as result of complex chemical reactions at higher temperatures. The reaction takes place at temperatures typically ranging between 200-250°C. The process of intumescent paint reaction is shown in Figure 2-11. This expansive nature makes it appealing fire protective material to preserve aesthetic appearance of structural steel members in buildings. Depending on the type and manufacturer of intumescent paint, it can expand up to 50 times its original thickness (Bradely and Sizemore, 2014). The disadvantage of using intumescent paint material is its high application and maintenance cost.

Although intumescent paint material is appealing for fire protection purposes, the modeling process is difficult due to its changing nature. Chen and Shen (2011) have proposed an engineering model that makes this process simple. Table 2-3 gives all the parameters proposed by them and are used for the analysis in this study.

2.5.1 Intumescent Paint Thermal Conductivity and Specific Heat

Thermal conductivity of intumescent paint depends on its temperature (Figure 2-12). At lower temperatures, thermal conductivity has a constant value, but as the temperature rises, it begins to react and expand. This expansion increases the thickness of intumescent paint layer and causes amplified thermal resistance. Chen and Shen (2011) divides this entire process of expansion and degradation into five stages (Table 2-2). The first stage includes the normal condition. As is shown in Figure 2-12, within this stage, intumescent paint is inert without changing its original thickness and thus constant thermal conductivity. The second stage begins with T_1 which is the time this material starts the reaction process

and expands. The conductivity of material drops linearly until it reaches certain temperature T2. The third stage starts with T2, the time that the process of expansion stops and material remains expanded. In stage four, after T3, material starts to degrade and lose its thickness. Figure 2-12 shows that as it loses its thickness, its conductivity rises to the same level as it was in its original state at T4 and remains constant in stage five.

2.6 Sprayed Fire Resistant Material (SFRM)

SFRM is used as thermal insulation due to its low thermal conductivity which slows down the transfer of heat to the steel section. SFRMs are lightweight plasters made of cementitious (gypsum or Portland cement) binders and inorganic porous aggregates (perlite, vermiculite, etc.) or mineral wools. Among those, cementitious SFRMs are commonly used; many of which are Portland cement based. SFRM's structure provides excellent fire resistance due to its low thermal conductivity. Up to four hours of fire rating can be achieved with SFRM material. They are applied through spraying process, which significantly shortens the installation time and therefore lowers the cost. It also allows SFRM to cover detailed features easily, like bolts and connections. Most importantly, they are very cost effective compared to other fire protection materials.

2.6.1 SFRM Thickness Calculation

The amount of thickness for SFRM depends on the size and the shape of the member's cross section and the amount of fire rating required by the building code. There are various ways to calculate thickness of SFRM, but it mainly depends on their type and manufacturer. In this section, two calculation methods presented are: International Building Code (IBC) and SFRM manufacturer catalog (Isolatek International Product

Manual, 2016). The thickness of SFRM for 8xx tube is calculated for 1 hour (1-h) and 2 hour (2-h) fire rating as follow using both methods.

IBC Method

Section 720.5.1.3 of the IBC includes an equation for the determination of the required SFRM thickness as a function of the fire rating R, the W/D ratio of the column and coefficients, which reflect the thermal properties of the insulating material.

$$R = \left[C_1 \left(\frac{W}{D} \right) + C_2 \right] h \quad \text{(Equation 2.6)}$$

where h is SFRM thickness (in.), R is fire rating (hours), W is the column weight (lbs per ft), D is the perimeter of the column at the interface of the SFRM (in.), C1 and C2 are Material dependent constants (see Table 2-3 copied from AISC provide these constants for some SFRM manufactures).

Thickness Calculation for 1-h Rating

$$C_1 = 0.86$$

$$C_2 = 0.97$$

Coefficients for Isolatek 800 SFRM

$$W = 72.42 \text{ lb/ft}$$

Weight of 8xx steel tube

$$D = 8 \text{ in}$$

Diameter of 8xx steel tube

$$h = \frac{R}{\left[C_1 \left(\frac{W}{D} \right) + C_2 \right]} = 0.29 \text{ in}$$

Thickness of SFRM required for 1-h fire rating

A similar calculation was performed for 2-h fire rating which resulted in 0.58-in thickness.

Method 2: Supplier Data for Blaze Shield II from Isolatek International

From manufacturer data manual for Blaze Shield II, the following equation is used to find the thickness of SFRM.

$$h = \frac{R-0.38}{3.58 \left(\frac{A}{P} \right)} \quad \text{(Equation 2.7)}$$

where R is the hourly rating (hours), h is the thickness of protection material (in), A is the cross-sectional area (sq in.), and P is the heated perimeter (in.).

Equation 2.7 is used to find 1-h and 2-h fire rating thicknesses.

$R = 1 \text{ hours}$	Duration of fire rating
$d_1 = 8 \text{ in}$	Outer diameter of 8xx tube
$d_2 = 8 - 2 \times 0.875 = 6.25 \text{ in}$	Inner diameter of 8xx tube
$A = \pi \frac{d_1^2 - d_2^2}{4} = 19.6 \text{ in}^2$	Area of the section
$P = \pi d_1 = 25.1$	Perimeter of the 8xx tube
$h = \frac{1 - 0.38}{3.58 \left(\frac{19.6}{25.1} \right)} = 0.222 \text{ in}$	Thickness of SFRM for 1-h fire rating

The same calculation was applied for two-hour fire rating and the thickness resulted in 0.58-in. For the purpose of achieving one hour and two-hour fire ratings, 0.25in (6.35 mm) and 0.6in (15.2 mm) thick SFRM material are used in this study.

2.6.2 Behavior of SFRM at Elevated Temperatures

According to NIST (2005), the thermal conductivity and specific heat of Blaze Shield II type SFRM were determined as a function of temperature up to 1200°C. Figure 2-13 illustrates thermal conductivity of SFRM as a function of time. As can be seen from this figure, thermal conductivity of SFRM increases when the temperature rises. Figure 2-14 shows variation of specific heat for SFRM as a function of time. Specific heat of SFRM also increases with an increase in its temperature.

2.7 Properties of Concrete at Elevated Temperatures

Concrete can function as thermal insulation when it is applied on the exterior surface of structural steel members. The drawback of using concrete as thermal insulation on

exterior of the structural members is its high construction cost. Labor work required for formwork, placement and curing are the main reasons of high cost. In this study, concrete is not considered as an exterior insulation, but instead it is investigated as thermal mass inside the steel column. In order to perform this investigation, thermal and mechanical properties of concrete are required.

2.7.1 Thermal Conductivity and Specific Heat of Concrete

As shown in Figure 2-15, the thermal conductivity of concrete decreases linearly as a function of time until it reaches 800°C and then stays constant. Since concrete has low thermal conductivity, it can be used as thermal protective material. Specific heat for concrete does not change dramatically according to EC3 (2001). Therefore, the value of 880 J/Kg-C for a normal weight concrete is used in this study.

2.7.2 Compressive Strength of Concrete

Figure 2-16 shows variation of concrete compressive strength as a function of temperature. The shaded area shows the range of values achieved from tests by various researchers. This figure shows that at elevated temperatures, the compressive strength of concrete decreases.

Figure 2-17 demonstrates that at elevated temperatures, the ultimate strength and modulus of elasticity of concrete decreases. All of the stress-strain curves shown in this figure begin with a linear elastic region, followed by a parabolic region until the concrete reaches the maximum strength. After the resistance of concrete reaches its maximum value, the resistance drops down until failure occurs. For this study, concrete is only treated as a heat sink to absorb heat energy from the steel casing. The compressive strength behavior of concrete is ignored in the strength analysis.

2.7.3 Density of Concrete

The density of normal weight concrete is approximately 2400 Kg/m³. Depending on whether lightweight or heavyweight concrete is used, the density will change. An increase in temperature has a small effect on the density of concrete. Due to the fact that density has small influence on heat transfer calculation, a constant value of 2400Kg/m³ will be used in this study. In addition, a 28 Mpa compressive strength concrete is assumed in this report, and the modulus of elasticity is taken as 1.73 E8 Mpa.

2.8 Heat Transfer Finite Element

Steady state heat transfer analysis for a small one dimensional elements can be done with direct calculations, but when the geometry of the problem gets complex, a numerical approach is needed. Finite element method of heat transfer is a useful tool for performing this analysis. Equation 2.7 shows the general formula for heat transfer analysis.

$$-\left(\frac{\partial q_x}{\partial x} + \frac{\partial q_y}{\partial y} + \frac{\partial q_z}{\partial z}\right) + Q = \rho \cdot cp \cdot \frac{\partial T}{\partial t} \quad (\text{Equation 2.7})$$
$$q_x = -k \frac{\partial T}{\partial x}$$
$$q_y = -k \frac{\partial T}{\partial y}$$
$$q_z = -k \frac{\partial T}{\partial z}$$

q_x , q_y and q_z are components of heat flow in a unit area (W/m²), $Q(x, y, z, t)$ is the internal generation of heat per unit volume (W/m³), ρ is the density (kg/m³), c is the specific heat (J/K), T is the temperature (K), t is the time (s), and k is the thermal conductivity of material (W/m-K).

The means in which heat enters the systems depends on boundary conditions. The boundary conditions assumed to be as follow: S_1, S_2, S_3, S_4 are the boundary surfaces.

- a. Fixed temperature

$$T_s = T_1(x, y, z, t) \text{ on } S_1$$

b. Specified heat flow

$$q_x n_x + q_y n_y + q_z n_z = q_2 \text{ on } S_2$$

c. Convection boundary conditions

$$q_x n_x + q_y n_y + q_z n_z = (T_s - T_e) \text{ on } S_3$$

d. Radiation boundary condition

$$q_x n_x + q_y n_y + q_z n_z = \sigma \varepsilon T_s^4 - \alpha q_r \text{ on } S_4$$

In the equations above, h is the convection coefficient; T_s is an unknown surface temperature; T_e is a convective exchange temperature; σ is the Stefan–Boltzmann constant; ε is the surface emission coefficient; α is the surface absorption coefficient, n is a vector normal to the surface area, and q_r is the incident radiant heat flow per unit surface area.

Finite element for heat transfer works in a similar manner to finite element for structural analysis of solid bodies. Objects are discretized into smaller elements and matrix of thermal conductivity is created instead of stiffness matrix. The general equation for solving heat transfer problems with finite element is as follows:

$$[K_T]\{T\} = \{Q\} \quad \text{(Equation 2.9)}$$

where $[K_T]$ is thermal conductivity matrix (W/m-K), $\{T\}$ is nodal temperature (K), and $\{Q\}$ is matrix of thermal loads (W). From this equation, after imposing boundary condition, nodal temperature in all the nodes of the finite element model can be determined.

Table 2-1 Reduction in yield strength and modulus of elasticity of steel at elevated temperatures (EC3, 2001).

Steel temperature θ_a	Reduction factors at temperature θ_a relative to the value of f_y or E_a at 20 °C			
	Reduction factor (relative to f_y) for effective yield strength $k_{y,\theta} = f_{y,\theta}/f_y$	Modified factor (relative to f_y) for satisfying deformation criteria $k_{x,\theta} = f_{x,\theta}/f_y$	Reduction factor (relative to f_y) for proportional limit $k_{p,\theta} = f_{p,\theta}/f_y$	Reduction factor (relative to E_a) for the slope of the linear elastic range $k_{E,\theta} = E_{a,\theta}/E_a$
20 °C	1,000	1,000	1,000	1,000
100 °C	1,000	1,000	1,000	1,000
200 °C	1,000	0,922	0,807	0,900
300 °C	1,000	0,845	0,613	0,800
400 °C	1,000	0,770	0,420	0,700
500 °C	0,780	0,615	0,360	0,600
600 °C	0,470	0,354	0,180	0,310
700 °C	0,230	0,167	0,075	0,130
800 °C	0,110	0,087	0,050	0,090
900 °C	0,060	0,051	0,0375	0,0675
1000 °C	0,040	0,034	0,0250	0,0450
1100 °C	0,020	0,017	0,0125	0,0225
1200 °C	0,000	0,000	0,0000	0,0000

NOTE: For intermediate values of the steel temperature, linear interpolation may be used.

Table 2-2 Emissivity of steel taken from different sources. (Note: this table is copied from Keller (2012). References of the sources Keller used are included in reference list of this report).

Reference	Emissivity
Eurocode 3 (BSI, 2001)	0.6
(Wang, 2002)	0.7
(Lie, 1992)	0.9
(Holman, 2010)	0.8 (oxidized)
(Lamont et al., 2001)	0.7
(Bejan, 1993)	0.79
(Siegel and Howell, 1980)	0.3 (polished)
	0.81 (oxidized)
(Brewster, 1992)	0.3 (polished)
	0.8 (oxidized)

Table 2-3 Intumescent paint parameters based on Chen and Shen (2011).

Variable	Description	Value (FPS;SI)
k: BTU/[in-s-°F] ; (W/[m-K])	Thermal conductivity	1.3x10 ⁻⁶ , 2.7x10 ⁻⁶ , 6.7x10 ⁻⁶ , 1.3x10 ⁻⁵ ; (0.1, 0.2, 0.5, 1.0) ^a
N	Expansion Ratio	30
d: in; (mm)	Initial Thickness	0.079; (2)
ρ: lb/in ³ ; (kg/m ³)	Density	0.0325; (900)
cp: BTU/[lb _m -°F] ; (J/[kg-K])	Specific Heat	0.478; (2000)
T ₀ : °F ; (°C)	Initial Temperature	68 ; (20)
T ₁ : °F ; (°C)	Start of Expansion	499; (200)
T ₂ : °F ; (°C)	End of Expansion	850; (450)
T ₃ : °F ; (°C)	Char consumption	1200 ; (650)
T ₄ : °F ; (°C)	All char consumed	1450 ; (800)

a) Thermal conductivity for four different types of intumescent material. The values in bracket shows the SI values for the thermal conductivity and the values outside the bracket in US Customary units.

Table 2-4 Coefficients of C₁ and C₂ for common SFRM manufacturers (based on AISC Design Guide 19 (2003)).

Material	C ₁	C ₂
Grace MK6 All W/D	1.05	0.61
Isolatek 800 All W/D	0.86	0.97
Isolatek 280 W/D 0.33 to 2.51	1.25	0.53
Isolatek 280 W/D 2.51 to 6.68	1.25	0.25
Isolatek D-C/F W/D 0.55 to 7.00	1.01	0.66
Isolatek D-C/F W/D 0.30 to 0.55	0.95	0.45

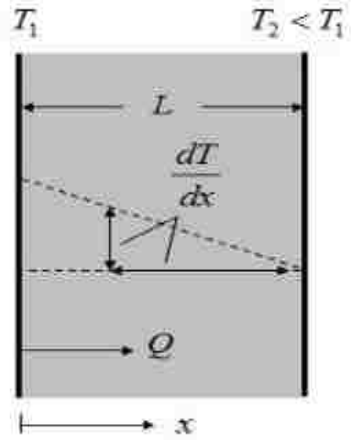


Figure 2-1 Heat conduction mechanism through a material of thickness L (Wang, 2002).

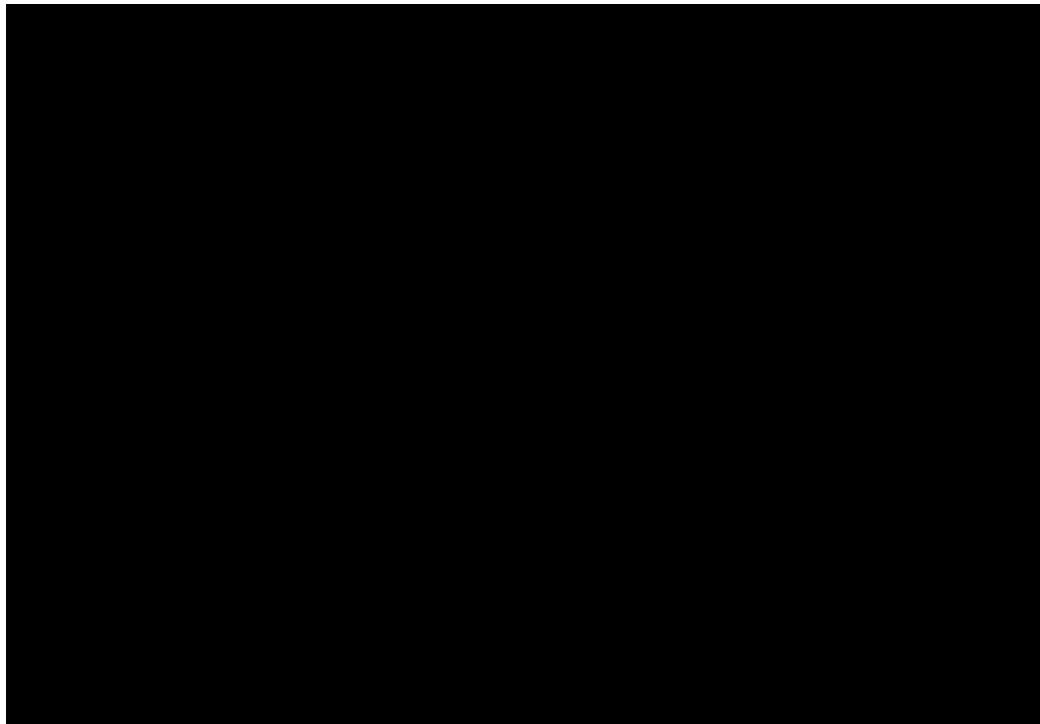


Figure 2-2 Surface configuration factor for radiating and receiving surfaces adapted from Drysdale (1998).

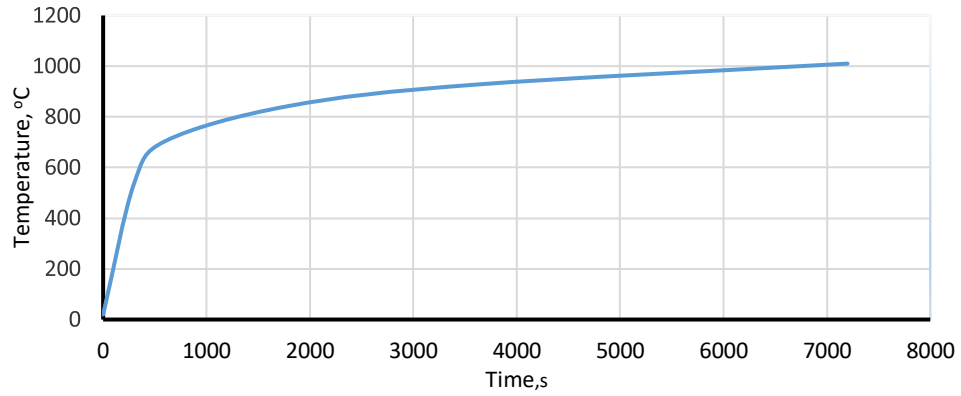


Figure 2-3 Temperature-time profile for the E119 fire taken from ASTM E119.

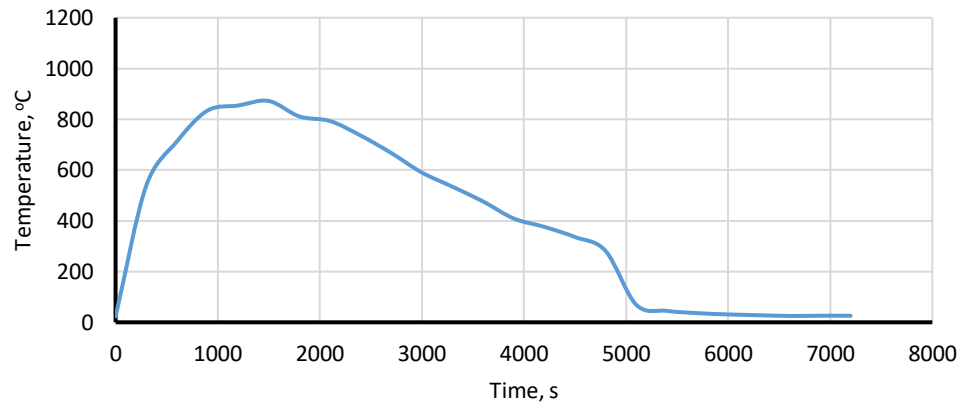


Figure 2-4 Temperature-time profile for the small compartment Cardington fire (digitized from British steel, 1999).

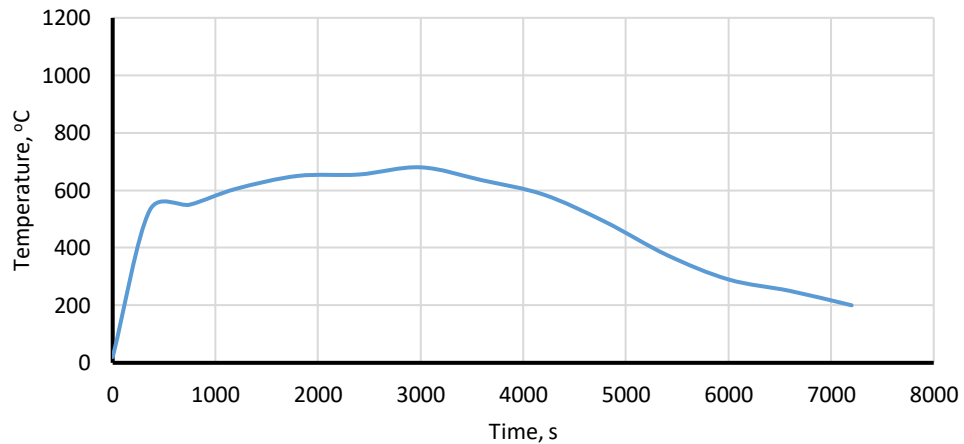


Figure 2-5 Temperature-time profile for the large compartment Cardington fire (digitized from British Steel, 1999).

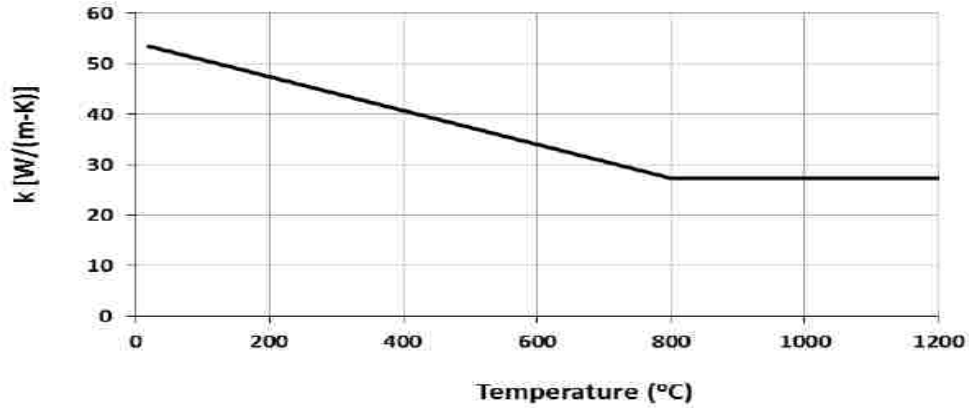


Figure 2-6 Thermal conductivity of steel as a function of temperature (EC3, 2001).

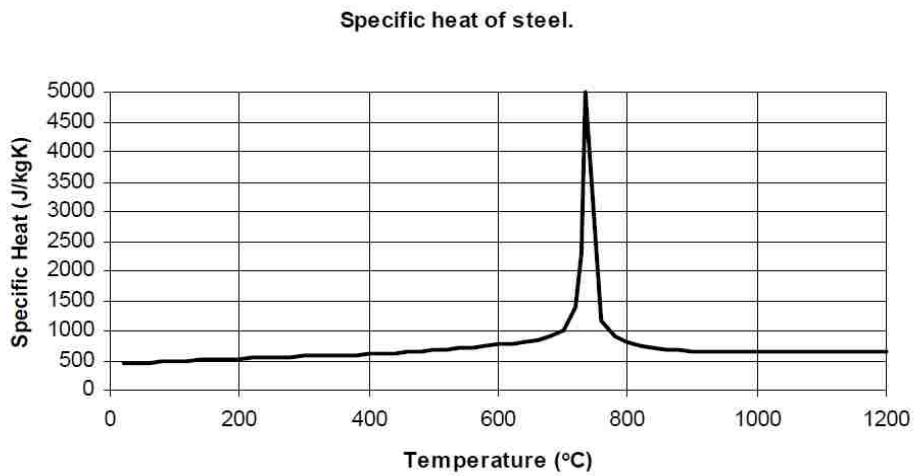


Figure 2-7 Specific heat of steel as a function of temperature (EC3, 2001).

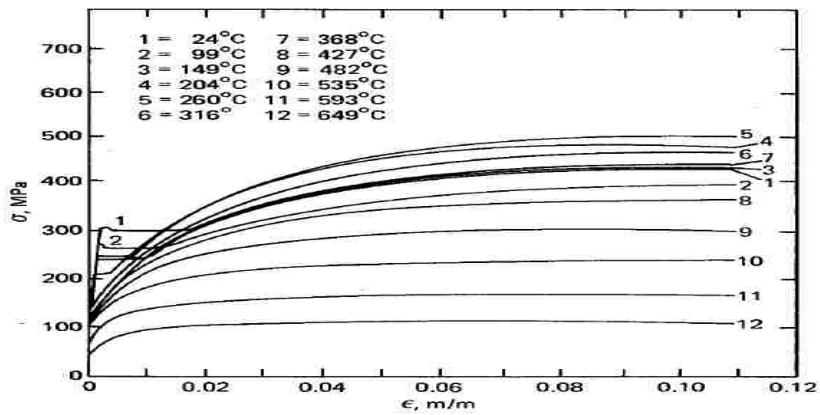


Figure 2-8 Stress-strain curves for steel at higher temperatures (SFPE, 1998).

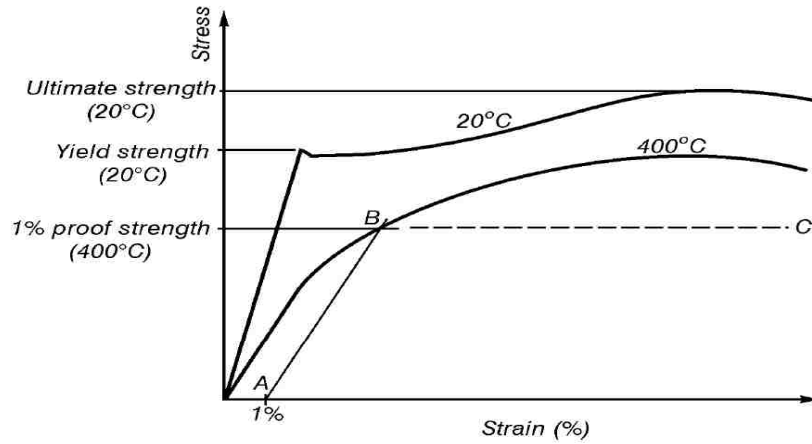


Figure 2-9 Effective yield strength proposed Kirby and Preston (1988).

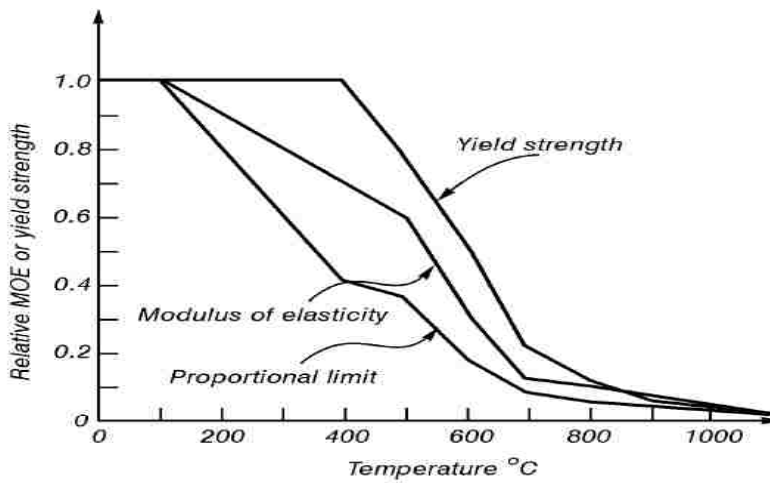


Figure 2-10 Reduction in yield strength and modulus of elasticity at elevated temperatures (EC3, 2001).

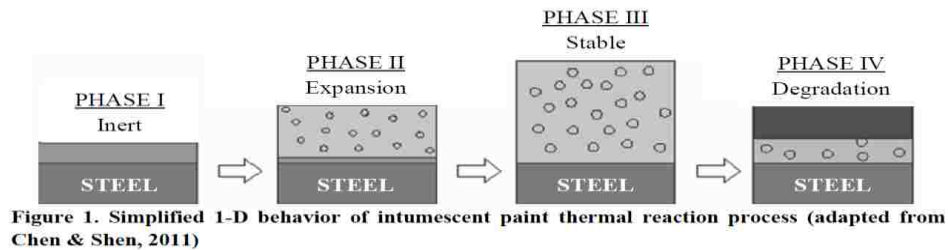


Figure 1. Simplified 1-D behavior of intumescent paint thermal reaction process (adapted from Chen & Shen, 2011)

Figure 2-11 Reaction process of intumescent paint at elevated temperatures (Bradley and Sizemore, 2014).

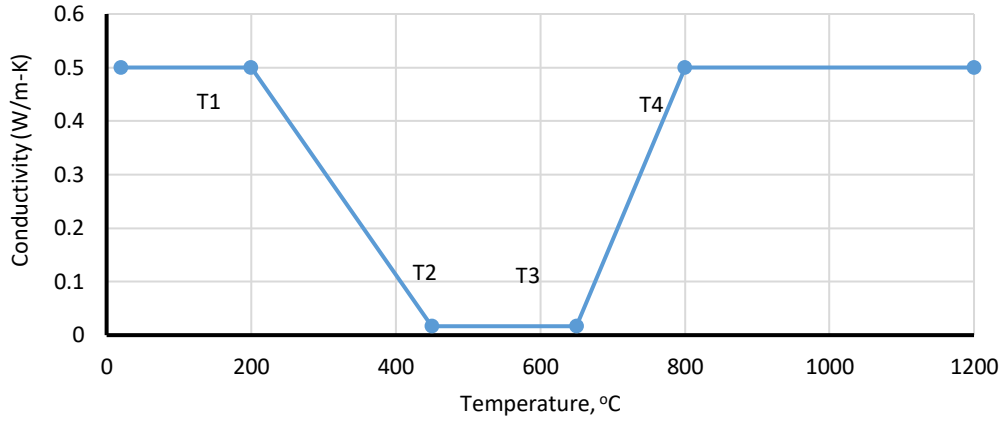


Figure 2-12 Thermal conductivity of intumescent paint as a function of temperature based on Chen and Shen (2011).

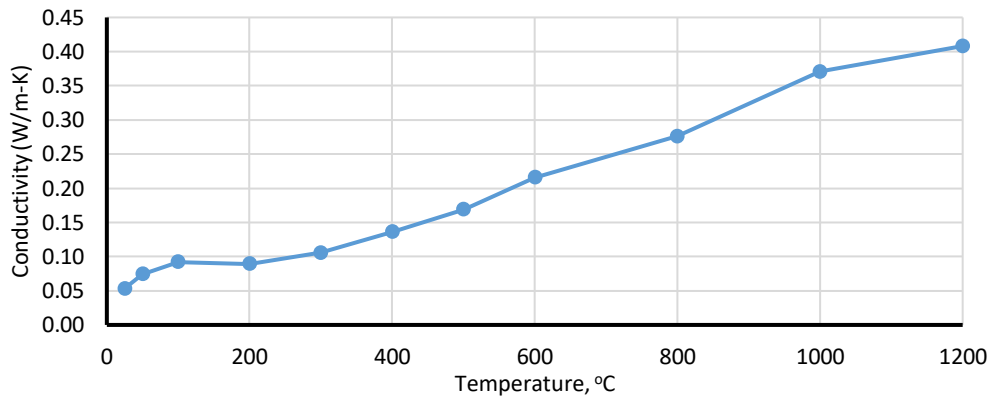


Figure 2-13 Thermal conductivity of Blaze Shield II SFRM as a function of temperature based on NIST (2005).

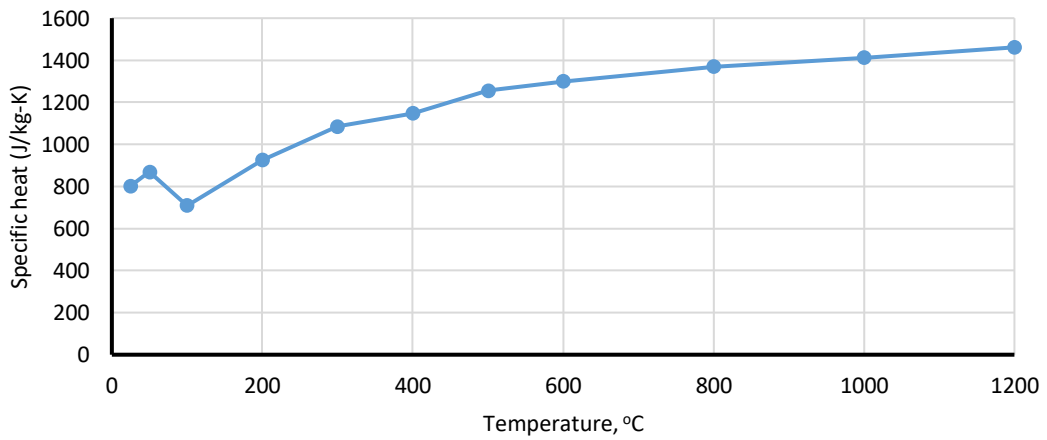


Figure 2-14 Specific heat of Blaze Shield II as a function of temperature based on NIST (2005).

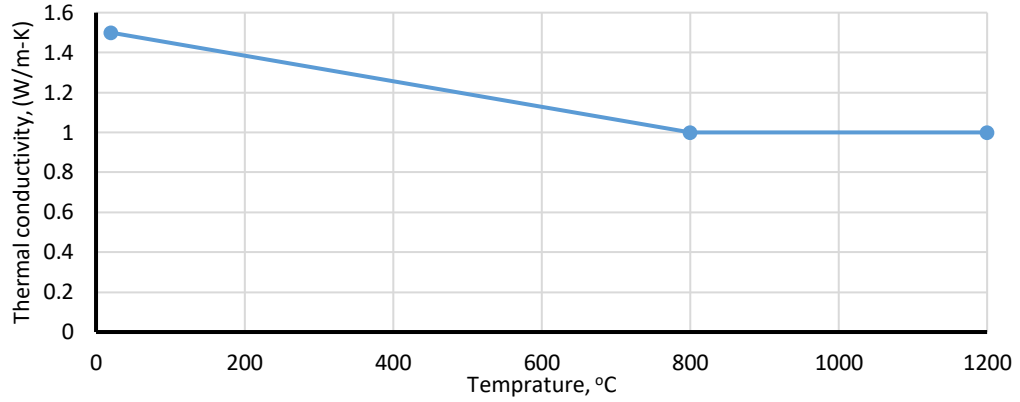


Figure 2-15 Concrete thermal conductivity as a function of temperature (Buchanan, 2002).

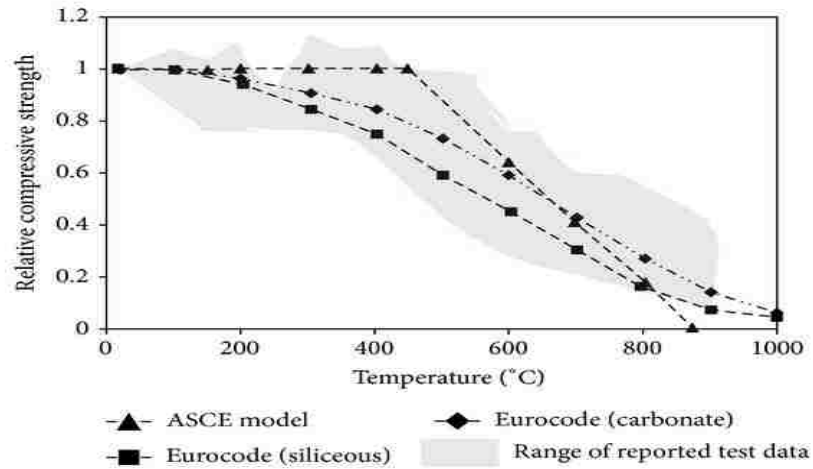


Figure 2-16 Variation in compressive strength of concrete at elevated temperatures (Kodur, 2014).

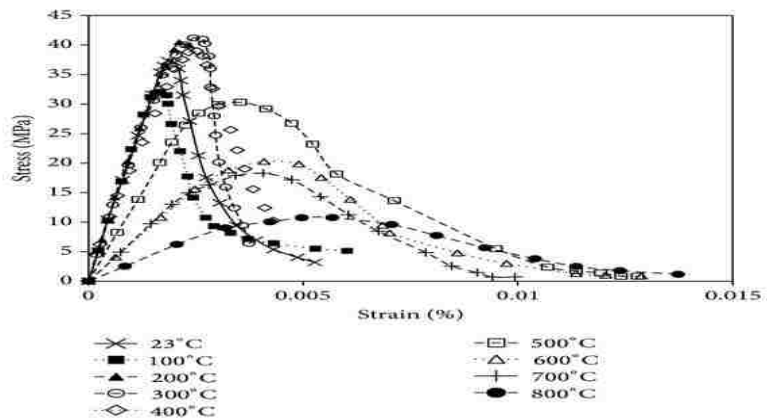


Figure 2-17 Concrete stress and strain curves at elevated temperatures (Kodur, 2014).

CHAPTER 3

ANALYSIS MODELS AND METHODS

3.1 Introduction

This chapter presents the analysis models and methods used to achieve the objectives of this study. Analysis models for both unprotected and fire protected columns are presented, followed by a description of the analysis matrix developed to isolate specific variables including bare steel, SFRM, intumescent paint and concrete fill. This chapter also explains the analytical tools used and the modeling procedure for heat transfer mechanisms for this study.

3.2 Analytical Models

Two methods to determine the thermal and strength response of structural members in a fire exposure includes experiment and analysis. Since experimental tests are usually time consuming and very expensive, this study uses analysis to evaluate heat transfer and strength of various column sections.

Two-dimensional finite element heat transfer models for the specific case of an 8xx steel tube column are considered in this study. 8xx tubes are circular hollow steel sections with an 8in (203.2 mm) outside diameter and 0.875in (22.2 mm) thickness as shown in Figure 3-1(d). In these analyses, heat is modeled from the fire source around the perimeter of the column to the surface of the column through convection and radiation mechanisms. Once it reaches the surface, the heat is transmitted within the section through the conduction heat transfer mechanism. The modeling procedure for heat transfer mechanisms are explained in Section 3.4.

Three fire scenarios are considered for the analysis in this report: E119, small compartment, and large compartment fires. The properties of these fires were explained in Section 2.3.

3.3 Analytical Matrix

Eighteen analytical models with various column section sizes, fire protective material and fire load cases are implemented as shown in Table 3-1. As shown in this table, for each model, an analysis ID is generated that represent the insulation type, section size, and the exposed for fire curve type in order to simplify their identification in later chapters. All the analysis scenarios in this study are divided into 5 cases.

1. Case 1 is the analyses of unprotected steel columns to study the effects of increasing wall thickness (i.e. total area) of the cross section on temperature distribution in the cross section of steel tubes. In this case, four analytical models for the 8in (203mm) diameter steel tube with various section's wall thicknesses starting from 0.5in (13mm) to 1.5in (38mm) are analyzed (see Figure 3-1). The outer diameter of the section remains constant. All four models are considered under the E119 fire exposure.
2. Case 2 studies the 8xx unprotected tube section under the exposure of the real fires. The objective of this case to investigate the effect of real fires on an unprotected column section. In this case, two models for large and small compartment fire exposures are studied.
3. Case 3 studies the 8xx tube section with 1-h fire rating thick SFRM on the outer surface of the column as shown in Figure 3-2(b). From the calculations in Section 2.6, it was found that the thickness of SFRM required for 1-h fire rating is 0.25in

(6.4mm). Three models will be created for a standard and compartment fire cases. Within the same case, an increased thickness of SFRM for 2-h fire rating is analyzed (Figure 3-2(a)).

4. Case 4 examines the intumescent paint insulated 8xx steel tube with different fire exposure scenarios. According to Table 2-2, one layer of intumescent paint is 2mm thick. Figure 3-3c shows schematic of the model created for the intumescent paint applied 8xx tube column. In this case, three analyses will be piloted, one for E119 and two for the real fires.
5. Case 5 is an analysis for concrete-filled 8xx tube section as shown in Figure 3-2(d) under the exposure of three fire types. Concrete will solely function as a heat sink for these models and will act to absorb heat energy from the steel section.

3.4 Analytical Tool

Two-dimensional heat transfer finite element analyses are performed with Abaqus software in this study. Abaqus is a commercially available finite element software used for a variety of purposes, including thermal analysis.

For the finite element meshing purpose, the 8-noded quadratic heat transfer quadrilateral (DC2D8) element is used in all of the analytical models. Mesh arrangements for the 8xx bare steel, intumescent paint applied, concrete-filled, SFRM applied models are shown in Figure 3-4. The interface between insulation material and steel tube are tied with each other to allow the flow of heat from the insulation to the steel tube. By doing this, the nodes at the interface from insulation material transfers temperature to the nearest nodes in steel tube section.

In all analysis cases, except for concrete filled sections, adiabatic boundary conditions for interior surface of the steel tube is used due to the reason that the columns are empty and the effect of cavity radiation is negligible (the reason that cavity radiation was ignored is discussed in Section 3.4.3). However, with concrete filled cross sections, heat transfer interaction occurs between interior surface of the steel tube and outer surface of the concrete.

Abaqus is used to calculate the temperature-time profile for each node in the model cross section throughout the analysis time. The analysis time increment is selected based the amount of time that the fire temperature increases by 20°C. The analysis time increment is based on variation in temperature of fire. When the variation in fire temperature is steep, the analysis time steps are small and when the variation in temperature is slight, the analysis time increments are longer.

Since this is a two-dimensional analysis, heat can only be transferred across the section not through the length of the member. The fire curves used in Abaqus models are E119, small and large compartment fires based on analysis cases. Note that the fire temperature is assumed to be consistent around the perimeter. This means that the fire intensity is assumed to be the same from all directions.

3.4.1 Convection and Radiation Heat Transfer Modeling

Convection and radiation boundary conditions are imposed on the outer surface of the column. Heat transfer is modeled to the column surfaces due to convection by creating a surface film condition interaction using Abaqus. Film condition interactions define heating or cooling due to convection by surrounding fluids. Film coefficients can also be a function of temperature, but for this analysis, it is considered instantaneously to

25 w/m²K (EC3 2001). It is also assumed that the temperature of the fire compartment is uniform, which is a reasonable assumption after flashover happens.

With Abaqus, heat transfer is modeled between a non-concave surface and a nonreflecting environment due to radiation by creating a surface radiation interaction and using emissivity value of 0.8. The emissivity value can be considered variable, but in this analysis, it is assumed that the column surface has a constant emissivity value. The ambient temperature is the fire temperature in the fire related models and is considered based on E119 and real fire curves.

3.4.2 Cavity Radiation Modeling

For the inner surface, effects of cavity radiation are considered. To understand the consequences of cavity radiation, two models of unprotected 8x1.5 tube section are examined, one with cavity radiation, and the other with adiabatic boundary conditions on the inner surface of the tube. Figure 3-3 shows the case with the fire applied symmetrically around the column. Both analysis with and without cavity radiation yields the same results. This is because the amount of heat emitting is equal to the amount of heat entering into the interior surface of the tube section. This proves that cavity radiation is equivalent of having an adiabatic boundary condition when fire load is applied symmetrically on tube sections. If fire is applied unsymmetrical on the section, cavity radiation effects should be considered. Figure 3-4 shows temperature distribution across the section when half of the column exterior surface is exposed to the fire and the other half is exposed to an environment with a constant temperature of 20°C. This figure shows that if the section or the fire load is unsymmetrical, effects of cavity radiation are significant.

3.5 Summary

For this analytical study, eighteen analytical models, six for unprotected column sections and twelve for the fire protected column sections are considered (see Table 3-1). Abaqus is used as an analysis tool to compute the temperature for each node across the section throughout the fire exposure. Heat is modeled to move to the column via convection and radiation heat transfer mechanisms and across the section through conduction mechanism. The values of $h=25 \text{ w/m}^2\text{K}$ and $\varepsilon=0.8$ will be used for convection heat transfer coefficient and the emissivity in this study respectively. Cavity radiation is not included in these analyses because the column section and the applied fire are symmetrical. The resulting temperatures are recorded for every 20°C increment in fire temperature at the three nodes across the section (exterior surface, midsection and interior surface).

Table 3-1 Analytical matrix for the models considered for analysis.

Case No.	Model Type	Wall Thickness inches, (mm)	Fire Protection	Applied Fire Curve	Analysis ID ^(a)
Case 1	Bare steel	1.5 (38.1)	None	E119 Fire	BS-8x1.5-E119
		1 (25.4)	None	E119 Fire	BS-8x1-E119
		0.5 (12.7)	None	E119 Fire	BS-8xx-E119
		0.875 (22.2)	None	E119 Fire	BS-8x0.5-E119
Case 2	Bare steel	0.875 (22.2)	None	LC Cardington Fire	BS-8xx-LC
		0.875 (22.2)	None	SC Cardington Fire	BS-8xx-SC
Case 3	1-h SFRM insulated column	0.875 (22.2)	(6.4mm) SFRM thick	E119 Fire	SFRM1h-8xx-E119
		0.875(22.2)	(6.4mm) SFRM thick	LC Cardington Fire	SFRM1h-8xx-LC
		0.875 (22.2)	(6.4mm) SFRM thick	SC Cardington Fire	SFRM1h-8xx-SC
	2-h SFRM insulated column	0.875 (22.2)	(15.2mm) SFRM thick	E119 Fire	SFRM2h-8xx-E119
		0.875 (22.2)	(15.2mm) SFRM thick	LC Cardington Fire	SFRM2h-8xx-LC
		0.875 (22.2)	(15.2mm) SFRM thick	SC Cardington Fire	SFRM2h-8xx-SC
Case 4	Intumescent paint insulated column	0.875 (22.2)	One layer of intumescent	E119 Fire	IP-8xx-E119
		0.875 (22.2)	One layer of intumescent	LC Cardington Fire	IP-8xx-LC
		0.875 (22.2)	One layer of intumescent	SC Cardington Fire	IP-8xx -SC
Case 5	Concrete-filled column	0.875 (22.2)	Concrete filled	E119 Fire	CF-8xx -E119
		0.875 (22.2)	Concrete filled	LC Cardington Fire	CF-8xx -LC
		0.875 (22.2)	Concrete filled	SC Cardington Fire	CF-8xx-SC

(a) The first letter in analysis ID is the insulation type, the second letter is the section type and the third one is the fire curve.

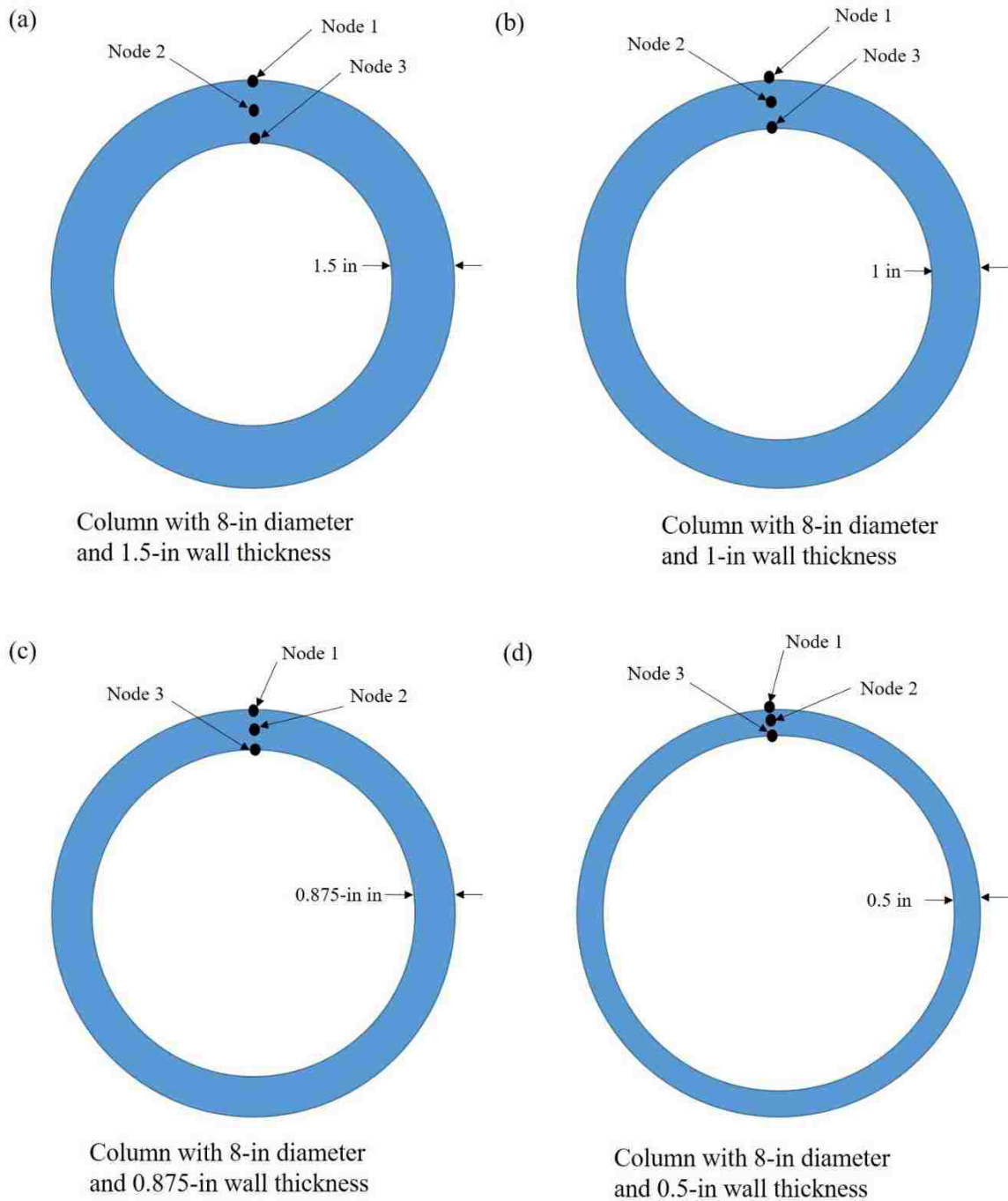


Figure 3-1 Unprotected circular steel section with different wall thicknesses used in this study: (a) 8x1.5; (b) 8x1; (c) 8xx; (d) 8x0.5.

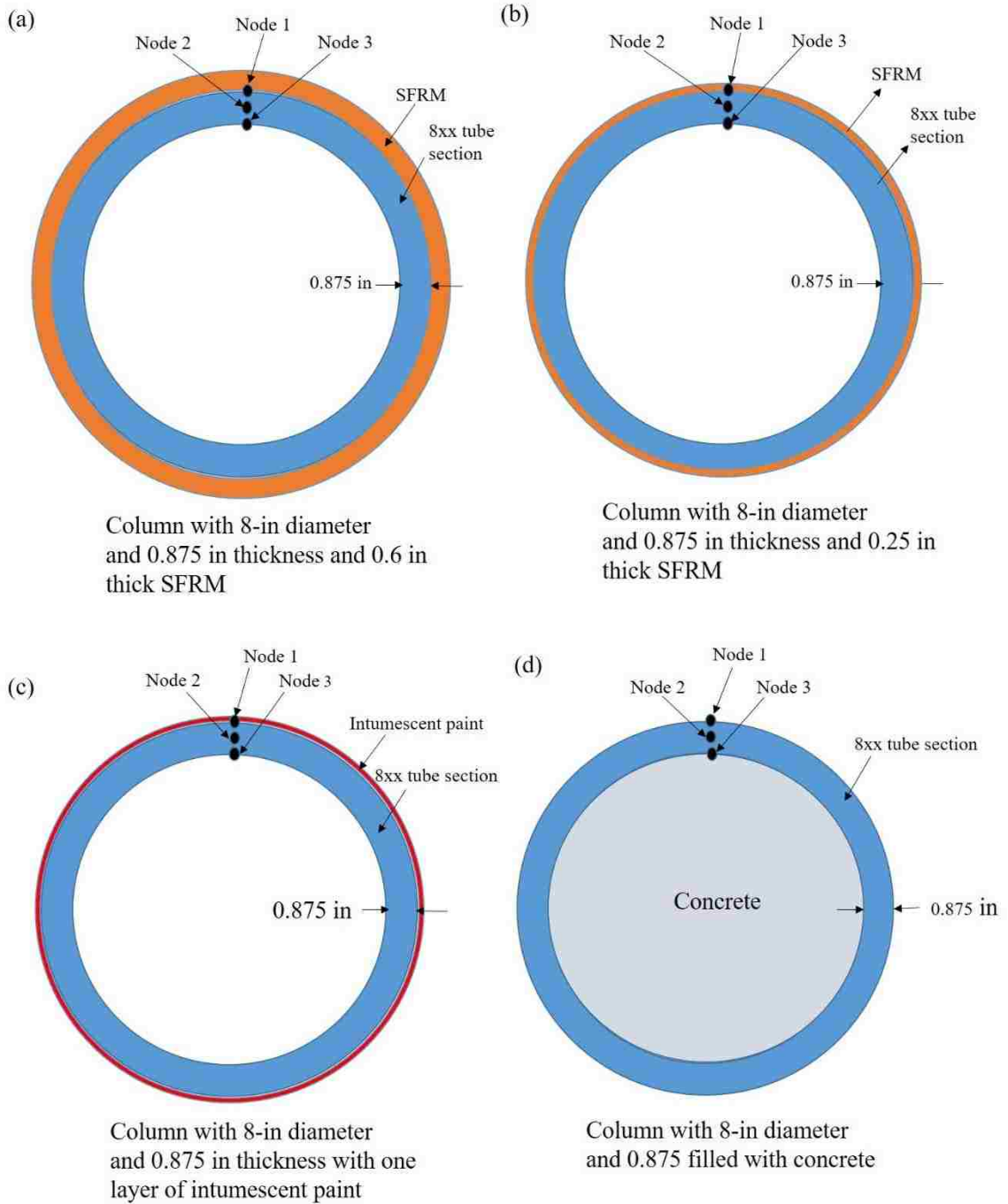


Figure 3-2 Protected 8xx tube section with different types of insulations applied: (a) 8xx with 2-h thick insulation; (b) 8xx with 1-h thick insulation; (c) 8xx with one layer of intumescent paint; (d) concrete fill 8xx.

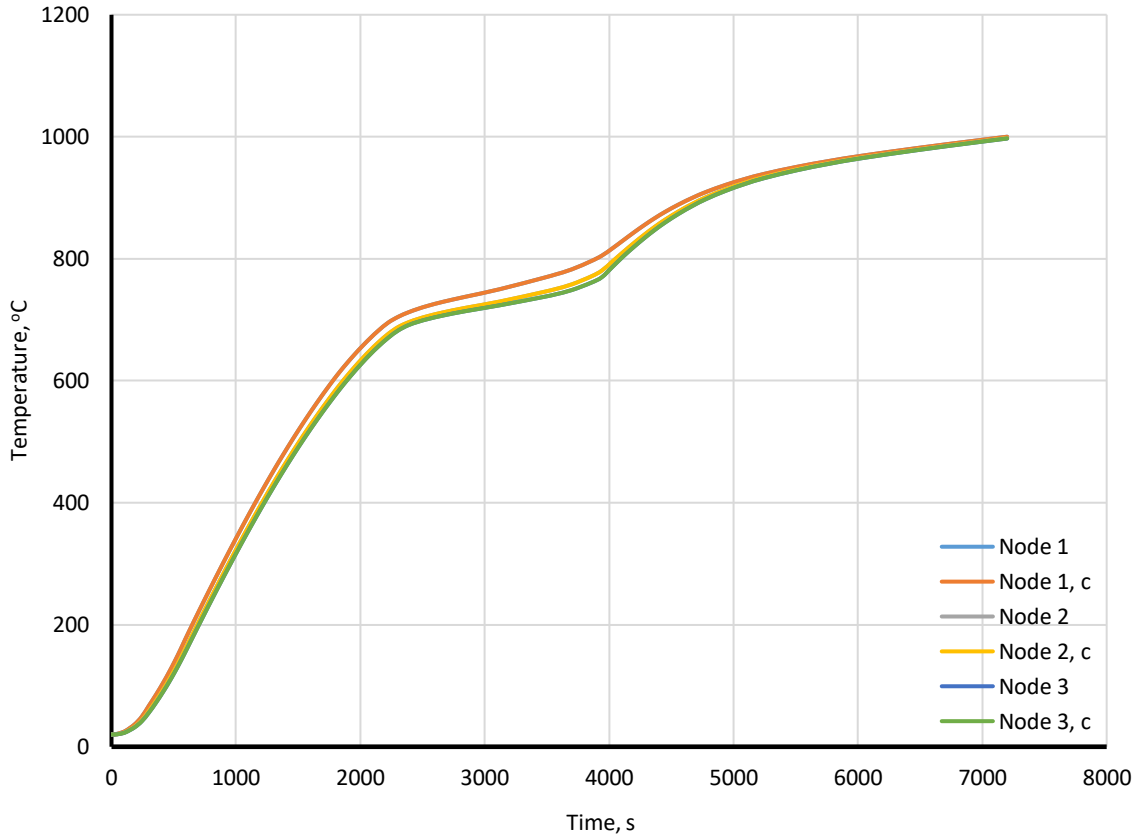


Figure 3-3 Heat transfer analysis with and without considering cavity radiation for 8x1.5 tube column under E119 fire exposure. 'c' means cavity radiation has been included.

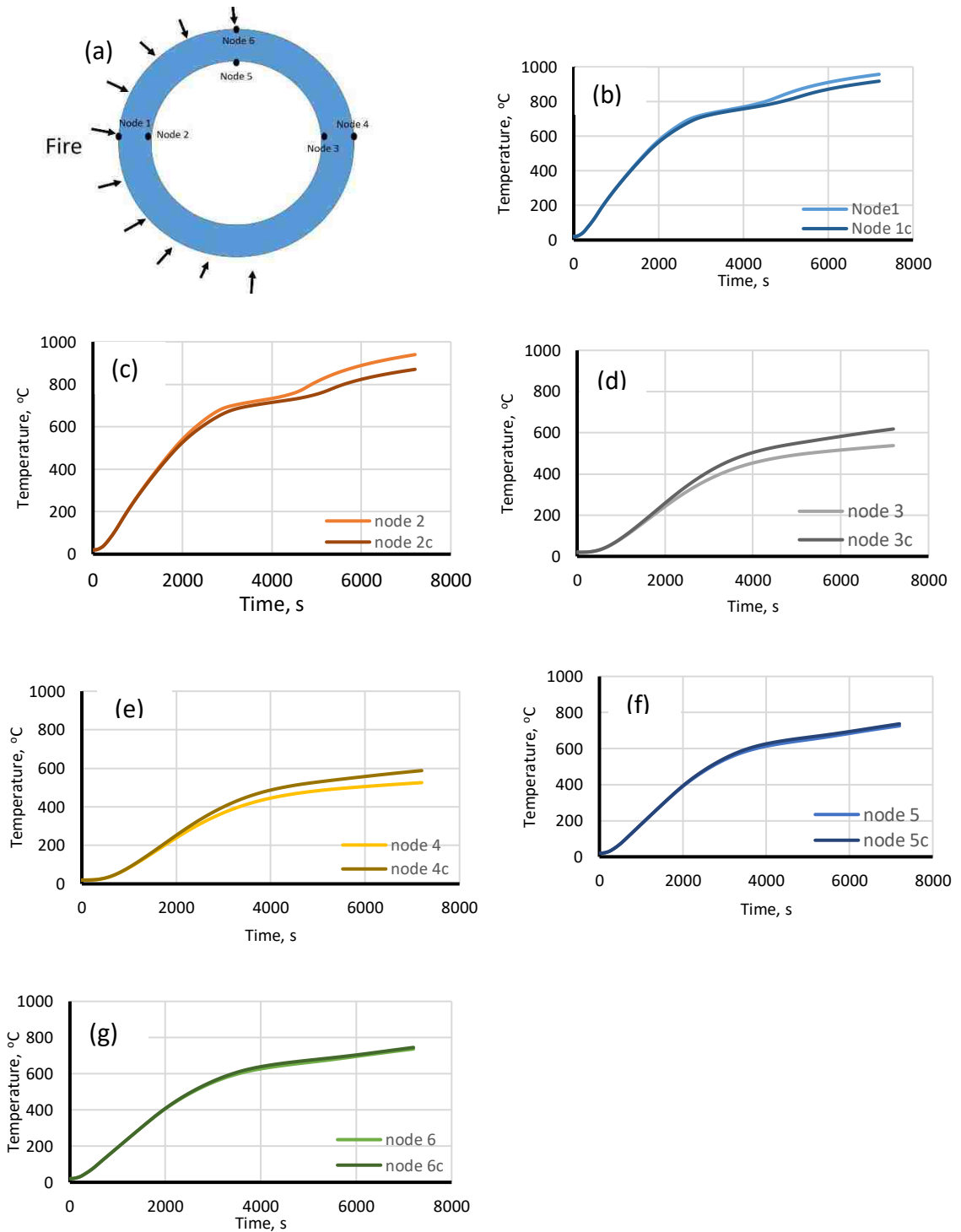


Figure 3-4 Results of cavity radiation analysis on 8x1.5 steel tube when half of the column surface is under E119 fire exposure. ‘c’ means with cavity radiation. (a) location of each nodes where data is extracted; (b) temperature-time profile for node 1; (c) node 2; (d) node 3; (e) node 4; (f) node 5; (g) node 6.

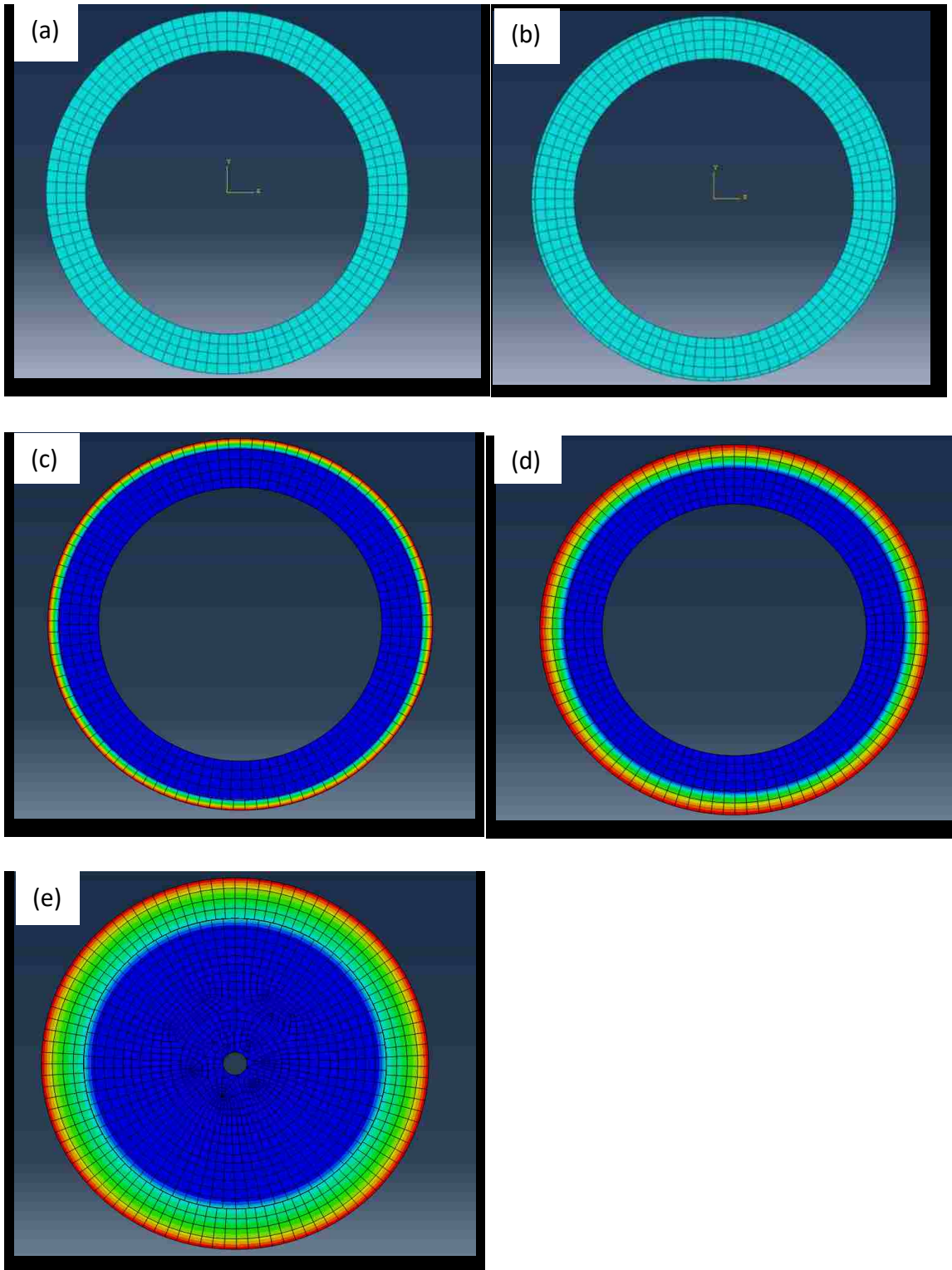


Figure 3-5 Mesh arrangements for the 8xx steel tube created for the study in this report: (a) Bare steel; (b) with one layer of intumescent paint; (c) with 1-h thick SFRM; (d) with 2-h thick SFRM; (e) concrete-filled.

CHAPTER 4

THERMAL ANALYSIS RESULTS

4.1 Introduction

This chapter presents the results of the two-dimensional heat transfer finite element analyses conducted on the eighteen analytical models. As discussed in Section 3.3, these models are divided into five analytical cases: analyses for unprotected columns under the E119 and real fire exposures (Case1 and 2), SFRM and intumescent paint insulated (Case 3 and 4), as well as concrete-filled tube sections (case 5). Based on temperature distribution results presented in this chapter, the strength analyses are conducted in Chapter 5.

4.2 Unprotected Columns with Various Section Sizes in E119 Fire

Exposure (Case 1)

Columns that are considered for analyses in this case are: 8x1.5, 8x1, 8xx and 8x0.5 unprotected steel tubes (see Figure 3-1) under the exposure of the E119 fire.

The 8x1.5 steel tube is the heaviest column considered for the analysis in this study. For two hours duration of E119 fire exposure, the nodal temperature at every point in the cross section is obtained. Figure 4-1 shows temperature versus time results obtained for three nodes: outer surface, midsection and inner surface. As shown in this figure, the temperature increases rapidly as a function of time at the beginning of the E119 fire. When the E119 fire reaches its almost steady value, temperature of the member converges to the temperature of fire.

The drop in temperature-time profile observed at point A is due to the existence of the transient increase in specific heat of steel at 735°C (see Figure 2-7). Since specific heat

is the amount of energy required to raise temperature of a unit mass by one degree Celsius, more energy is required to raise steel's temperature at 735°C.

Referring to Figure 4-1, the difference in temperature amongst Nodes 1, 2 and 3 is not substantial. Therefore, there is not significant temperature gradient within the section, which is due to the small distance between these nodes and the high thermal conductivity of steel. Figure 4-2 displays the temperature difference between the exterior and interior surfaces for the 8x1.5 tube section. The peak temperature difference observed between the exterior and interior surface for this heavy section is only 36 °C during the fire exposure.

Figure 4-3 displays temperature-time profile for the 8x1 tube section in E119 fire exposure. The maximum temperature difference between the exterior and interior surface of the column is 18.3 degrees Celsius (Figure 4-4), which is lower in comparison to the value achieved for 8x1.5 tube (Figure 4-2). The reason for this lower value is the smaller wall thickness of the tube cross section.

Figure 4-5 and 4.7 shows temperature-time profile for 8xx and 8x0.5 tube cross sections under the exposure of E119 fire. Since these cross sections have thinner walls than the first two, the temperature profile for the three nodes in the cross section are very close. This small variation in temperature between exterior and interior surface (node 1 and node 3) can be seen in Figures 4-6 and 4-8 for 8xx and 8x0.5 tubes, respectively. The maximum temperature difference observed for 8xx and 8x0.5 tube sections are 14.5°C and 6.7°C for the duration of fire exposure.

It can be interpreted from these results that in hollow section with smaller wall thicknesses (common for most structural members) the temperature change across the

section is not significant. Moreover, with all four unprotected-sections that are analyzed under E119 fire, there is a variation in rate of change of temperature at the point in which specific heat has maximum value. In addition, the temperature of steel section converges to the fire temperature after flashover occurs in E119 fires.

4.3 Unprotected 8xx Section in Real Fire Exposures (Case 2)

This section presents results of two-dimensional heat transfer analysis performed on an unprotected 8xx tube column under the real fire exposures in large and small compartments.

Figure 4-9 shows nodal temperatures for the Nodes 1, 2 and 3 under the large compartment fire exposure. The section's temperature rises to its maximum value of 635 °C after 57 minutes and then decreases. As shown in this figure, in real fires, temperature increases rapidly at the beginning and reaches to its maximum temperature. After it reaches the maximum value, its temperature starts to decay. This decay of fire decreases the room temperature but the column remains hot which causes flow of heat from the column back to the room. This is due to the reason that heat flows from higher temperature regions to the lower temperature regions.

Figure 4-10 shows temperature of unprotected 8xx steel section under the exposure of the small compartment fire. The maximum temperature observed is 725 °C, which occurs 37 minutes after the start of the fire. After the fire temperature reaches its maximum value, the temperature in fire starts to decay and the process of heat transfer reverses from column to the room similar to the large compartment case.

4.4 SFRM as Thermal Insulation (Case 3)

In this section, two-dimensional heat transfer analysis is conducted on a SFRM insulated 8xx steel tube column. Two subcases for 1-h and 2-h fire rating thicknesses of SFRM are studied. Both E119 and real fires are studied in three separate analyses for each subcases. Thickness of SFRM required for 1-h and 2-h fire rating was calculated in Section 2.6.

4.4.1 1-h Fire Rating SFRM

Figure 4-11 shows variation in temperature as a function of time obtained for Nodes 1, 2 and 3 in an E119 fire exposure. Due to the thermal resistance behavior of SFRM, the increase in temperature-time profile of the steel section is slow and steady. However, the nodal temperatures are in close proximity to each other. The maximum temperature occurs at the end of the fire, and is equal to 735°C.

Figures 4-12 and 4-13 shows variation in temperature for 1-h fire rating SFRM applied 8xx steel tube in large and small compartment fire exposures. The maximum temperature recorded for this column cross section under large compartment fire exposure is 407 °C after 86 minutes. The maximum temperature recorded under the exposure of small compartment fire is 434°C after 62 minutes. As expected, higher and earlier maximum section's temperature is obtained in small compartment fire in comparison to the large compartment fire.

4.4.2 2-h Fire Rating SFRM

Figure 4-14 shows the variation in temperature as a function of time under the E119 fire exposure on 2-h fire rating SFRM applied 8xx steel tube. The temperature increases almost linearly and reaches its maximum value of 606 °C at the end of the fire. This steady

rise in temperature is a result of the increased thickness of SFRM, which retards flow of heat to the steel column.

Figures 4-15 and 4-16 display the temperature-time profile of this same section in large and small compartment fire exposures. As shown in these figures, the temperature of the steel column raises to its maximum value of 265°C after 120 minutes when exposed to the large compartment fire and 274°C after 82 minutes when exposed to the small compartment fire. The process of heat transfer reverses from the column to the room after the fire temperature decays. From Figures 4-12, 4-13, 4-15 and 4-16, it appears that section's temperature does not change very much after the maximum temperature value is attained. SFRM acts as a thermal barrier to heat flow from the column to the room during temperature reversal and limits the steel's temperature to change much.

4.5 Intumescent Paint as Thermal Insulation (Case 4)

In this case, two-dimensional heat transfer analysis for the IP-applied 8xx tube section is conducted. Figure 4-17 displays the variation in section's temperature as a function of time in E119 fire exposure. In this case, the increase in temperature is slower compared to the case of unprotected steel due to fire resistance of intumescent paint. Because thermal conductivity of intumescent paint changes as a function of time, four regions can be observed in temperature profile of the model. By referring to the thermal conductivity of intumescent paint shown in Figure 2-11, the reasons for the irregularities in temperature profile can be understood.

When thermal conductivity of intumescent paint increases, the rate at which temperature increases slows down. This changes the slope of the curve and makes it concave downward. When thermal conductivity decreases, the rate of increase in

temperature rises and the plot concaves upward. At the end of analysis, the temperature of steel converges to the fire because intumescent paint disintegrates at higher temperatures.

The same 8xx steel tube with one layer of intumescent paint applied at its exterior surface is analyzed in real fire exposures. Figures 4-18 and 4-19 shows temperature-time profile of this model in large and small compartment fire exposures. Temperature reaches its maximum value of 435°C after 84 minutes in the large compartment fire, and 528°C in 55 minutes in the small compartment fire.

4.6 Concrete-Filled Columns (Case 5)

In this case, two dimensional heat transfer analysis for concrete-filled 8xx steel tube column under the E119 and real fire exposures in large and small compartments is performed. Concrete stores heat energy depending on its heating capacity and it's mass inside the column.

The behavior of the concrete-filled 8xx tube section under E119 fire is shown in Figure 4-20. The temperatures achieved are similar to the unprotected 8xx steel tube column except with slightly lower temperatures. This lower temperature is expected because concrete absorbs a portion of heat from the steel tube section. Due to the low thermal conductivity of concrete, heat transfer inside the concrete-filled section is slow. This causes the large portion of concrete to not receive the amount of heat it can store for the the two hours of fire exposure. Therefore, its effect on temperature-time profile of the section is not significant.

Figures 4-21 and 4-22 show variation in temperature of concrete-filled 8xx tube section in large and small compartment fire exposures. These figures resembles the results

achieved for unprotected steel sections displayed in Figures 4-9 and 4-10 with a slight difference. This is due to the reason that concrete cannot absorb more energy.

4.7 Summary

The objective of this chapter was to perform heat transfer analysis on unprotected and fire protected steel sections in standard and real fire exposures. Eighteen analytical model were studied in order to investigate effects of increasing section's size, adding various types of fire protective material and type of fire load on temperature response of the column section. Followings are the highlights of the findings in this chapter.

Four unprotected column members with different section sizes were analyzed. The resulting temperatures in the exterior and interior surfaces of the column were in close proximity of each other and the differences were not more than 40°C for all these sections throughout the fire duration.

Among the fire protective material selected for study in this chapter, SFRM provided the best thermal resistant to the member against fire and reduced the temperature of steel significantly. After SFRM, intumescent paint acted as a good thermal barrier, especially under compartment fires. Concrete-filled column section was the least effective way of fire insulation and its temperature was similar to the unprotected sections.

In E119 fire exposure, section's temperature increased throughout the burning and the maximum value occurred at the end (after two hours). In large and small compartment fire exposures, after the maximum value of compartment temperature was achieved, the steel temperature reduced as the transfer of heat reversed and flew from the column back to the environment.

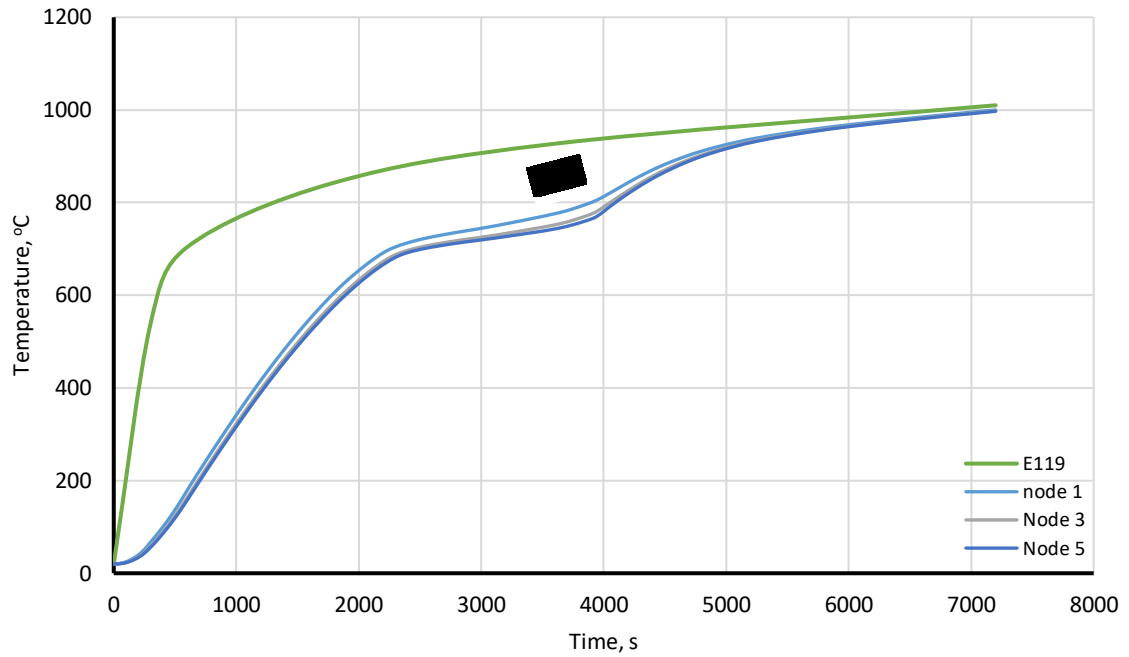


Figure 4-1 Variation in temperature for Nodes 1, 2 and 3 as a function of time for the analysis BS-8X1.5-E119.

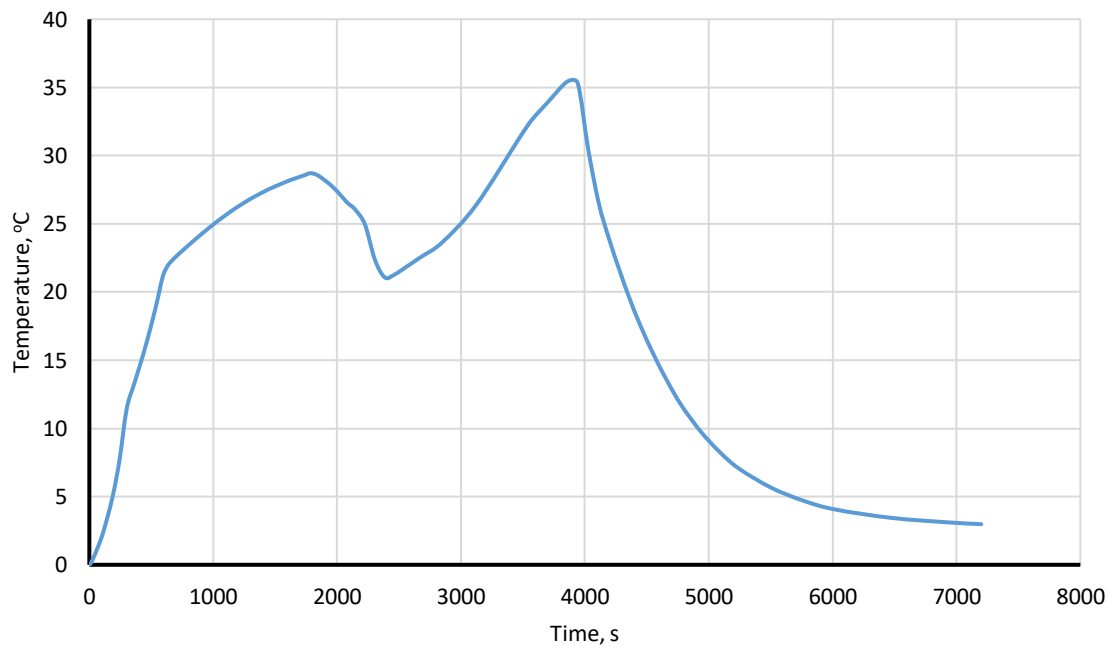


Figure 4-2 Temperature difference between exterior and interior surface of the column for the analysis BS-8X1.5-E119.

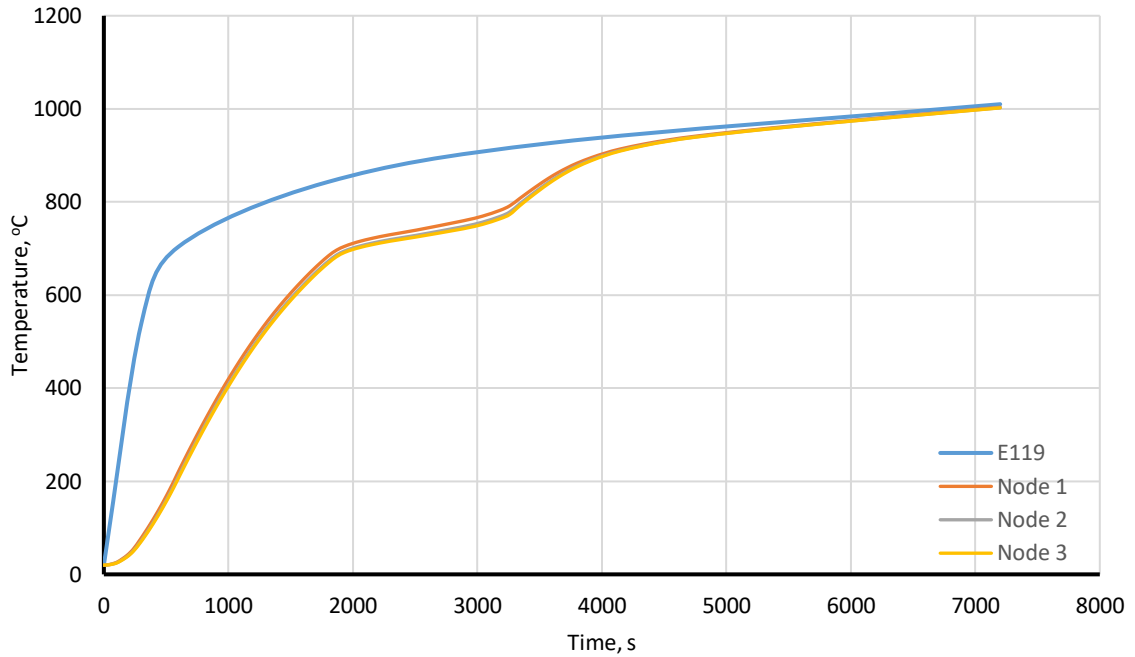


Figure 4-3 Variation in temperature for Nodes 1, 2 and 3 as a function of time for the analysis BS-8X1-E119.

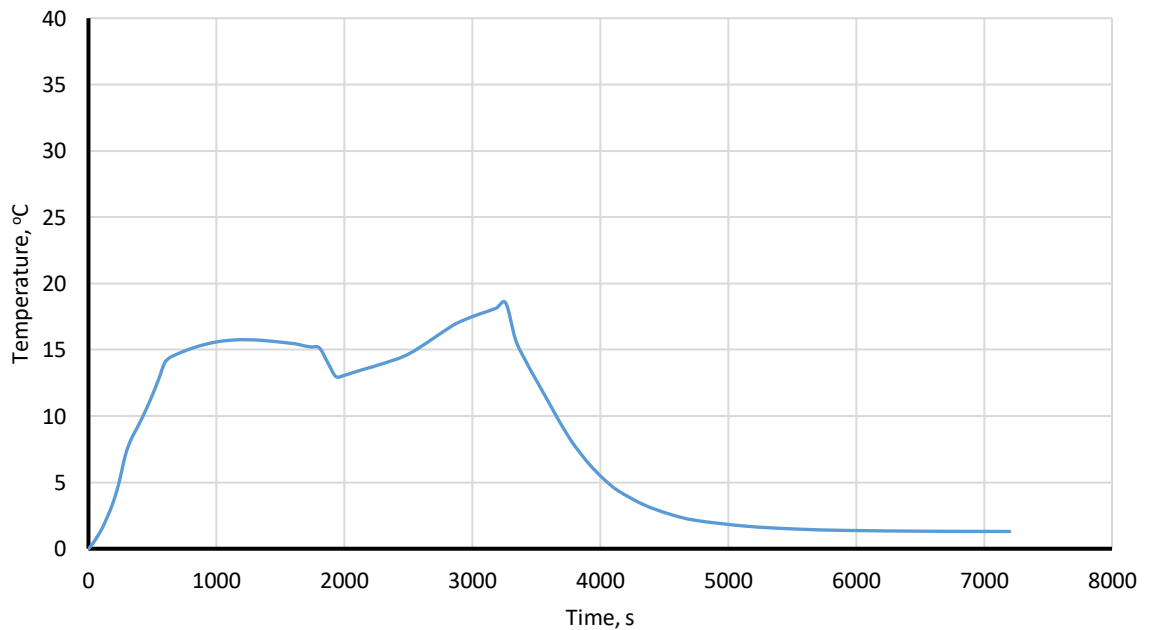


Figure 4-4 Temperature difference between exterior and interior surface of the column for the analysis BS-8X1-E119.

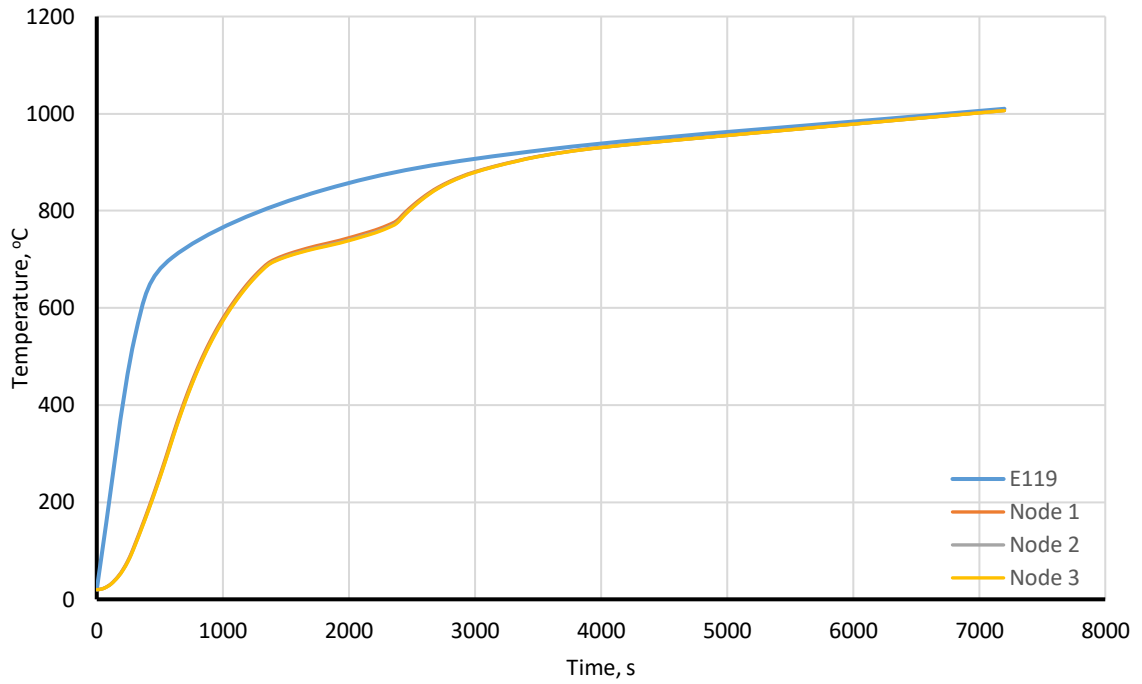


Figure 4-5 Variation in temperature for Nodes 1, 2 and 3 as a function of time for the analysis BS-8X0.5-E119.

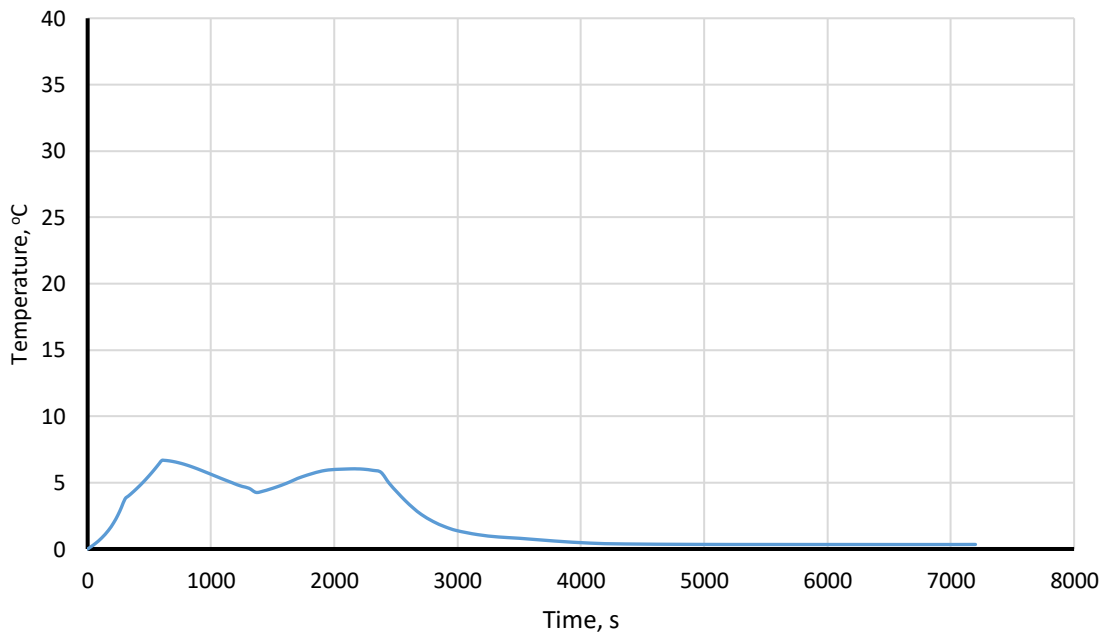


Figure 4-6 Temperature difference between exterior and interior surface of the column for the analysis BS-8X0.5-E119.

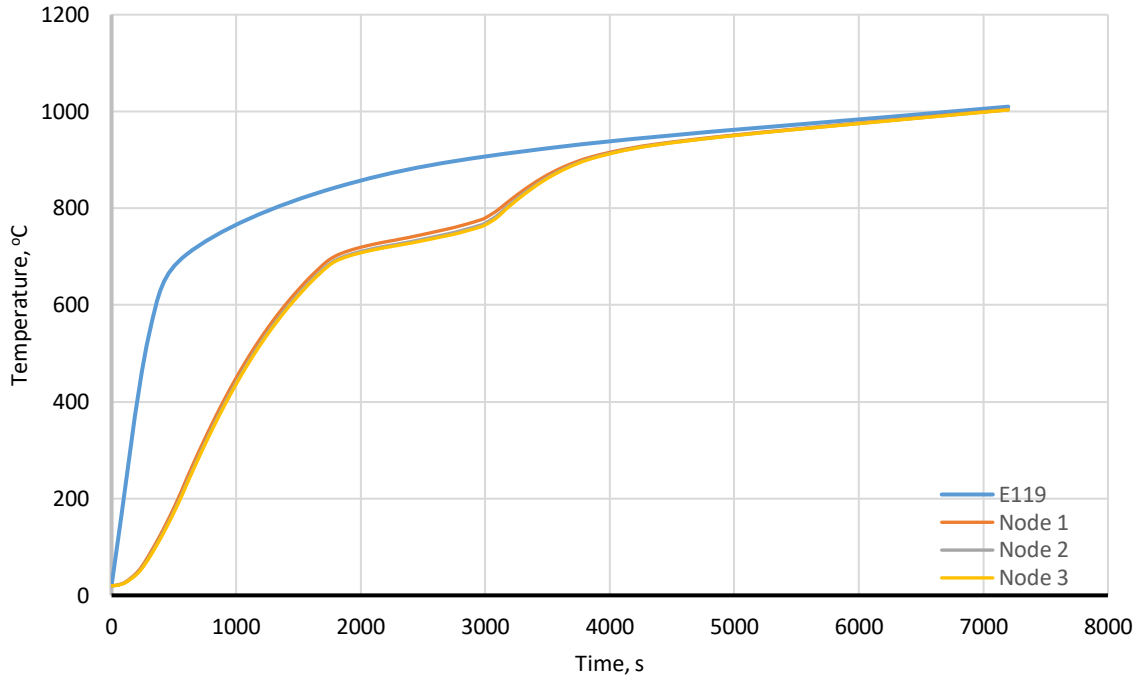


Figure 4-7 Variation in temperature for Nodes 1, 2 and 3 as a function of time for the analysis BS-8xx-E119.

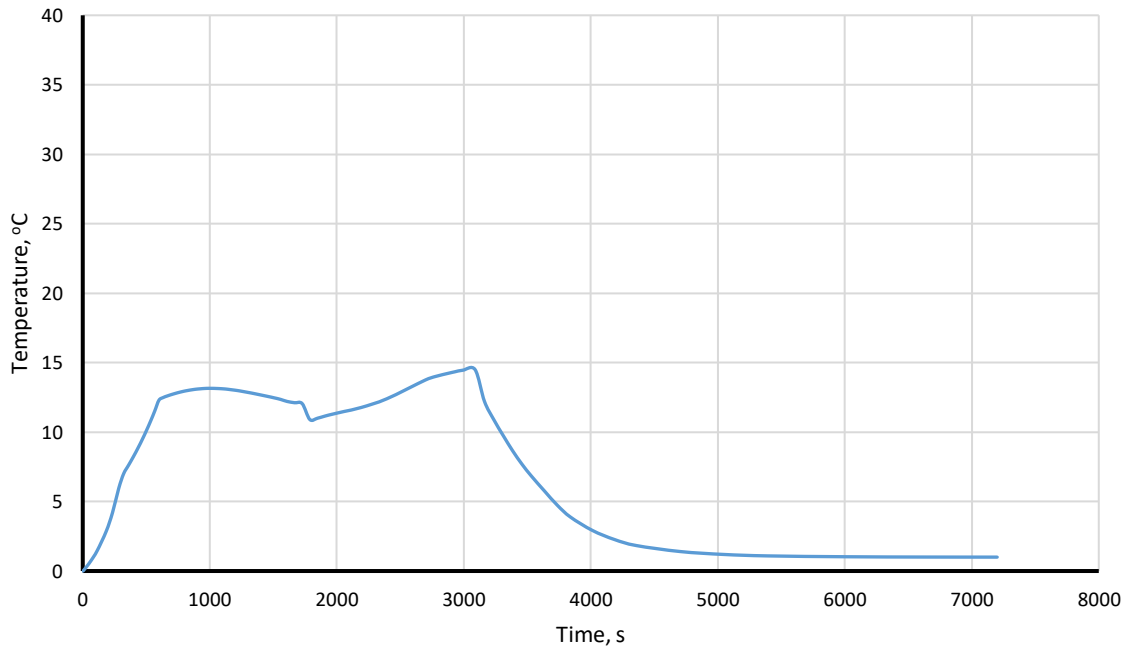


Figure 4-8 Temperature difference between exterior and interior surface of the column for the analysis BS-8xx-E119.

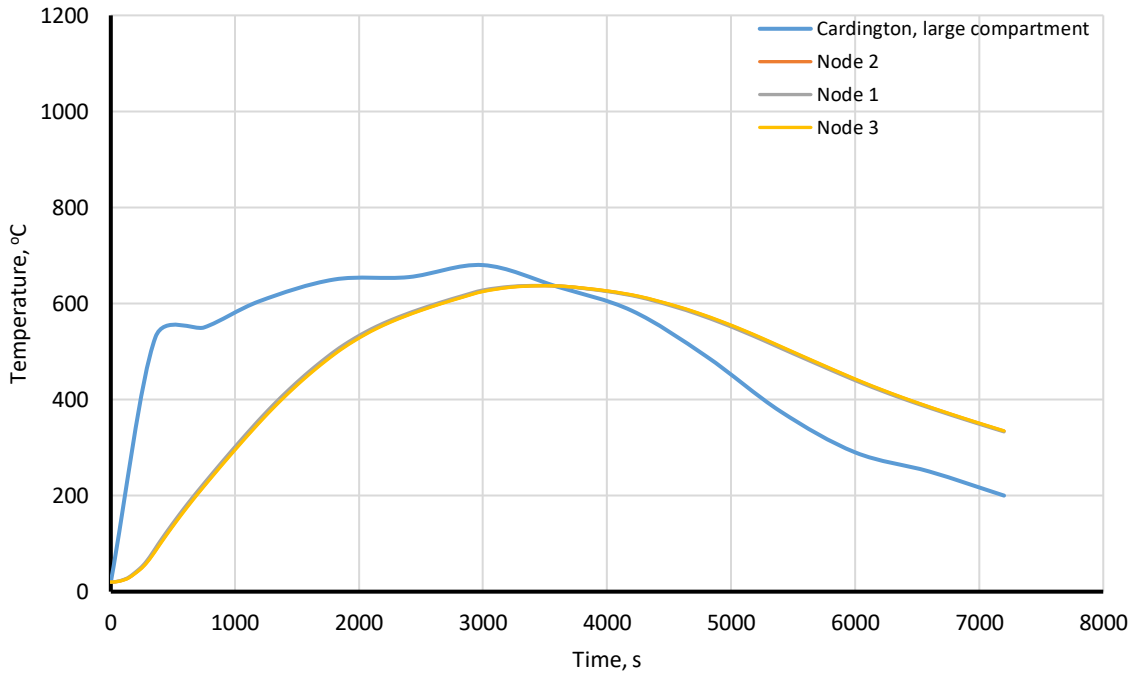


Figure 4-9 Variation in temperature for Nodes 1, 2 and 3 as a function of time for the analysis BS-8xx-LC.

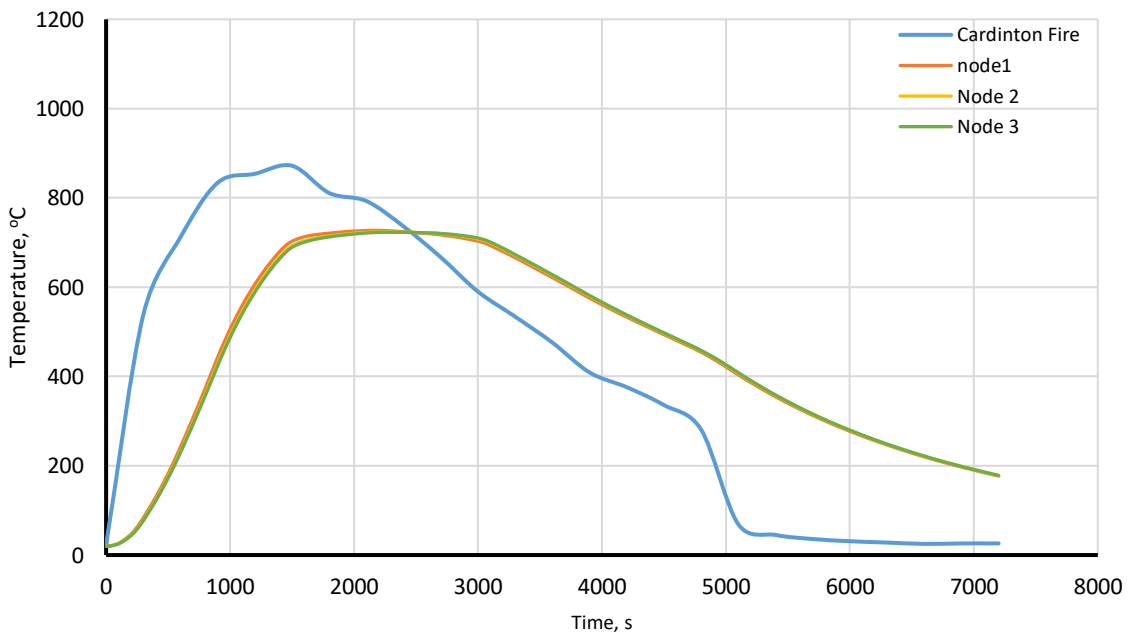


Figure 4-10 Variation in temperature for Nodes 1, 2 and 3 as a function of time for the analysis BS-8xx-SC.

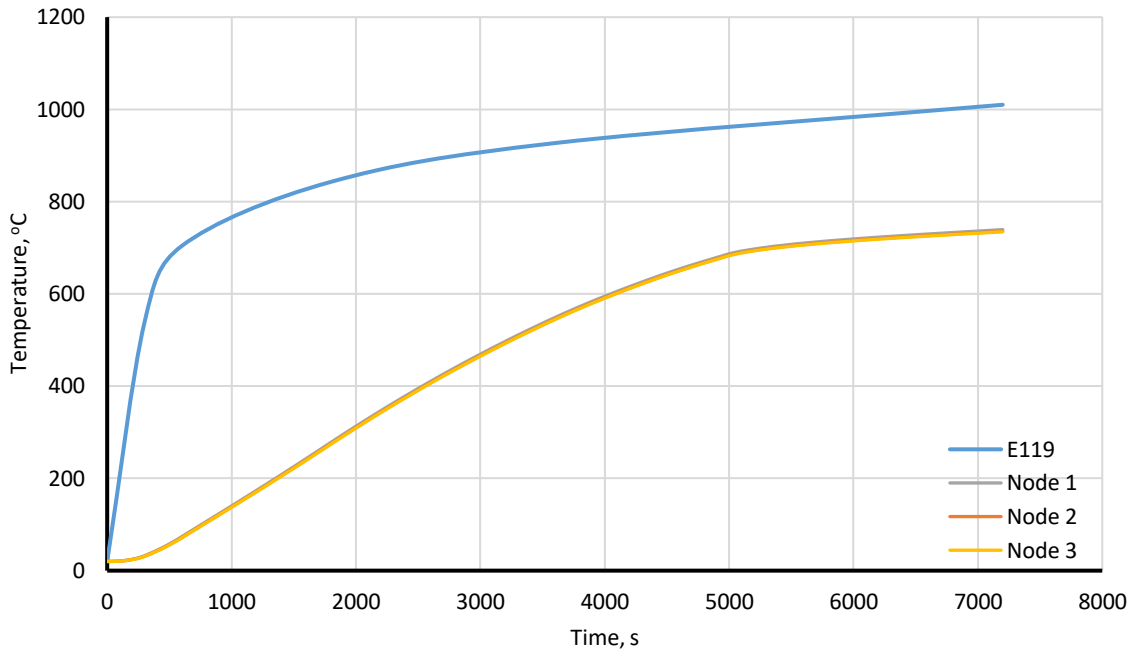


Figure 4-11 Variation in temperature for Nodes 1, 2 and 3 as a function of time for the analysis SFRM1h-8xx-E119.

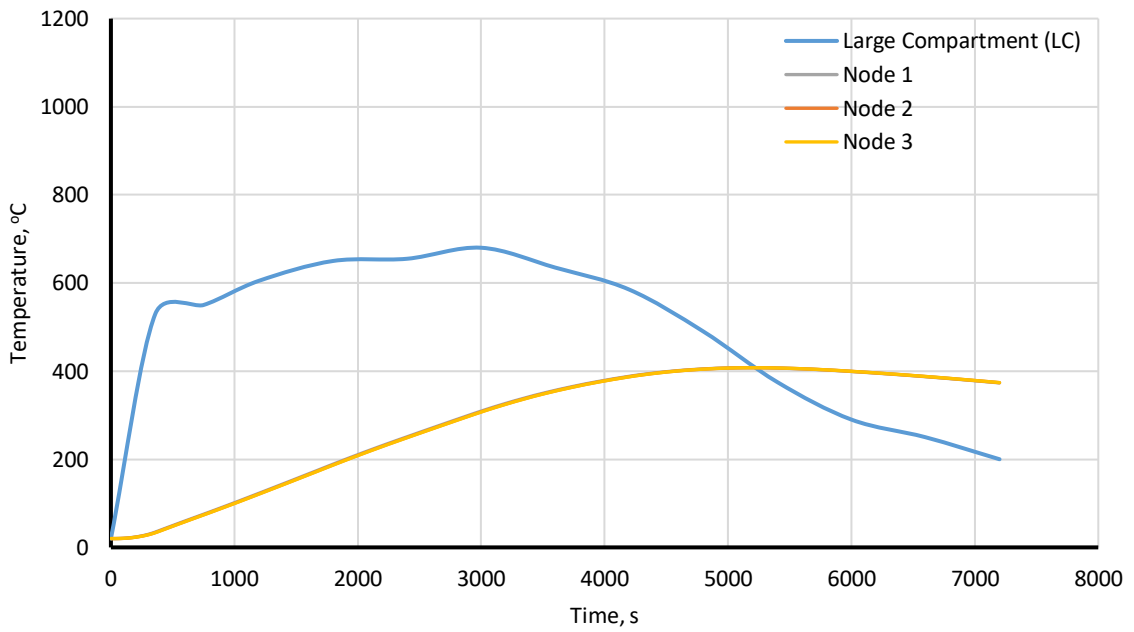


Figure 4-12 Variation in temperature for Nodes 1, 2 and 3 as a function of time for the analysis SFRM1h-8xx-LC.

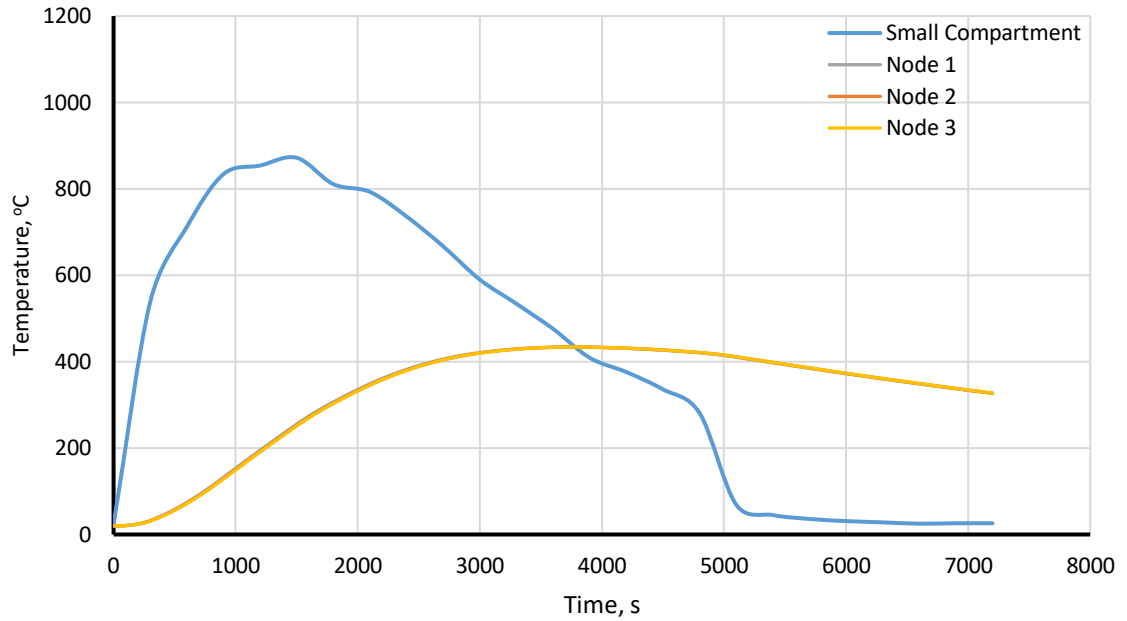


Figure 4-13 Variation in temperature for Nodes 1, 2 and 3 as a function of time for the analysis SFRM1h-8xx-SC.

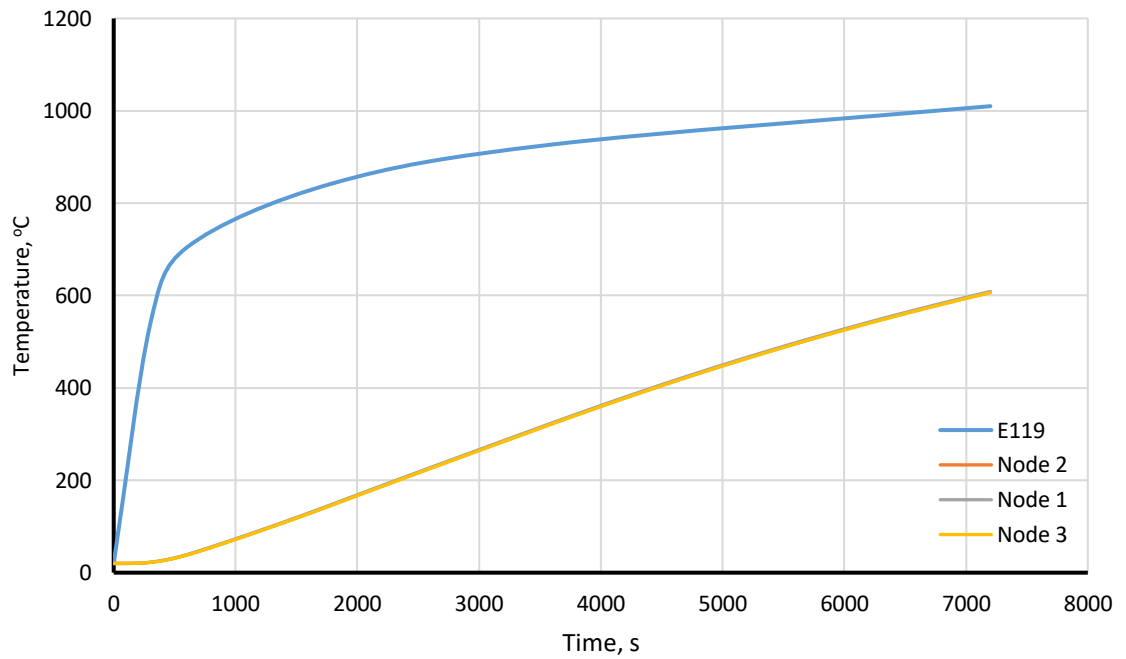


Figure 4-14 Variation in temperature for Nodes 1, 2 and 3 as a function of time for the analysis SFRM2h-8xx-E119.

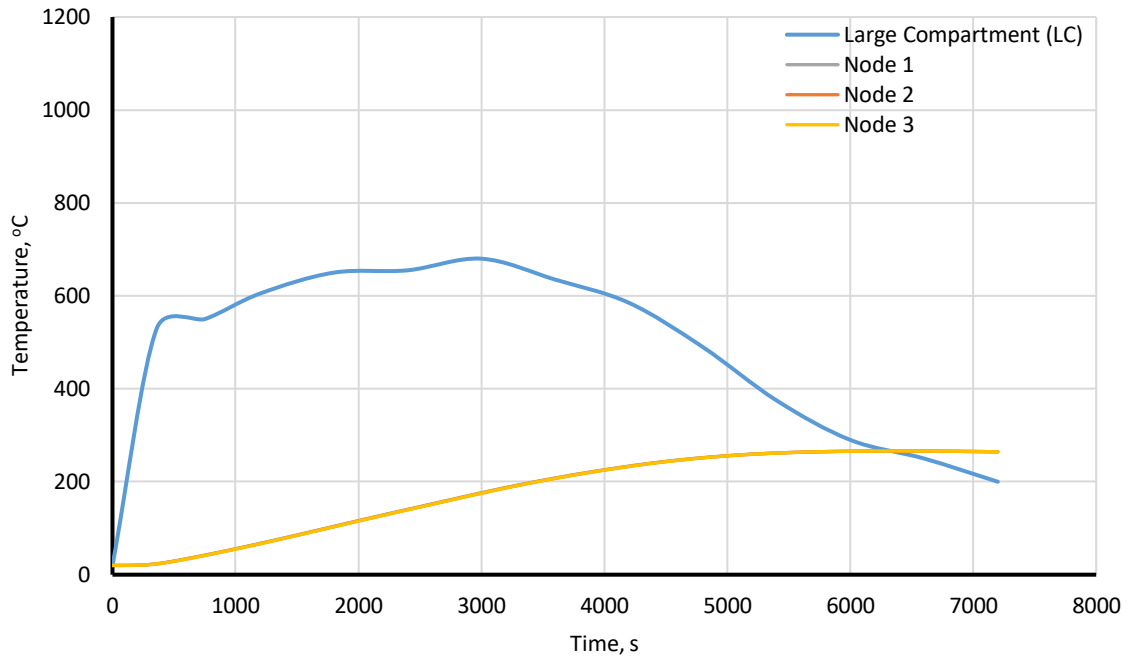


Figure 4-15 Variation in temperature for Nodes 1, 2 and 3 as a function of time for the analysis SFRM1h-8xx-LC.

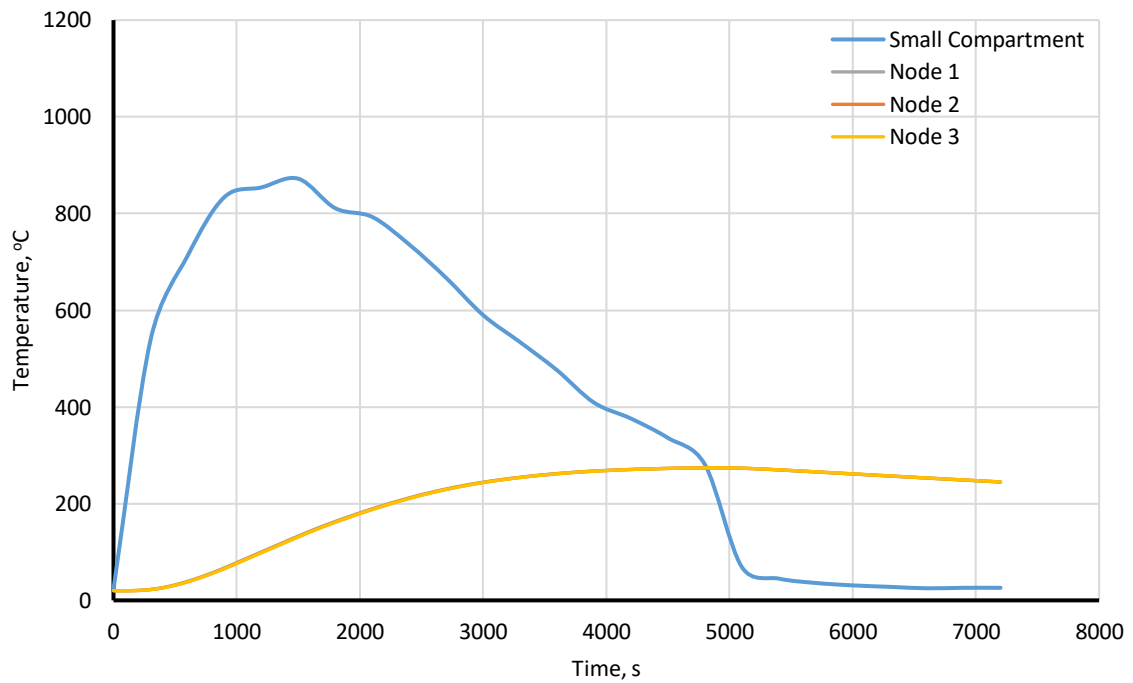


Figure 4-16 Variation in temperature for Nodes 1, 2 and 3 as a function of time for the analysis SFRM1h-8xx-SC.

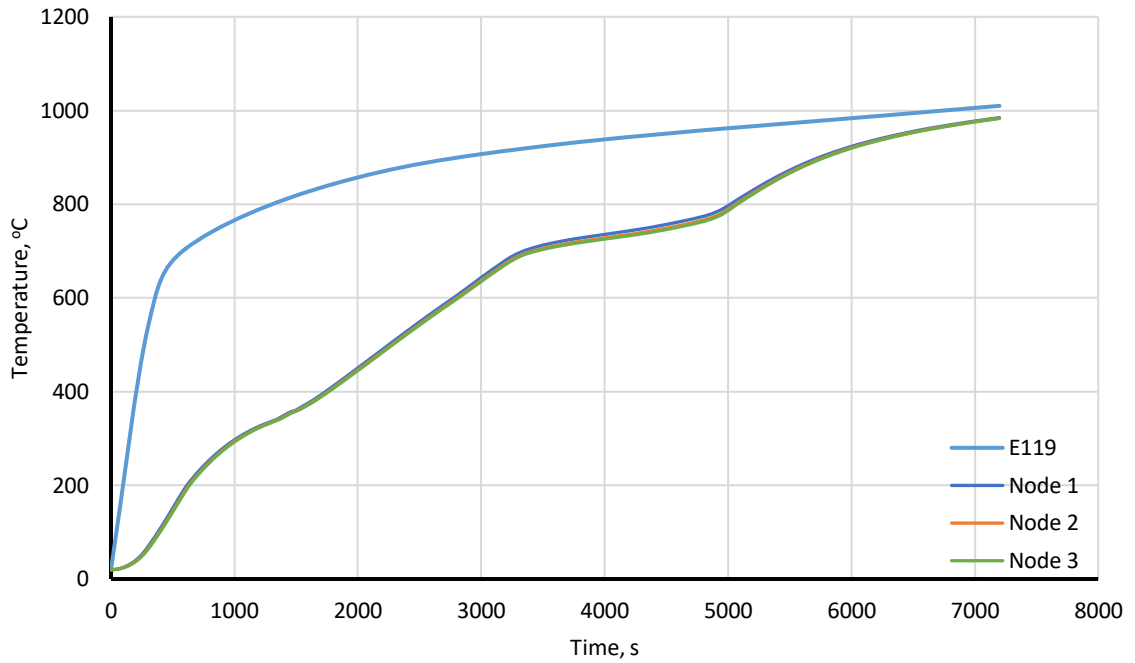


Figure 4-17 Variation in temperature for Nodes 1, 2 and 3 as a function of time for the analysis IP-8xx-E119.

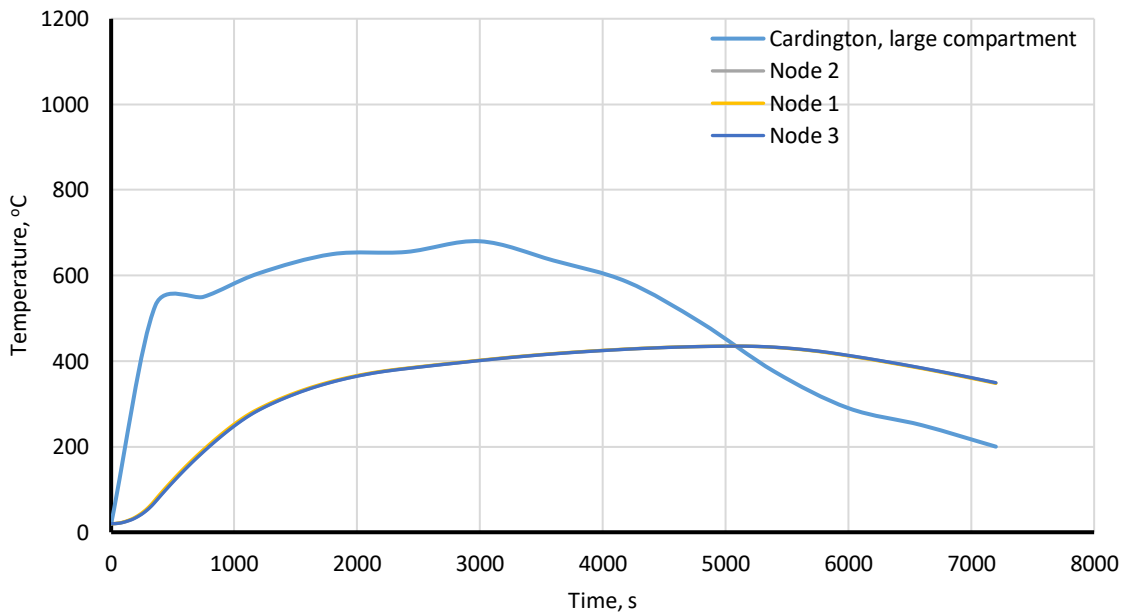


Figure 4-18 Variation in temperature for Nodes 1, 2 and 3 as a function of time for the analysis IP-8xx-LC.

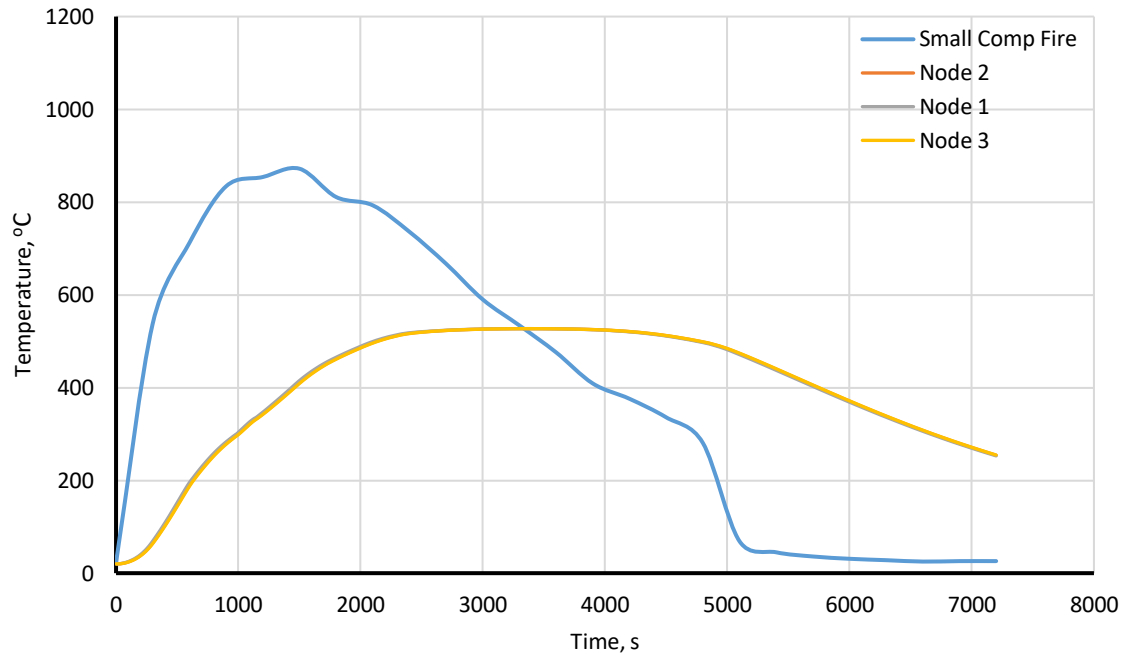


Figure 4-19 Variation in temperature for Nodes 1, 2 and 3 as a function of time for the analysis IP-8xx-SC.

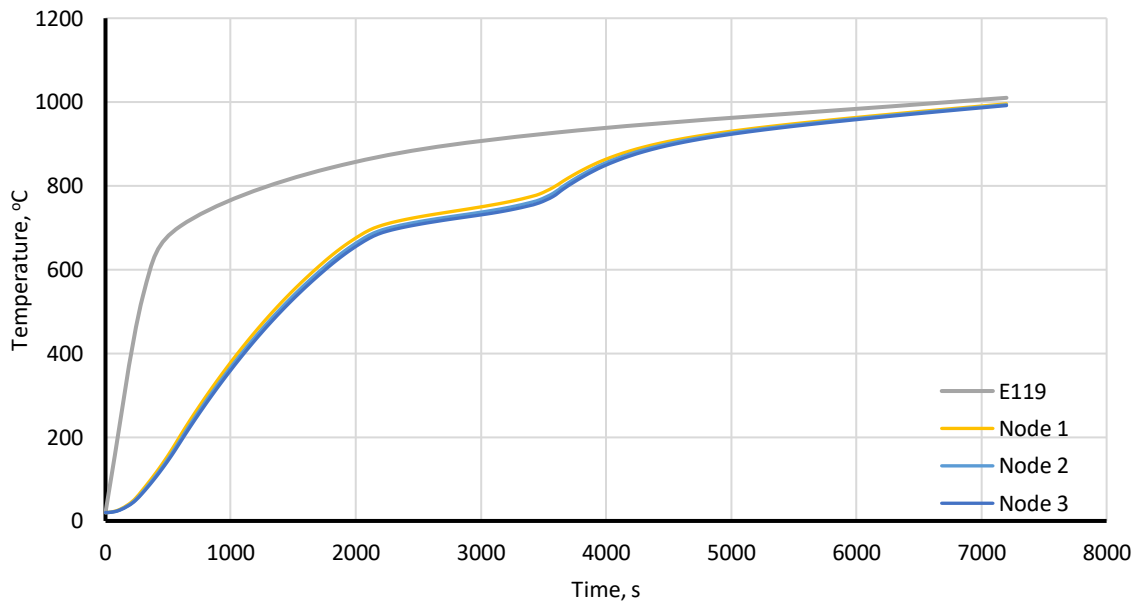


Figure 4-20 Variation in temperature for Nodes 1, 2 and 3 as a function of time for the analysis CF-8xx-E119.

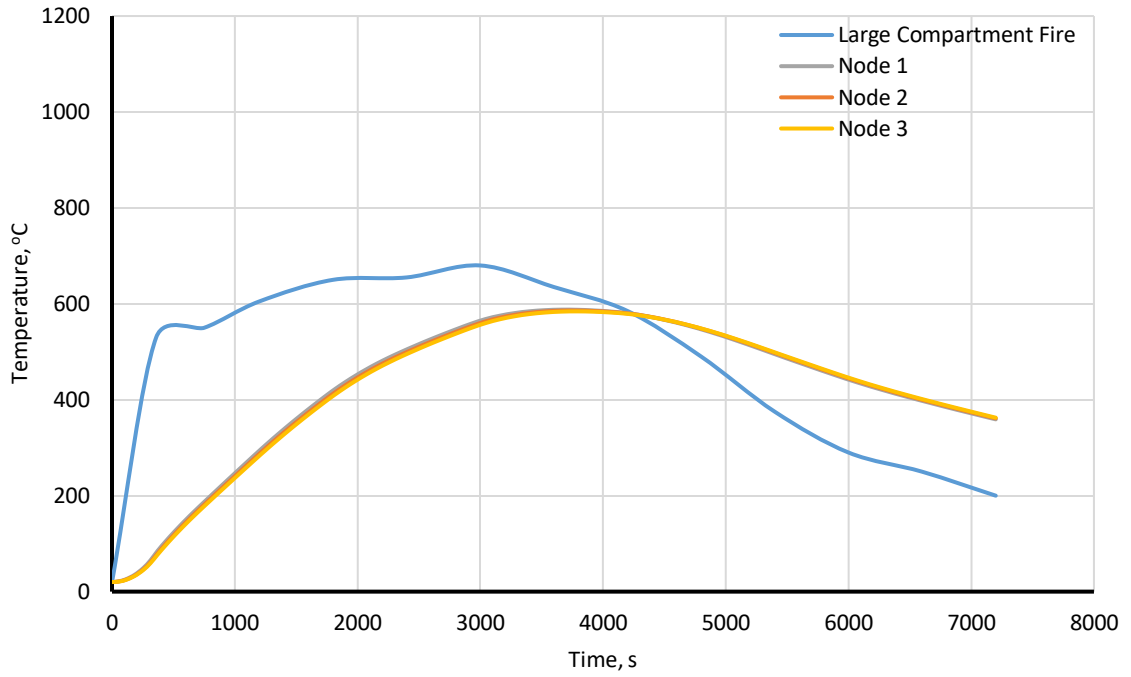


Figure 4-21 Variation in temperature for Nodes 1, 2 and 3 as a function of time for the analysis CF-8xx-LC.

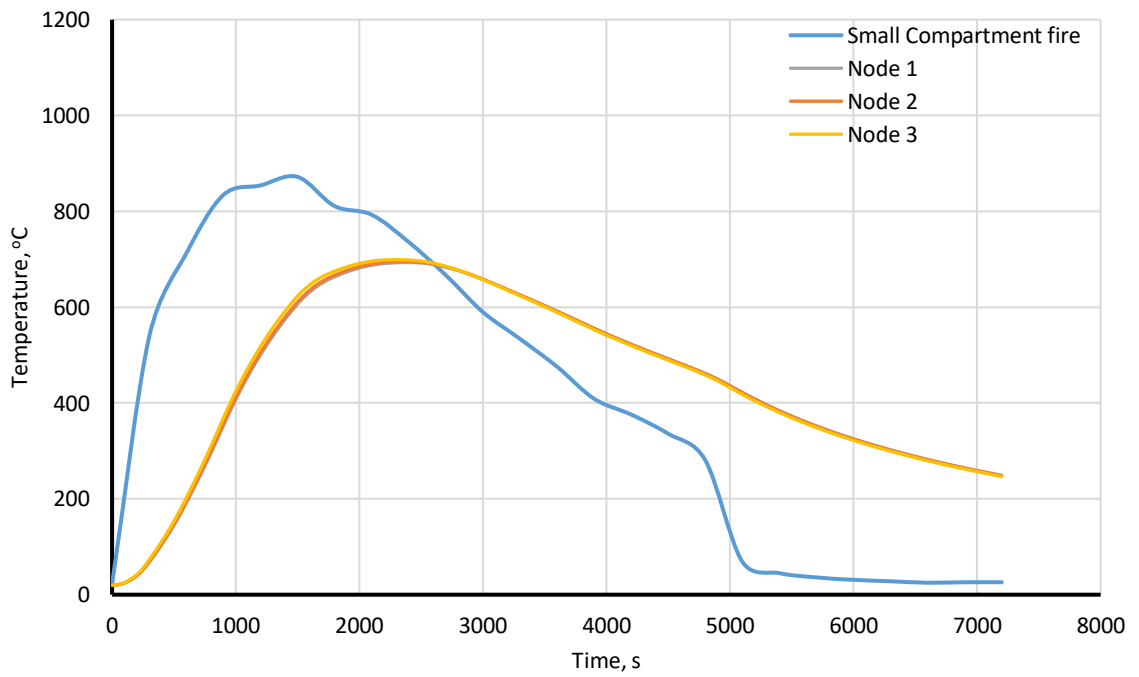


Figure 4-22 Variation in temperature for Nodes 1, 2 and 3 as a function of time for the analysis CF-8xx-SC.

CHAPTER 5

STRENGTH ANALYSIS RESULTS

5.1 Introduction

This chapter presents strength analysis for the analytical models explained in Section 3.3 and listed in Table 3-1. By using the section's temperature results obtained in Chapter 4 and reduction of yield strength and modulus of elasticity as a function of temperature from Table 2-1, the variation in strength of the column cross section during the fire exposure are calculated for each model. Columns are assumed to be short and the second order effects are neglected. The variation in modulus of elasticity calculated in this study can be used for the stability analysis in future works. The specific case of A992 steel with a yield strength of 345 MPa is used for the strength analysis.

5.2 Strength Analysis of Unprotected Steel Columns in E119 Fire

Exposure (Case 1)

Four models are analyzed for the case of an unprotected steel tube sections subject to the E119 fire exposure. Heat transfer analysis of these models were presented in Section 4.2. Referring to the results of heat transfer analysis in chapter 4, the difference between temperatures of Nodes 1, 2 and 3 in each section were insignificant. Therefore, it is assumed that the midsection temperature can represent overall behavior of the column and was used for strength analysis. The plots of variation in strength and modulus of elasticity in this chapter are normalized with respect to their values at normal temperature (f_y , E_0). In addition, the variation in yield strength, modulus of elasticity and yield forces for the duration of 2 hour fire exposure are included in Appendix A of this report for each analysis model.

Figure 5-1 shows variation in yield strength (F) and modulus of elasticity (E) for 8x1.5 steel tube under the E119 fire exposure for two hours. As shown in the figure, the section yield strength values converges to zero near the end of the fire in all analyses. The ratio of yield strength reaches 6.3% and 2.5% of their value at normal temperature after 1-h and 2-h fires respectively (Table A.1).

Figure 5-2 shows variation of yield strength and modulus of elasticity for 8x1 steel tube under the E119 fire exposure. Despite the half-inch decrease in wall thickness of the section, results obtained are very similar to Figure 5-1 for 8x1.5 tube, but with slightly smaller values. Yield strength of this section reaches 4.4% and 2.5% after 1-h and 2-h of fire exposure (Table A.2).

Figure 5-3 and Figure 5-4 display yield strength and modulus of elasticity for 8xx and 8x0.5 tubes under E119 fire respectively. For these sections, slightly lower yield strengths are achieved due to higher temperatures caused by their smaller wall thicknesses. For the 8xx tube, yield strength reaches 4.0% and 2.5% of their values at normal temperature after 1-h and 2-h of the fire (Table A.3). Moreover, for the 8x0.5 tube, yield strength of the section reduces to 3.5% and 2.4% of their original values after 1-h and 2-h of the E119 fire (Table A.4). Since temperature of steel converges to E119 fire in all tube sections, the reduced yield strength after 2 hours are similar for all column sizes (%2.5).

5.3 Strength of Unprotected 8xx Section in Real Fire Exposures (Case 2)

Strength analysis is performed on an 8xx steel tube section under the large and small compartment fire exposures to investigate their effects on the strength of this column. The heat transfer analyses for the unprotected 8xx tube section in real fires was presented in Section 4.3.

Figure 5-5 shows variation of yield strength and modulus of elasticity for 8xx tube section with the application of large compartment fire. The minimum value of yield strength and modulus of elasticity occurs after 1-h and is equal to 14.2% and 24.4% of their values at normal temperature (Table A.5).

Figure 5-6 shows yield strength and modulus of elasticity of 8xx tube as a function of time in small compartment fire exposure. The minimum value of 6.9% and 12.0% of their normal temperature value are recorded after 40 minutes for yield strength and modulus of elasticity respectively (Table A.6).

5.4 Strength of Columns with SFRM as Thermal Insulation (Case 3)

Two cases of 1-h and 2-h fire rating thickness are considered for study in the following subcases. Thermal analysis of this case was presented in Sections 4.4.1 and 4.4.2 for three fire scenarios.

5.4.1 1-h Fire Rating Thick SFRM

Figure 5-7 and Table A.7 show variation in yield strength and modulus of elasticity of an 8xx steel tube with 1-h fire rating thick SFRM (6.4 mm) in E119 fire exposure. The yield strength and modulus of elasticity reach to their minimum values of 6.6% and 11.6% after 2 hours of fire. The values of yield strength and modulus of elasticity reduces to 27.8% and 46.8% of their value at normal temperature after 1-h of fire exposure.

The same section is analyzed in real fire exposures for small and large compartments. Figure 5-8 and Table A.8 show yield strength and modulus of elasticity as a function of time for this section in a large compartment fire. Minimum values of 41.6% and 69.3% were obtained after 90 minutes of the fire for yield strength and modulus of elasticity of the cross section.

Figure 5-9 and Table 5.9 show variation in yield strength and modulus of elasticity caused by the small compartment fire. The minimum values of yield strength and modulus of elasticity observed are 40.1% and 66.9% of their original values after 70 minutes of burning.

5.4.2 2-h Fire Rating Thick SFRM

Figure 5-10 and Table A.10 shows yield strength and modulus of elasticity values for the 8xx steel tube with 2-h fire rating SFRM under the E119 fire exposure. Minimum values of 17.3% and 29.7% are observed at the end of the fire. The reduction in section capacity is slow due to the increased thickness of SFRM and its high thermal resistance.

Figure 5-11 and Table A.11 shows yield strength and modulus of elasticity values for this same column section in large compartment fire. The minimum values of 67.9% and 86.3% are achieved after 110 minutes of fire.

When small compartment is applied, yield strength and modulus of elasticity reduced to the minimal values of 66.3% and 82.6% after 80 minutes of fire. These results are shown in Figure 5-12 and Table A.12

5.5 Strength of Intumescent Paint Insulated Columns (Case 4)

To evaluate impacts of adding intumescent paint to the column as thermal insulation on its strength response, one layer of intumescent paint is modeled to an 8xx steel tube (Figure 3-2). Heat transfer analysis of this case was presented in Section 4.5.

Figure 5-13 and Table A.13 shows yield strength and modulus of elasticity of this section as a function of time in E119 fire exposure. Minimum section's strength is observed

to be after 2 hours of fire (end of E119 fire). The minimum yield strength and modulus of elasticity calculated are 2.7% and 4.8% of their values at normal temperatures.

Figure 5-14 and Table A.14 shows yield strength and modulus of elasticity ratios with respect to their original values in large compartment fire. The minimum values of 40.0% for yield strength and 67.0% for modulus of elasticity were observed after 80 minutes of fire.

The same section under small compartment fire yielded minimum values of 31% and 52.0% for yield strength and modulus of elasticity after 60 minutes of fire. Like temperature, minimum section's strength is lower in small compartment fires than large compartment fires

5.6 Strength of Concrete-Filled Models (Case 5)

In this research, it is assumed that the concrete inside the column does not contribute to the strength of the cross section for the strength analysis. Instead, the purpose of the concrete is to serve as a heat sink to reduce steel temperatures. Thermal analyses for 8xx concrete-filled steel tube columns were presented in Section 4.6.

Figure 5-16 and Table A.16 shows change in yield strength and modulus of elasticity for this column section as a function of time in E119 fire exposure. The minimum values of 2.6% and 4.6% for yield strength and modulus of elasticity are achieved after 2-h of fire is passed.

Figure 5-17 and Table A.17 shows material properties for this section in large compartment fire exposure. Minimum values of 41.6% and 69.3% was achieved after 90 minutes of burning. Figure 5-18 and Table A.18 shows variation in yield strength and

modulus of elasticity for the same cross section under the small compartment fire exposure. Minimum values of 40.1% and 66.9% has been achieved after 70 minutes of burning.

5.7 Summary

The purpose of this chapter was to study reduction in strength for the unprotected and fire protected circular hollow steel sections under E119 and real fires in large and small compartments. The following are highlights of the findings for this chapter.

The strength of unprotected steel sections drops significantly during the first 30 minutes of fire and can cause structural collapse if column members are not designed conservatively. The increase in column's cross section size small effect on the reduction in yield strength of the section. The members bearing force increases mainly due to the increase in cross sectional area of the column, not the preservation of the strength of material due to the reduction in temperature.

ASTM E119 is a most severe fire scenario on a structural member. Section's strength continuously drops and reaches to its minimal value after two hours (end of the fire). In real fires, strength of these models reaches a minimal value when the temperature of the section reaches to its maximum. After the fire temperature start to drop, strength of these sections begin to increase as the column loses its heat energy back to the environment. When the cross section is exposed to the small compartment fire, the strength of the section reaches to its minimum value sooner in comparison to the large compartment fir exposures.

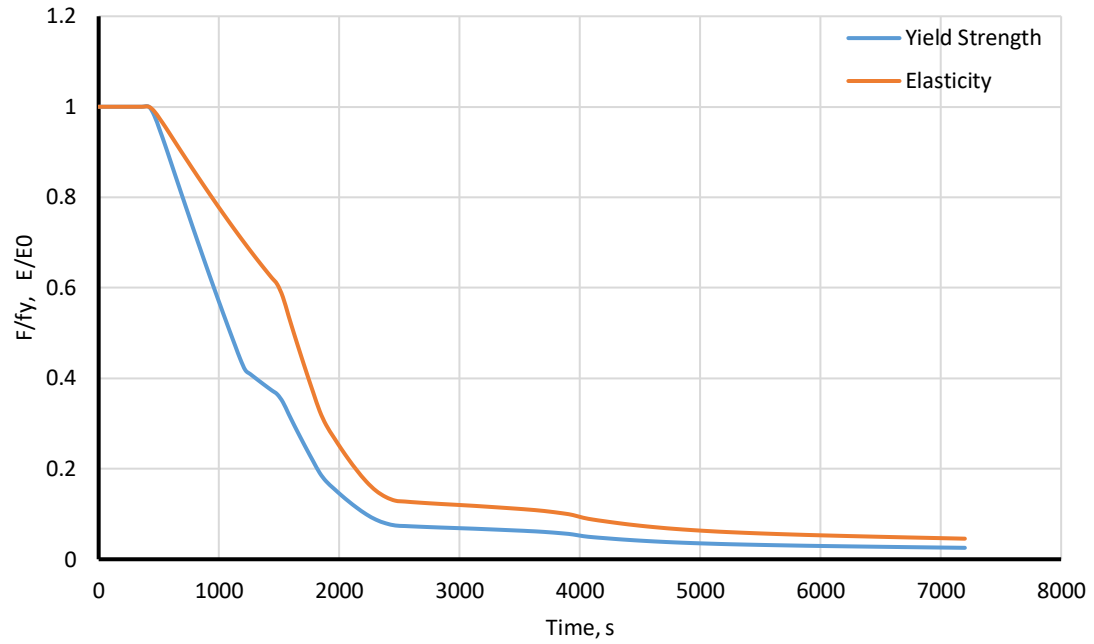


Figure 5-1 Variation in yield strength and modulus of elasticity for the model BS-8X1.5-E119.

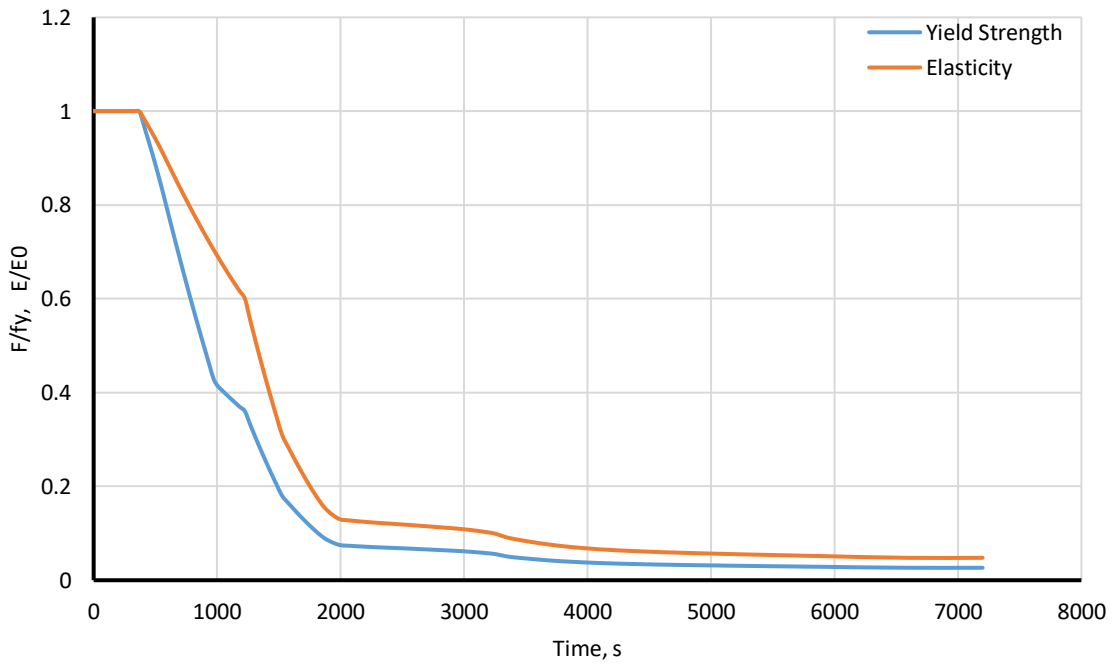


Figure 5-2 Variation in yield strength and modulus of elasticity for the model BS-8X1-E119.

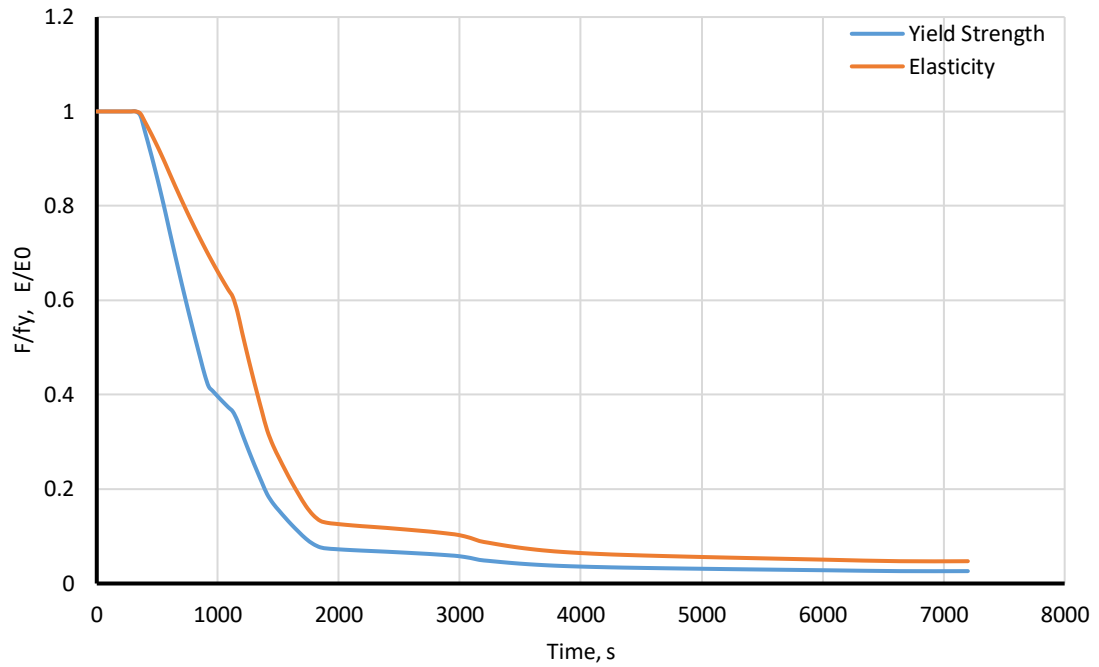


Figure 5-3 Variation in yield strength and modulus of elasticity for the model BS-8xx-E119.

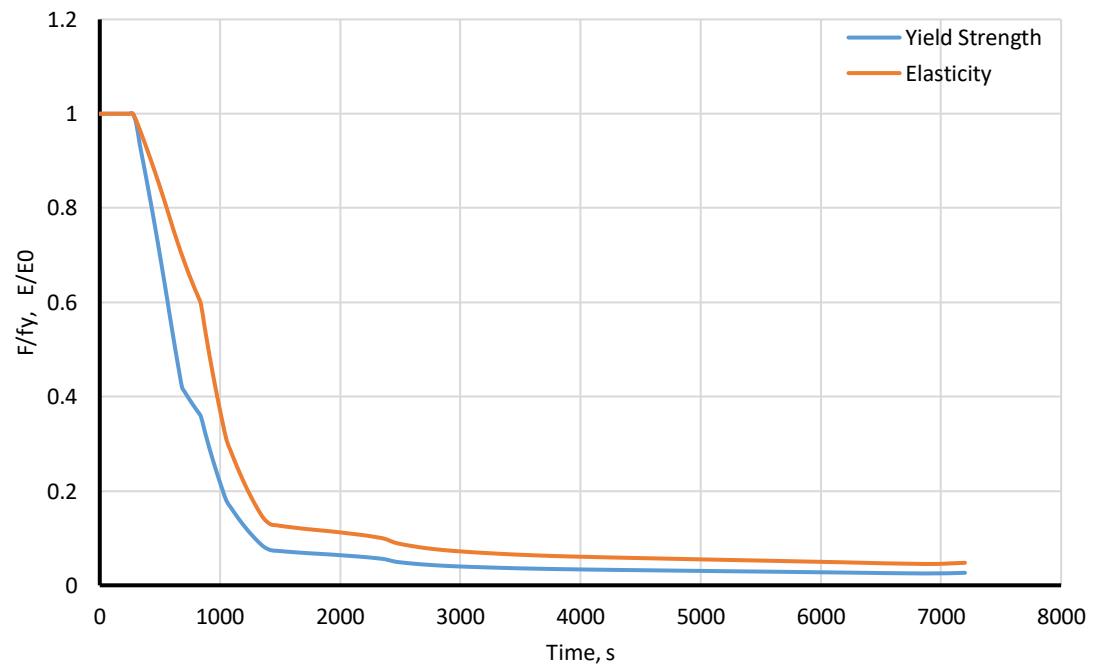


Figure 5-4 Variation in yield strength and modulus of elasticity for the model BS-8X0.5-E119.

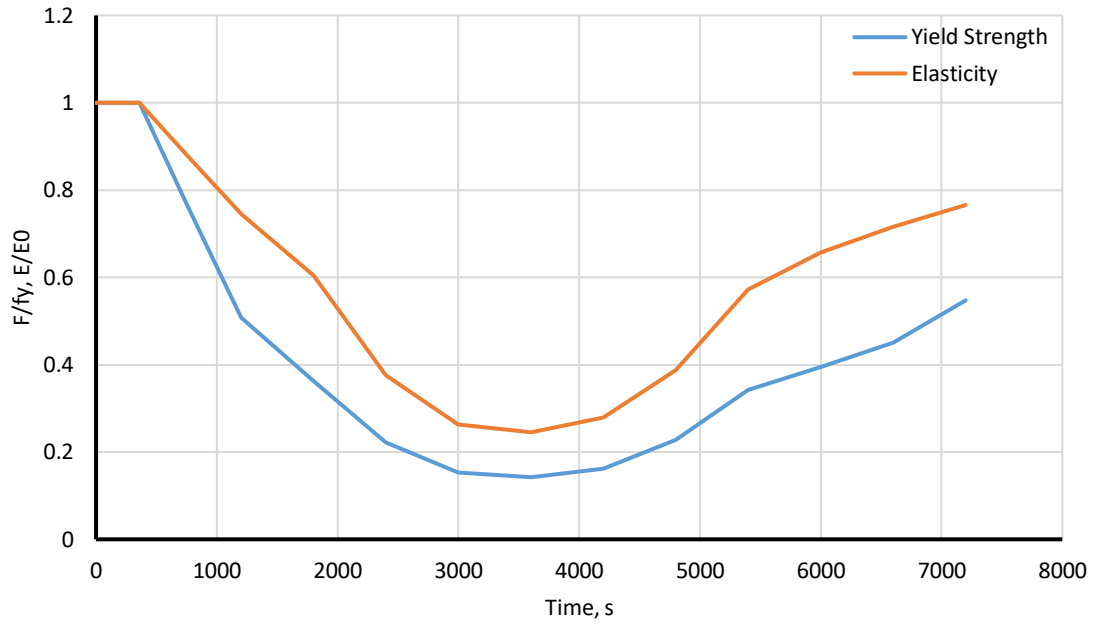


Figure 5-5 Variation in yield strength and modulus of elasticity for the model BS-8xx-LC.

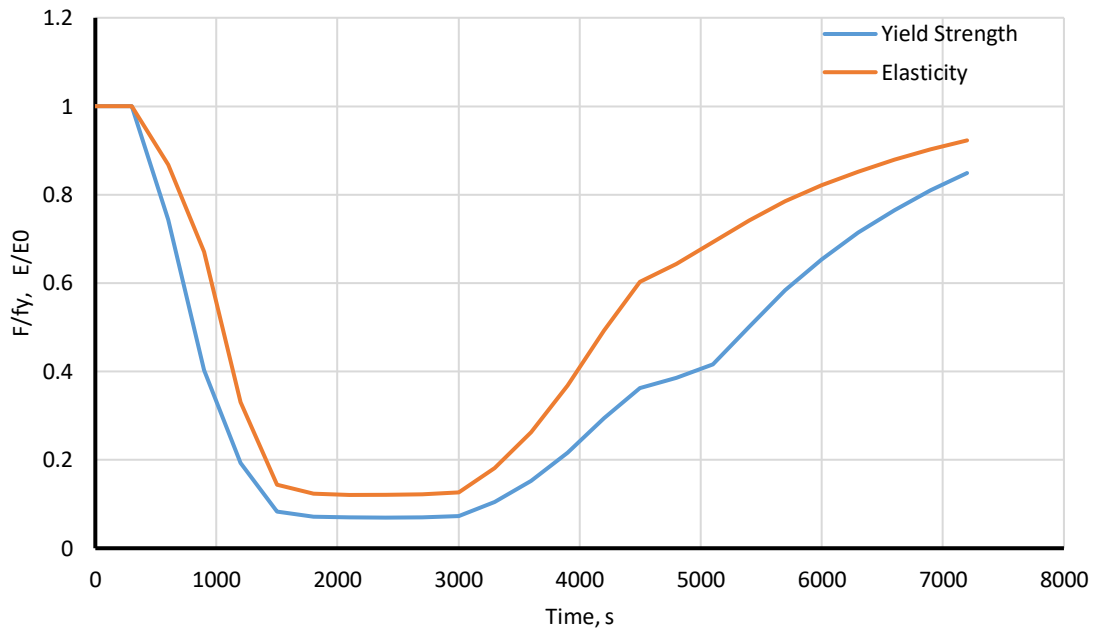


Figure 5-6 Variation in yield strength and modulus of elasticity for the model BS-8xx-SC.

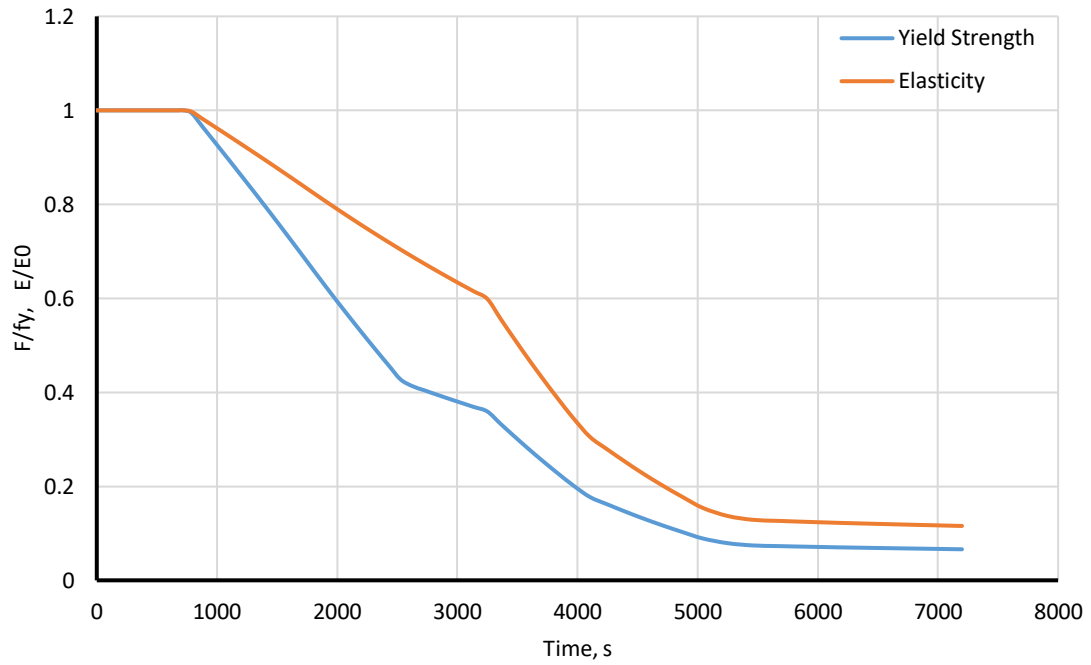


Figure 5-7 Variation in yield strength and modulus of elasticity for the model SFRM1h-8xx-E119.

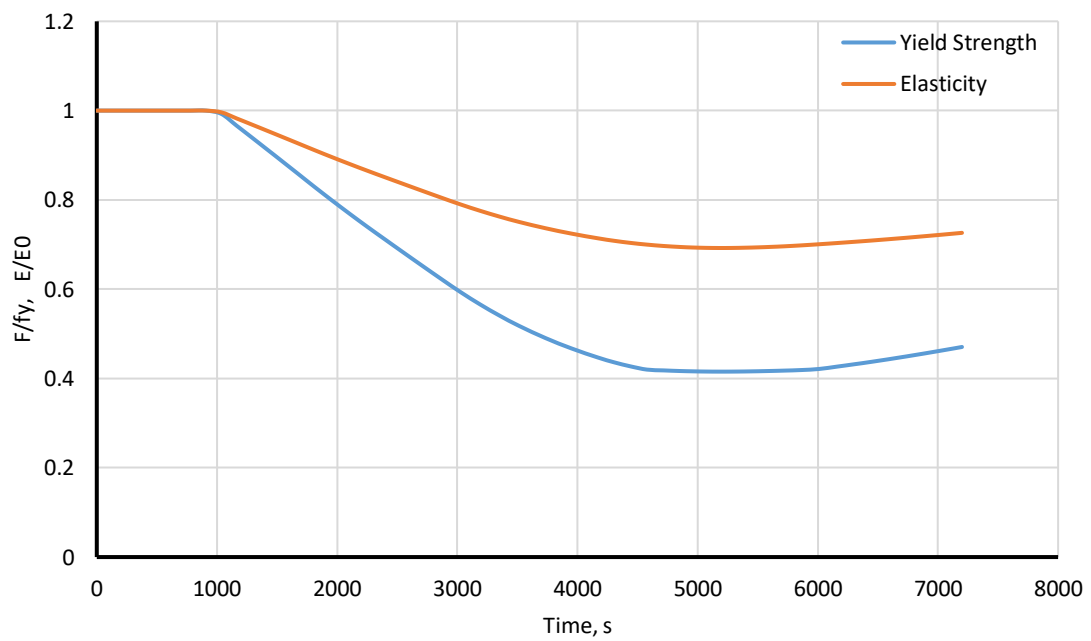


Figure 5-8 Variation in yield strength and modulus of elasticity for the model SFRM1h-8xx-LC.

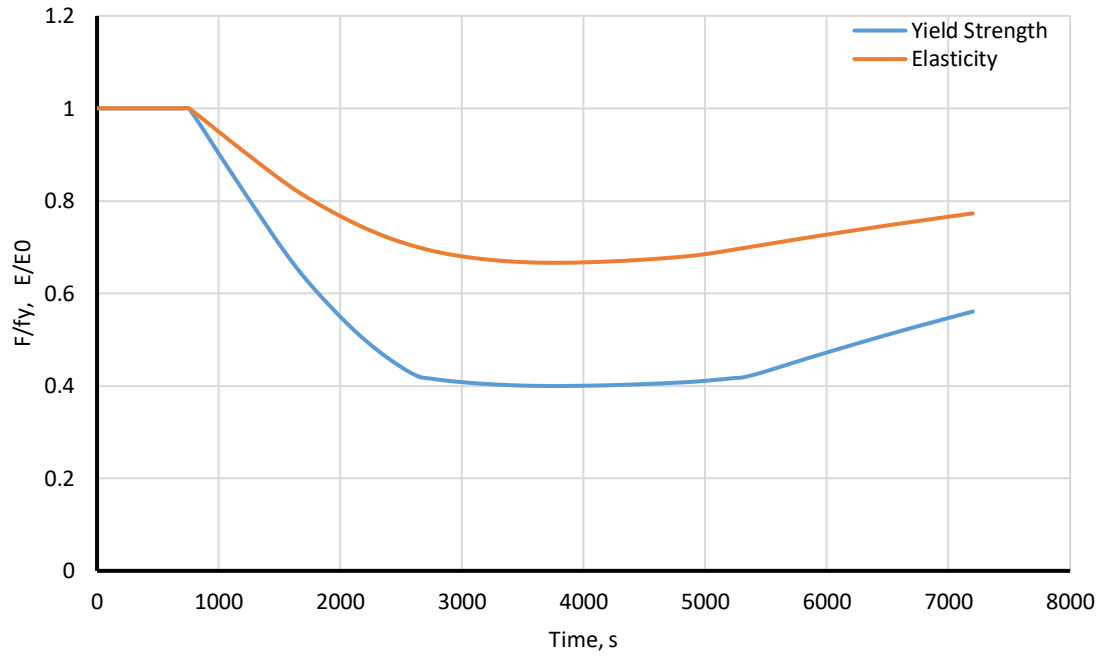


Figure 5-9 Variation in yield strength and modulus of elasticity for the model SFRM1h-8xx-SC.

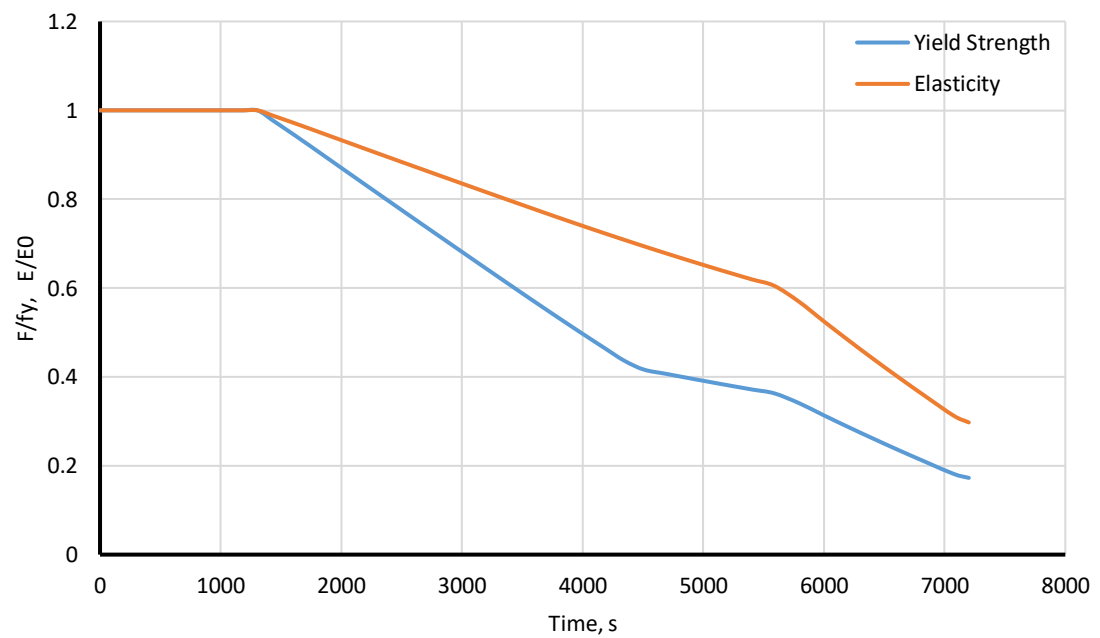


Figure 5-10 Variation in yield strength and modulus of elasticity for the model SFRM2h-8xx-E119.

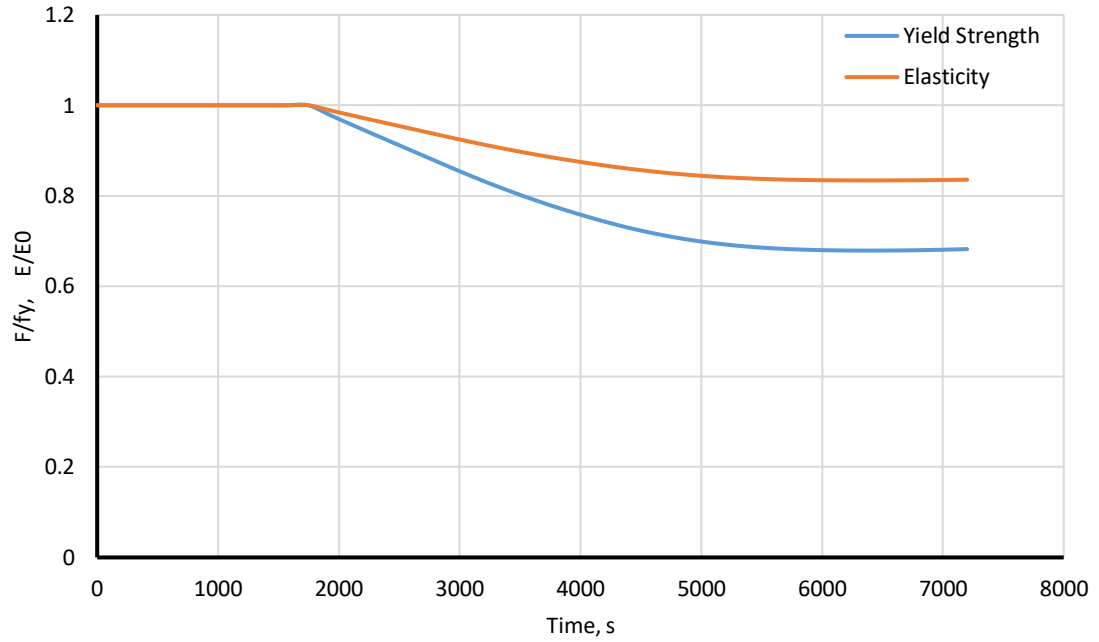


Figure 5-11 Variation in yield strength and modulus of elasticity for the model SFRM2h-8xx-LC.

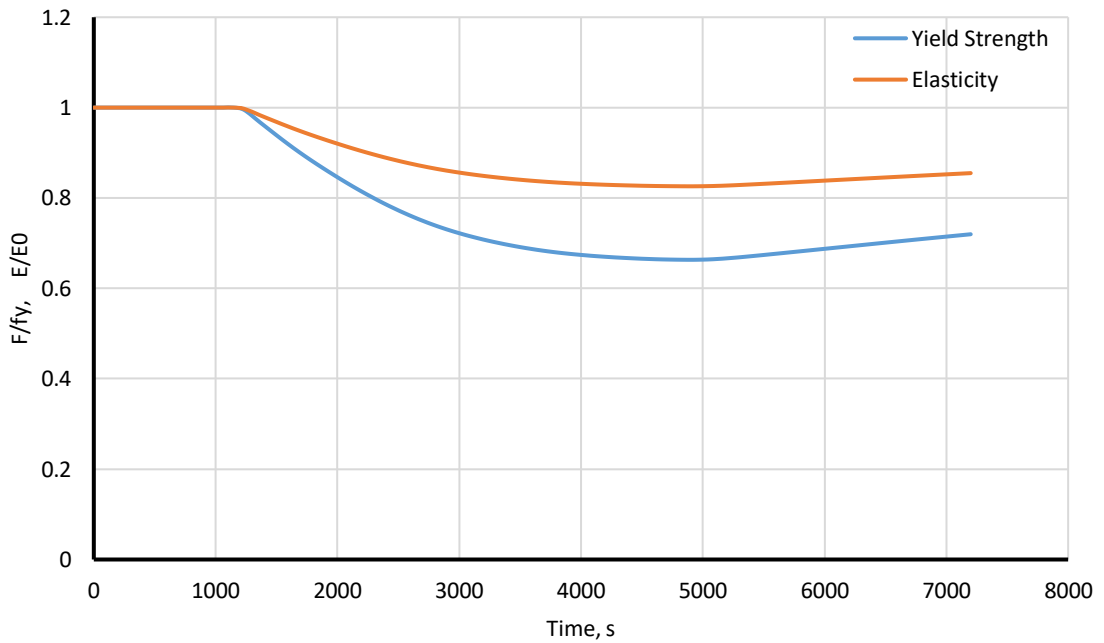


Figure 5-12 Variation in yield strength and modulus of elasticity for the model SFRM2h-8xx-SC.

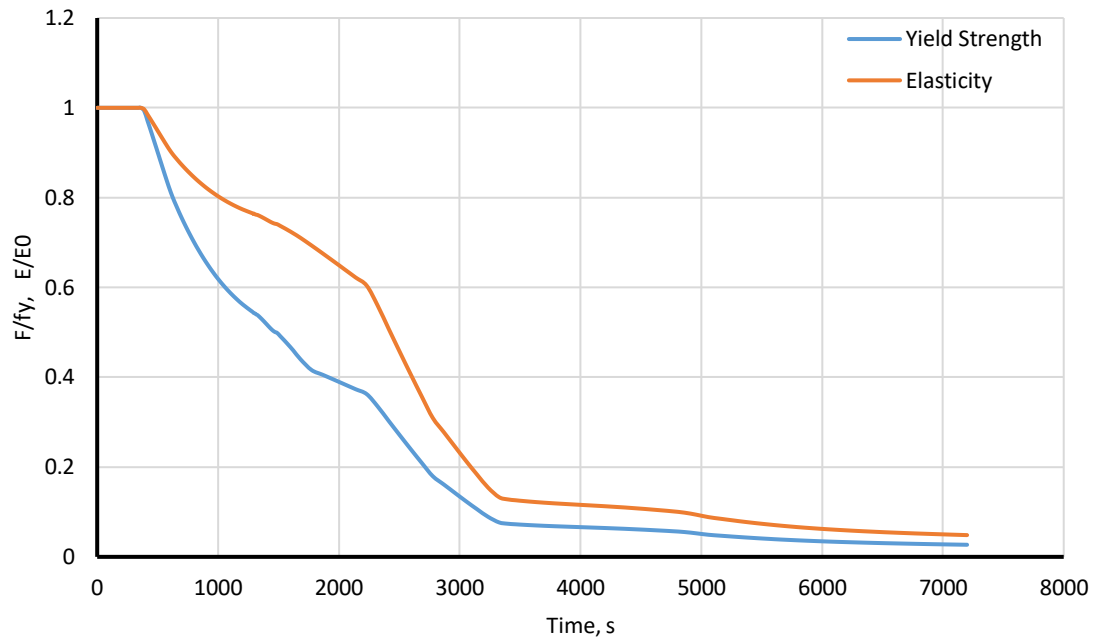


Figure 5-13 Variation in yield strength and modulus of elasticity for the model IP-8xx-E119.

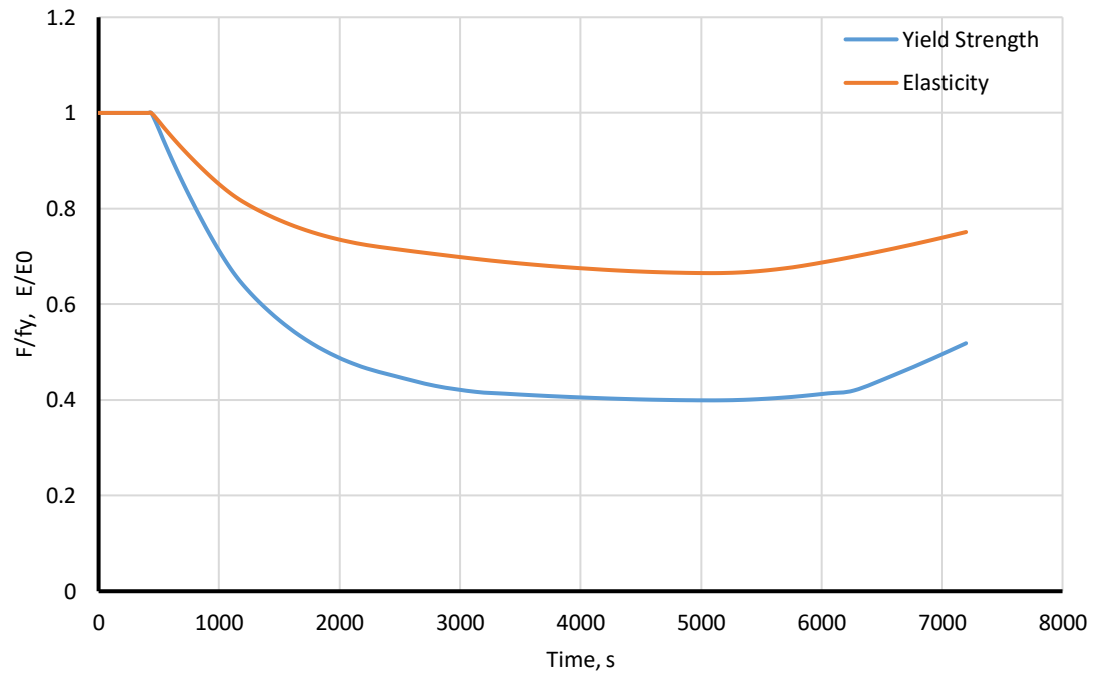


Figure 5-14 Variation in yield strength and modulus of elasticity for the model IP-8xx-LC.

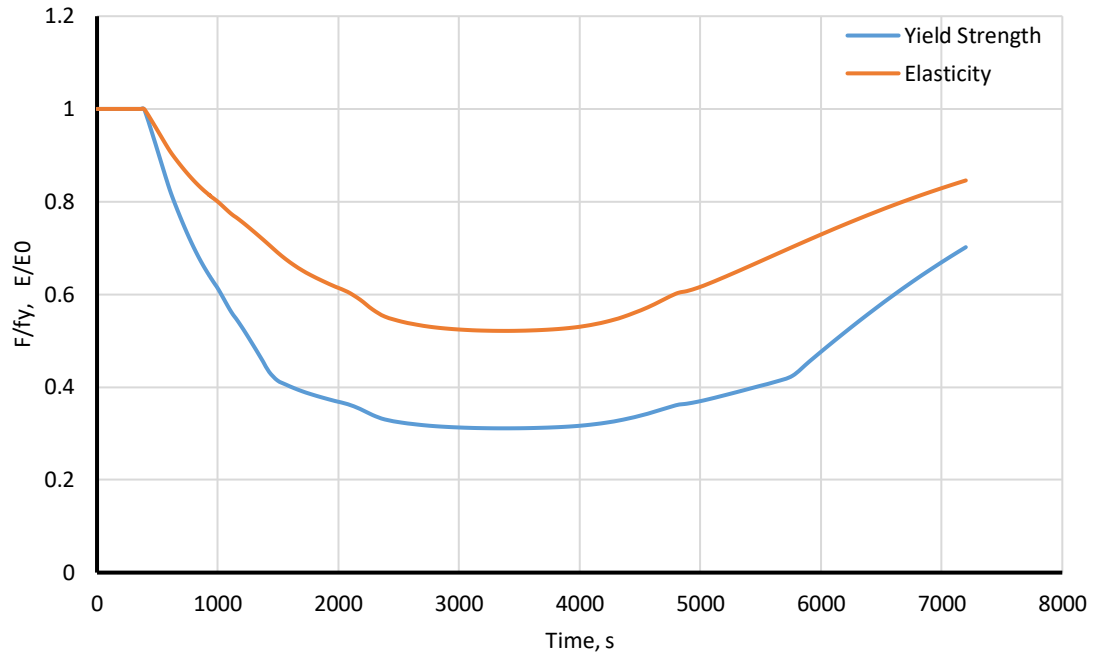


Figure 5-15 Variation in yield strength and modulus of elasticity for the model IP-8xx-SC.

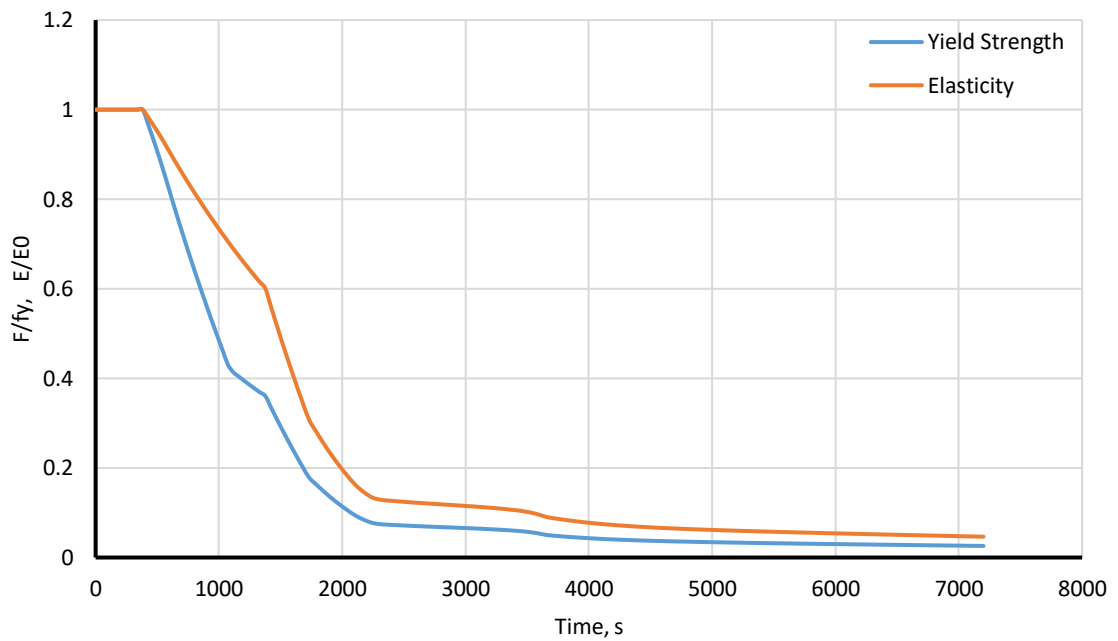


Figure 5-16 Variation in yield strength and modulus of elasticity for the model CF-8xx-E119.

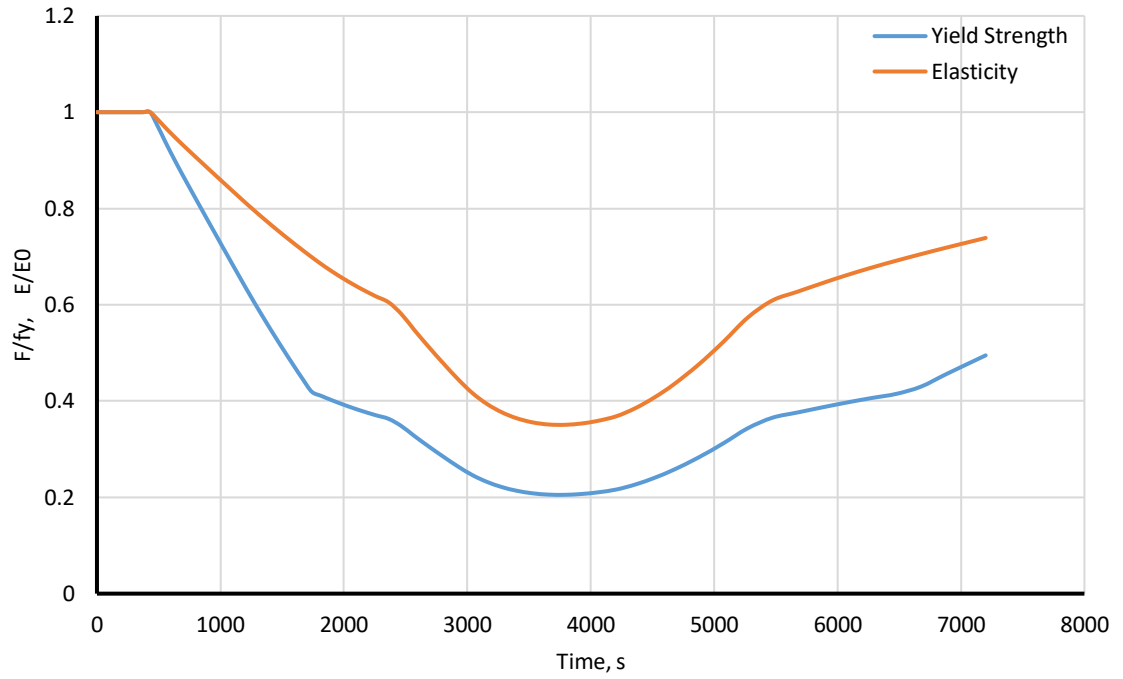


Figure 5-17 Variation in yield strength and modulus of elasticity for the model CF-8xx-LC.

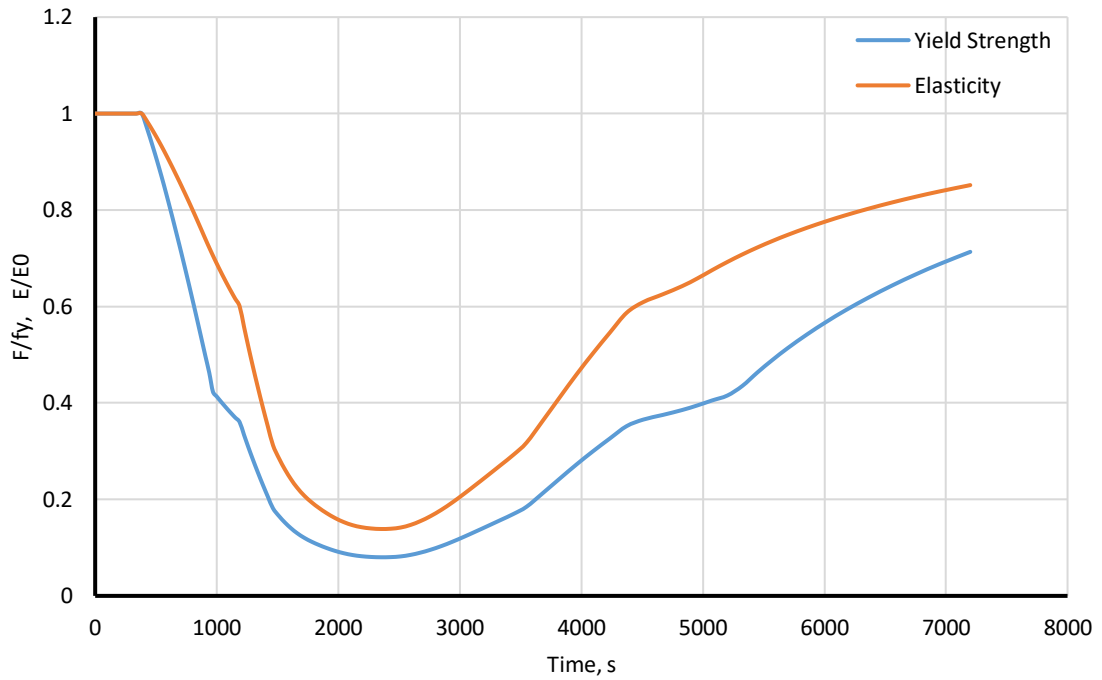


Figure 5-18 Variation in yield strength and modulus of elasticity for the model CF-8xx-SC.

CHAPTER 6

RESULTS COMPARSION AND DISCUSSION

6.1 Introduction

This chapter presents discussion and comparison of the results obtained in Chapters 4 and 5 for the thermal and strength analysis of circular hollow steel column sections. The effects of increasing size of the column cross section, effects of adding SFRM as thermal insulation, applying intumescent paint to the column surface, and filling the column with concrete on fire resistance of circular hollow steel column sections are discussed.

Referring to the results of heat transfer analysis in Chapter 4, the difference between temperatures of Nodes 1, 2 and 3 in each section were insignificant. Therefore, the midsection temperature is used to represent overall behavior of each column and was used for strength analysis in Chapter 5 and is used for discussion and comparison purposes in this Chapter.

6.2 Effects of Increasing Size of the Cross Section

This section discusses the results of heat transfer and strength analysis presented Sections 4.2 and 5.2. The purpose of these analyses were to investigate effects of increasing size of the cross section on thermal resistance of circular hollow steel section.

6.2.1 Heat Transfer

Figure 6-1 shows variation of temperature as a function of time for the 8x1.5, 8x1, 8xx and 8x0.5 steel tube models (see Figure 3-1) for two hours of the E119 fire exposure. It can be seen from this figure that the temperature-time profile for 8x0.5 tube section is closest to the E119 curve due to its thin wall thickness. When the size of the column section

is increased, this rise in temperature is less in comparison to the lighter sections. Since 8x1.5 is the heaviest section, its temperature increase at any given time is lowest at any given time is lowest (see Figure 6-1). The irregularity at point A in all four analyzed models is due the peak in specific heat value of steel at 735°C.

Figure 6-2 shows the temperature difference between node 1 and node 2 (exterior and exterior wall surfaces) of these models. The maximum temperature difference is 36°C for 8x1.5 and 6.5°C for 8x0.5 tube sections. It can be seen from Figure 6-2 that due to the small wall thickness and the high thermal conductivity of steel, the change in temperature within these sections are insignificant.

6.2.2 Strength

Figures 6-3 and 6-4 display variation of yield strength and modulus of elasticity as a function of time for unprotected 8x1.5, 8x1, 8xx and 8x0.5 tube sections. Since these columns are unprotected and the applied fire curve is E119, strength of these sections reduces rapidly and reaches their minimum value at the end of the fire. Significant reduction occurs during the first 30 minutes of the fire exposure. After the flashover occurs, the temperature and the section's strength does not experience large variation. Approximately 40% of section's strength will remain after 22, 17, 16 and 12 minutes from the beginning of the fire for unprotected 8x1.5, 8x1, 8xx and 8x0.5 tube columns respectively. Midsection temperature, yield strength and modulus of elasticity values for every 10 minutes are tabulated in Appendix A of this report for each of these column sections.

Figure 5-5 shows force resistance of these members as a function of time under the E119 fire exposure. The axial force resistances of these columns are obtained by multiplying the reduced section's yield strength to the cross sectional area of the column.

From Figures 6-1 and 6-3, it is observed that the section's size is increased significantly with a small improvement in strength of these members. It can be concluded that increasing column size does not provide adequate fire resistance to the unprotected steel members. The increase in size of the cross section increases the force resistance of the cross section because of the increased load bearing area.

6.3 Effects of Using SFRM

This section discusses the results of heat transfer and strength analysis presented in Sections 4.3 and 5.3. The purposes of these analyses was to investigate the benefits of using SFRM to the column surface on fire resistance of circular hollow steel column sections.

6.3.1 Heat Transfer

As expected, adding SFRM to the column provides a substantial increase in fire resistance. Figure 6-6 displays the temperature-time profile of the unprotected and SFRM-applied 8xx tube columns in an E119 fire exposure. The increase in section's temperature depends on the thickness of SFRM. A 15.2mm SFRM thickness (for 2-h fire rating) impedes the increase in temperature more as compared to 6.4mm SFRM thickness (for 1-h fire rating). In all three curves, the temperature increases to its maximum value at the end of the fire.

Figure 6-8 and 6-10 shows variation in temperature of unprotected and SFRM-applied 8xx tube sections under large and small compartment fire exposures. For the SFRM-applied sections, 1-h and 2-h fire rating thicknesses are used. The maximum

temperatures and the times at which they occurred are listed in Table 6-1. In comparison to E119 fire, the time when each section's temperature is maximum, and yield strength as well as modulus of elasticity is minimum, occurs before the fire ends. This point happens earlier in the small compartment fire in comparison to the large compartment fire due to the reasons explained in Section 2.3.

6.3.2 Strength

Figure 6-7 shows variation in yield strength of these models under the E119 fire exposure. Steel section's strength reduces when the temperature increases above 100°C (Table 2-1). This reduction starts after 6 minutes for unprotected 8xx steel tube. By adding SFRM, it starts after 13 and 22 minutes for 1-h and 2-h fire ratings respectively. The section's yield strength reduces constantly until it reaches a minimum value at the end of the fire. 40% of yield strength remains after 16, 45 and 81 minutes in unprotected, 1-h and 2-h fire rating SFRM-applied 8xx steel tube columns. Adding fire protective material delays reduction of section's strength depending on the type of SFRM and its thickness.

Figure 6-9 and 6-11 display the change in values of yield strength when SFRM is added to the column in real fire exposures. Significant differences are observed by adding SFRM under compartment fires in comparison to the E119. Table 6-1 shows the minimum value of yield strength obtained for each model. By referring to this table, it can be seen that the minimum yield strength values changes from 14% for unprotected to 41% and 68% for 1-h and 2-h fire rating thick SFRM-applied 8xx tube section under the exposure of the large compartment fire. These values change from 7% for unprotected to 40% and 66% for 1-h and 2-h fire rating thick SFRM-protected 8xx tube section in an exposure to the small compartment fire (Table 6-1)

6.4 Effect of Using Intumescent Paint as Thermal Insulation

This section discusses the results of heat transfer analysis and strength analysis conducted in Sections 4.4 and 5.4 on intumescent paint insulated 8xx steel tube. The purposes of these analysis were to investigate the benefits of using intumescent paint to the column surface on fire resistance of circular hollow steel column sections.

6.4.1 Heat Transfer

The variation of temperature under the E119 fire exposure for both bare steel and intumescent paint protected 8xx section is displayed in Figure 6-12. The increase in temperature reduces due to the presence of the intumescent paint. As per Table 2-1, after the temperature increases above 800 °C (T4), intumescent paint degrades and its fire resistance capacity diminishes. Thus, after losing the effectiveness of the intumescent paint, the temperature of the tube section converges to that of the E119 fire, similar to the unprotected sections.

Figures 6-13 and 6-14 display behavior of the intumescent paint insulated section under the large and small compartment fire exposures. The maximum temperature during the period of fire exposure changes from 636°C for unprotected 8xx tube section to 435°C when one layer of intumescent paint is applied (Table 6-1).

6.4.2 Strength

Figure 6-15 displays variation in yield strength of a bare steel and intumescent paint protected steel column under the E119 fire exposure. The minimum section's strength occurs at the end of the fire and is similar to the unprotected section's strength. The time that yield strength of the section reduces to its 40% or its value at normal temperature is extended from 16 minutes for bare steel to 33 minutes by adding one layer of intumescent

paint. When column is exposed to the E119 fire, the benefit of having intumescent paint insulation is to slow the reduction of yield strength at the beginning of the fire exposure.

Figures 6-16 and 6-17 show variation of yield strength for unprotected and intumescent paint applied 8xx steel tube section in large and small compartment fires. As listed in Table 6-1, column section's minimum yield strength increases from 14% to 40% when one layer of intumescent paint is added to the column under large compartment fire exposure. Section's strength does not decrease more than 40% of their original value the whole time, which is a modest amount of strength for the service loads during fire in a building. This shift in minimum yield strength is from 7% to 31% under small compartment fire.

6.5 Effect of Concrete-Filled Sections

This section discusses the results of heat transfer analysis and strength analysis presented in Sections 4.5 and 5.6 on concrete filled 8xx steel tube. The purposes of these analysis were to investigate the benefits of filling circular hollow steel sections with concrete on fire resistance of these cross sections.

6.5.1 Heat Transfer

Concrete inside the column absorbs some of the heat energy from the steel casing. This behavior of concrete depends on its specific heat as explained in Section 2.7.1. Since the thermal conductivity of concrete is small, a minor amount of heat energy find its way to concrete core in column during the two hours of fire exposure. Because of this, it absorbs a small portion of heat from steel. As is shown in Figure 6-18, concrete-filled columns' temperature decreases in comparison to the unprotected sections, but by an insignificant

amount. Temperature increases to its maximum value at the end of E119 fire and is very similar to the unprotected column sections' temperatures.

Figures 6-19 and 6-20 display temperature of concrete-filled 8xx column section under the large and small compartment fires exposures. Temperature-time profile for this model is similar to the unprotected section except for slightly smaller temperature values. The maximum temperature decreases from 636°C in unprotected section to 586°C when the section is filled with concrete under large compartment fire. In small compartment fire exposure, the maximum temperature observed changes from 723°C to 695°C by filling the section with concrete (see Table 6-1).

6.5.2 Strength

As discussed in heat transfer section, filling the column with concrete did not change temperature-time profile of the section significantly. Since strength of a steel section depend on its temperature, variation of yield strength does not change and is very similar to the unprotected column sections. Figure 6-21 shows variation of yield strength for an unprotected 8xx and concrete-filled 8xx steel tube section under E119 fire exposure. Contribution of concrete absorbing energy as heat sink is very small due to its low thermal conductivity.

Figures 6-22 and 6-23 display yield strength of concrete-filled 8xx steel tube section under large and small compartment fires. By using concrete-filled section, the minimum yield strength value of this section changes from 14% to 20% of their original values in large compartment fire (see Table 6-1). This value changes from 7% to 8% when it is exposed to the small compartment fire.

Of the fire protection methods considered, using concrete solely for the purpose of absorbing heat from steel column is the least effective way of protecting column members against structural fire. Usually concrete inside tube column is considered for load bearing purposes after steel loses its strength. The concrete inside the tube column can be plain or reinforced depending on the amount of axial load they will resist assigned by the designer.

6.6 Additional Comparison

This section sums up the effects of different methods of fire protection considered in this study including SFRM, intumescent paint and concrete filled tube sections. Figure 6-24 shows variation in temperature of the unprotected, SFRM applied, intumescent paint insulated and concrete filled 8xx tube sections under the exposure of the E119 fire.

Figures 6-25 and 6-26 show the variation in temperature of the unprotected, SFRM applied, intumescent paint insulated and concrete filled tube sections under the exposure of the large and small compartment fires. These figures proves that SFRM is the most effective method of insulating column members against fire. This is followed by intumescent paint insulated, and concrete-filled sections. Figure 6-27 compares the temperature-time profile of the concrete filled section with the unprotected tube sections with different sizes. It can be seen that temperature-time profile for the concrete filled section is between 8x1 and 8x1.5 tube sections, thus the effectiveness of concrete filled with respect to the unprotected sections depends on how much size of the cross section is increased.

6.6.1 Change in Strength after the First 20 and 30 Minutes

Figure 6-28 shows normalized strength of each model after the 20 and 30 minutes of standard and real fire exposure. In this Figure, values are normalized with respect to the

strength of the unprotected 8xx steel tube at normal room temperature. As is shown in this figure, increasing size of the cross section improves the performance of the column in the first 20 and 30 minutes and can prevent from the collapse of the building before the building is evacuated depending on its occupancy and the evacuation time required by the code.

In addition, it can be seen from this figure that adding intumescent paint to the column keeps its strength above 40% of its original value in the first 30 minutes of standard E119 fire and can be a useful method of fire protection to delay the reduction in strength. In real fire exposures, it was observed in Chapter 5 that intumescent paint can keep the strength of the steel column above 35% during the entire time. In concrete filled section, however, when the concrete is used solely as heat sink, there hasn't been any significant increase in strength of the column even in the first 20 and 30 minutes.

6.7 Summary

This chapter discussed and compared the results obtained in Chapter 4 and Chapter 5 for heat transfer and strength analysis. Following are the summary of findings in this chapter.

Increasing size of the section did not significantly reduce the temperature. It was shown that yield strength capacity of the section has not changed significantly by increasing size of the cross section. However, this increase in column cross section increases its force capacity which is obtained by multiplying its reduced yield strength to the cross sectional area of the column. This increase is considerable in the first 20 and 30 minutes of the fire.

As expected amongst the four methods of fire protection studied in this report, SFRM is the most effective method of insulating column members against fire. This is followed by intumescent paint insulated, concrete-filled sections.

Under compartment fire exposure, behavior of the protected columns change and they more effectively preserve their strength. Since the temperature increases to a maximum value of 680°C and 872°C in large and small compartment fires then it starts to degrade, the column perform well with these fire protective material.

Table 6-1 Maximum temperature, the minimum yield strength and minimum modulus of elasticity as well as the time they occur for the all analyzed models.

Case	Section ID	Type of Insulation	Fire Type	Time ^(a) (mins)	Maximum Temperature (°C)	Minimum (F/ly)	Minimum (E/E0)
Case 1	BS-8x1.5-E119	Unprotected	E119	120	998	0.025	0.045
	BS-8x1-E119	Unprotected	E119	120	1002	0.027	0.048
	BS-8xx-E119	Unprotected	E119	120	1003	0.026	0.047
	BS-8x0.5-E119	Unprotected	E119	120	1006	0.027	0.048
Case 2	BS-8xx-LC	Unprotected	LC Cardington	60	636	0.142	0.245
	BS-8xx-SC	Unprotected	SC Cardington	40	723	0.069	0.121
Case 3	SFRM1h-8xx-E119	1-h SFRM	E119	120	736	0.066	0.116
	SFRM1h-8xx-LC	1-h SFRM	LC Cardington	86	408	0.415	0.692
	SFRM1h-8xx-SC	1-h SFRM	SC Cardington	62	434	0.400	0.666
	SFRM2h-8xx-E119	2-h SFRM	E119	120	607	0.173	0.297
	SFRM2h-8xx-LC	2-h SFRM	LC Cardington	120	264	0.682	0.836
	SFRM2h-8xx-SC	2-h SFRM	SC Cardington	82	274	0.663	0.826
Case 4	IP-8xx-E119	IP applied	E119	120	984	0.027	0.048
	IP-8xx-LC	IP applied	LC Cardington	85	435	0.399	0.665
	IP-8xx-SC	IP applied	SC Cardington	57	527	0.311	0.521
Case 5	CF-8xx-E119	Concrete-Filled	E119	120	993	0.026	0.046
	CF-8xx-LC	Concrete-Filled	LC Cardington	63	586	0.205	0.351
	CF-8xx-SC	Concrete-Filled	SC Cardington	39	695	0.080	0.139

(a) This is the time where the maximum temperature, minimum yield strength and minimum modulus of elasticity occurs in the analysis models.

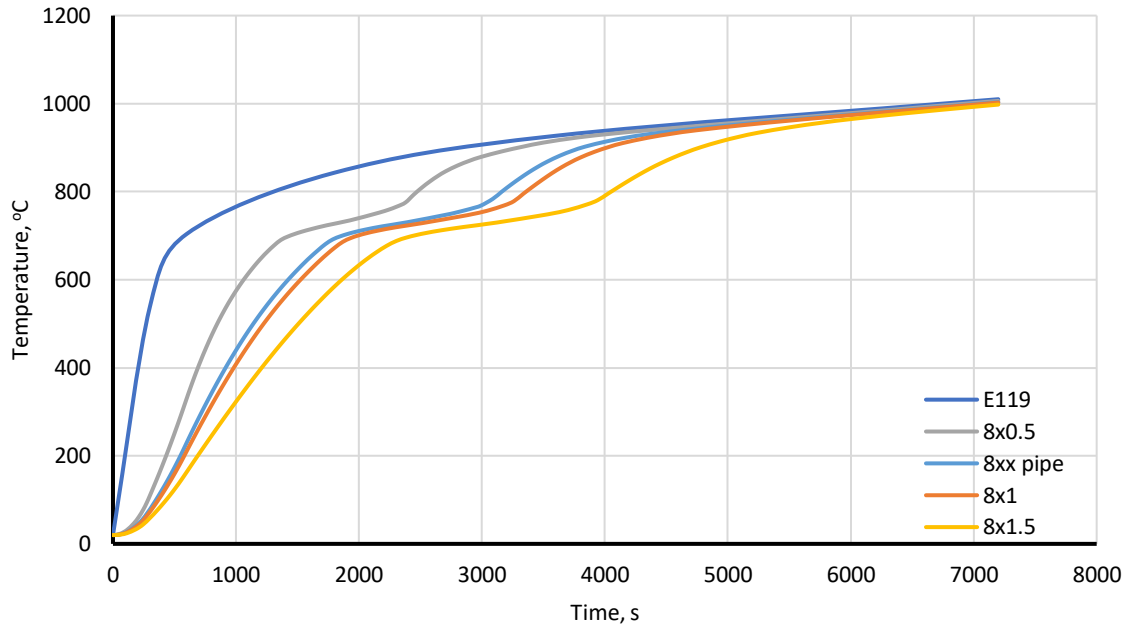


Figure 6-1 Temperature-time profile for unprotected 8x1.5, 8x1, 8xx, 8x0.5 tube sections under E119 fire exposure. Plotted curves are for mid-section temperatures.

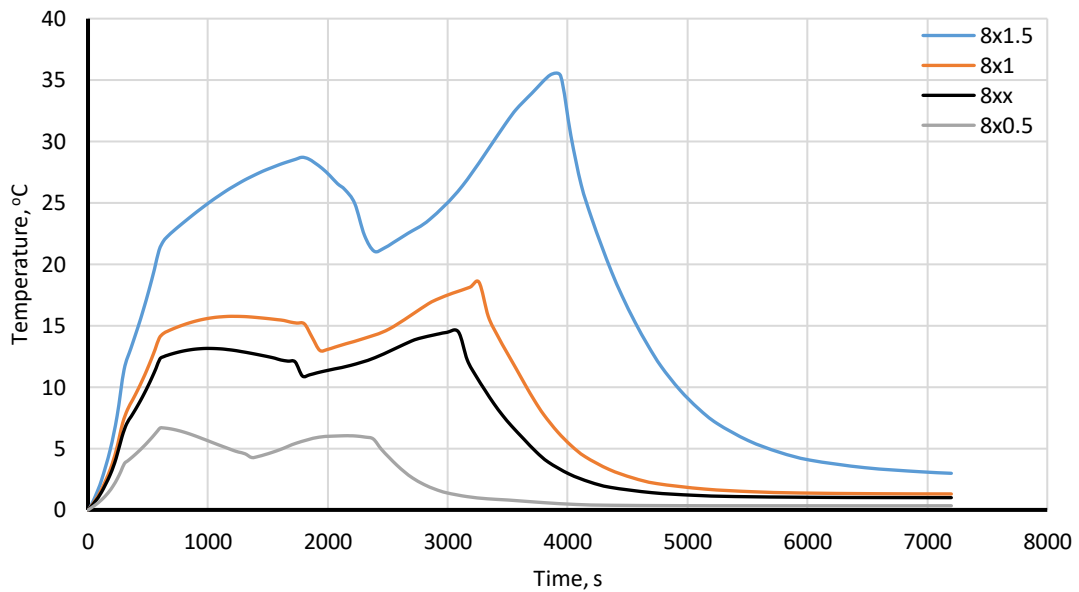


Figure 6-2 Variation in temperature difference between exterior and interior wall surface (Nodes 1 and 3) of unprotected 8x1.5, 8x1, 8xx, 8x0.5 tube sections under E119 fire exposure.

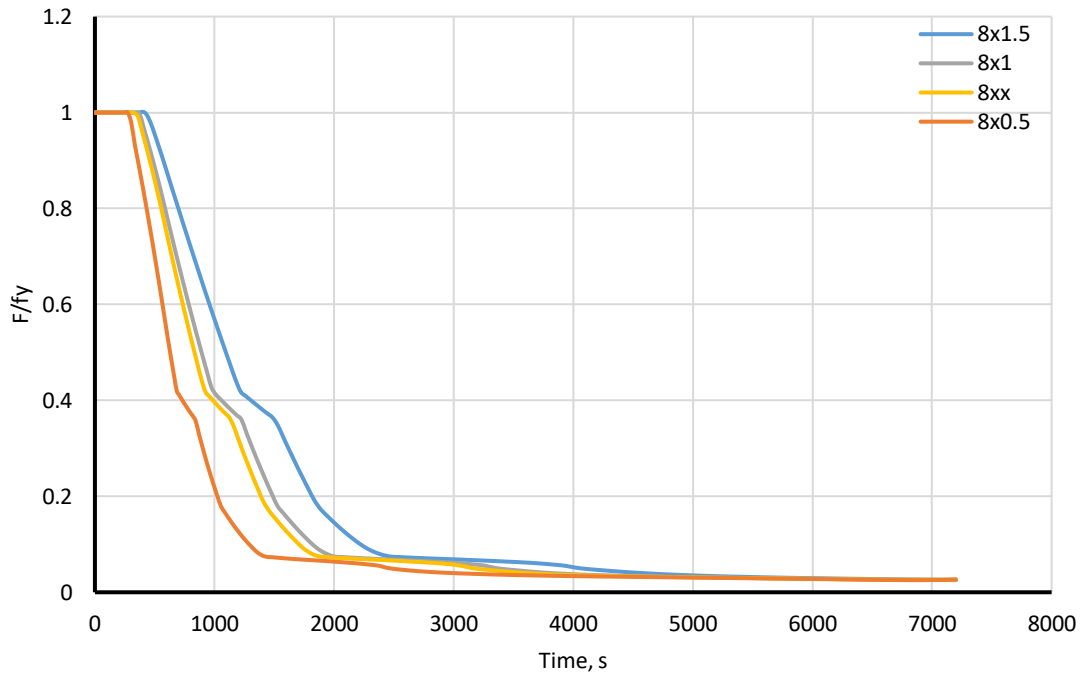


Figure 6-3 Variation in yield strength of unprotected 8x1.5, 8x1, 8xx, 8x0.5 tube sections under the E119 fire exposure.

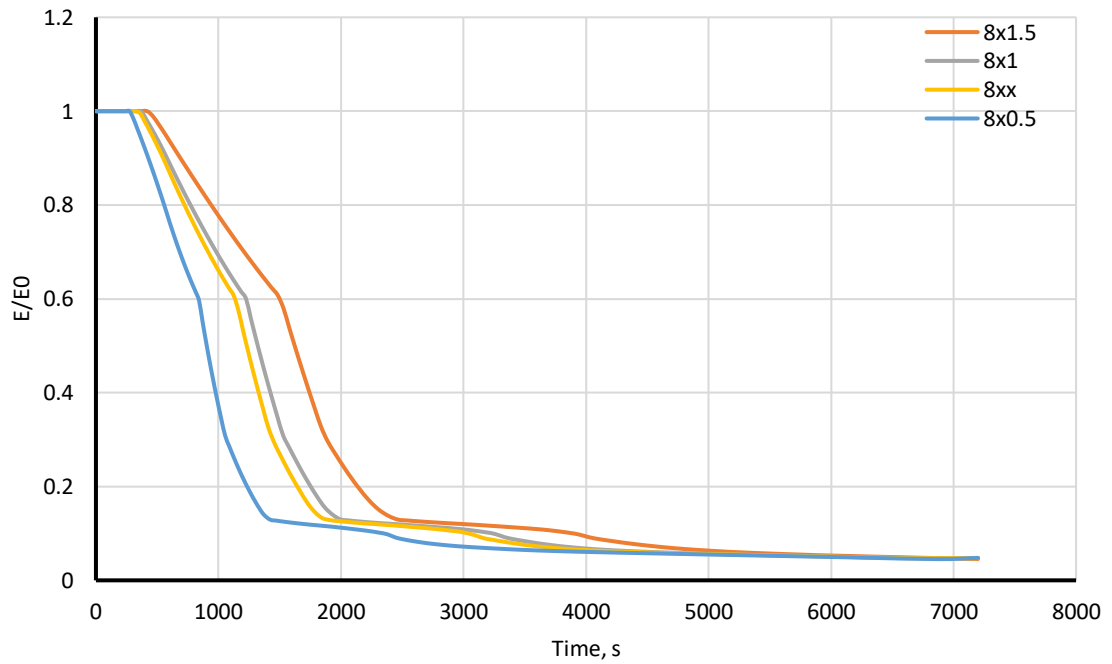


Figure 6-4 Variation in modulus of elasticity of unprotected 8x1.5, 8x1, 8xx, 8x0.5 tube sections under the E119 fire exposure.

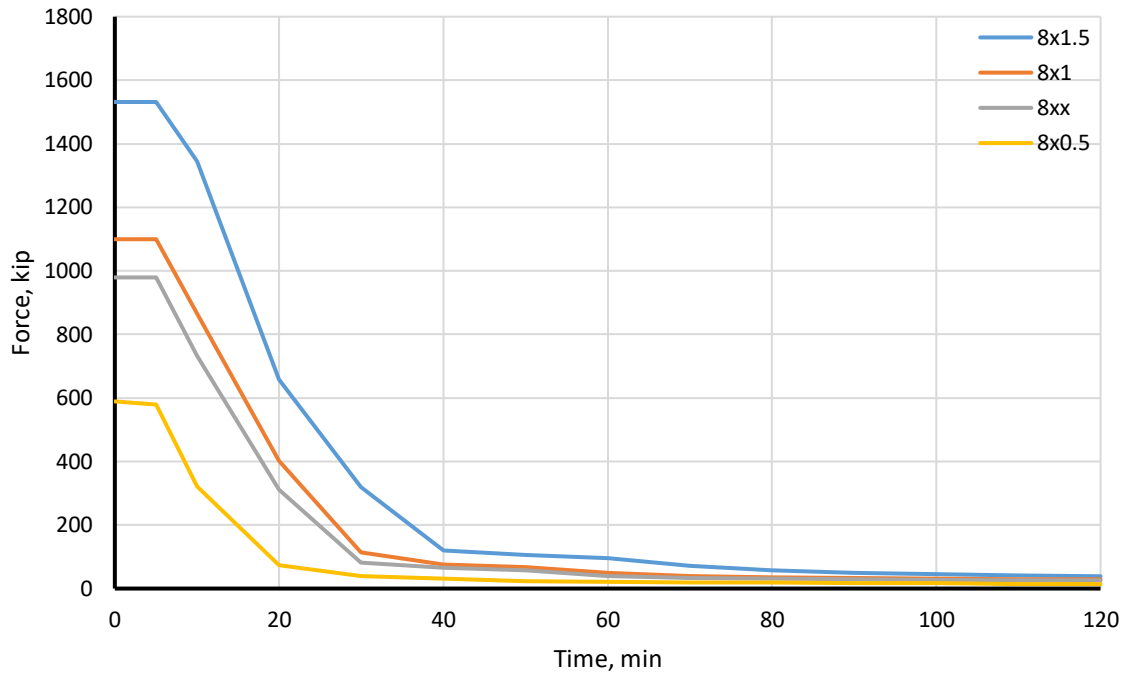


Figure 6-5 Variation in axial force resistance of unprotected 8x1.5, 8x1, 8xx, 8x0.5 tube sections under the E119 fire exposure.

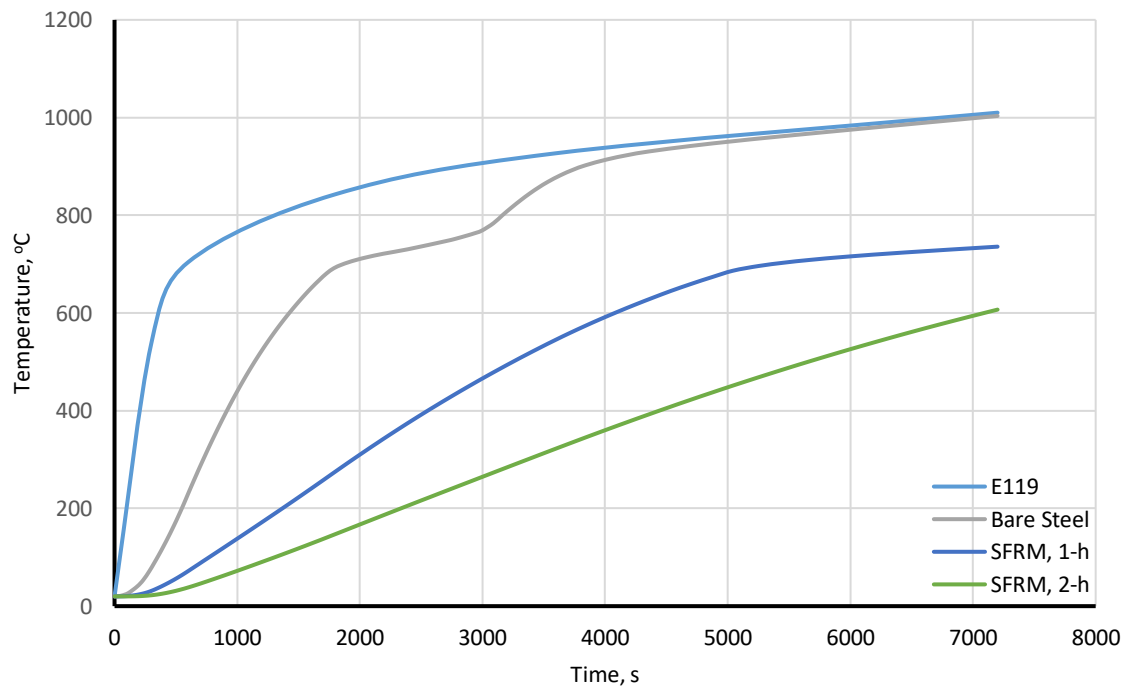


Figure 6-6 Effects of adding SFRM on temperature of 8xx section under the E119 fire exposure.

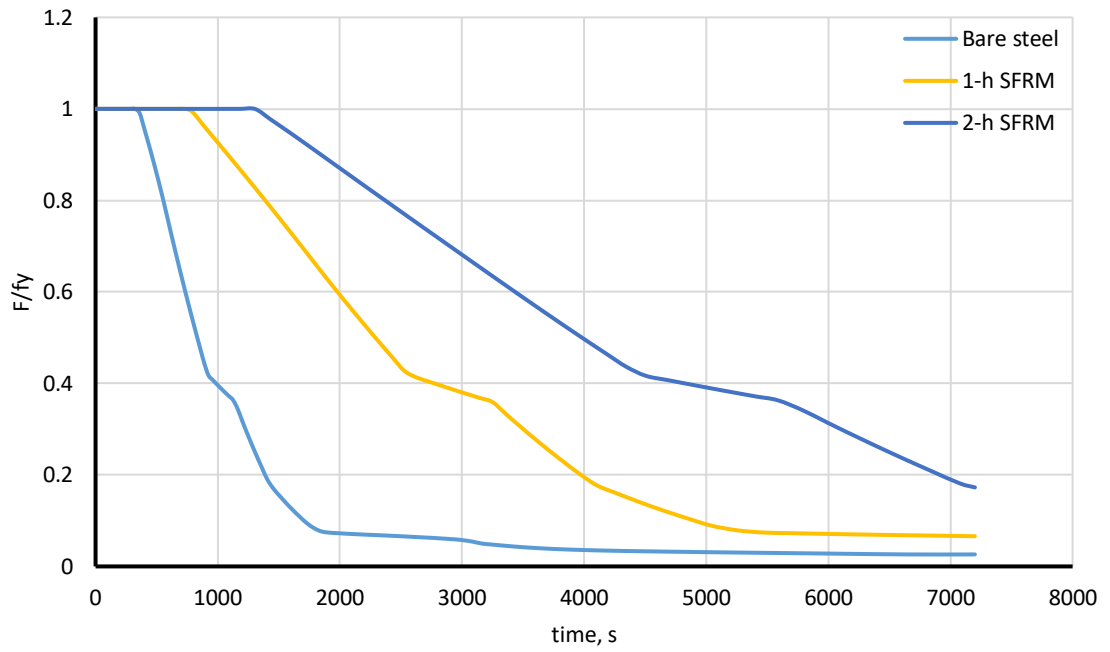


Figure 6-7 Effects of adding SFRM on strength of the 8xx section under the E119 fire exposure.

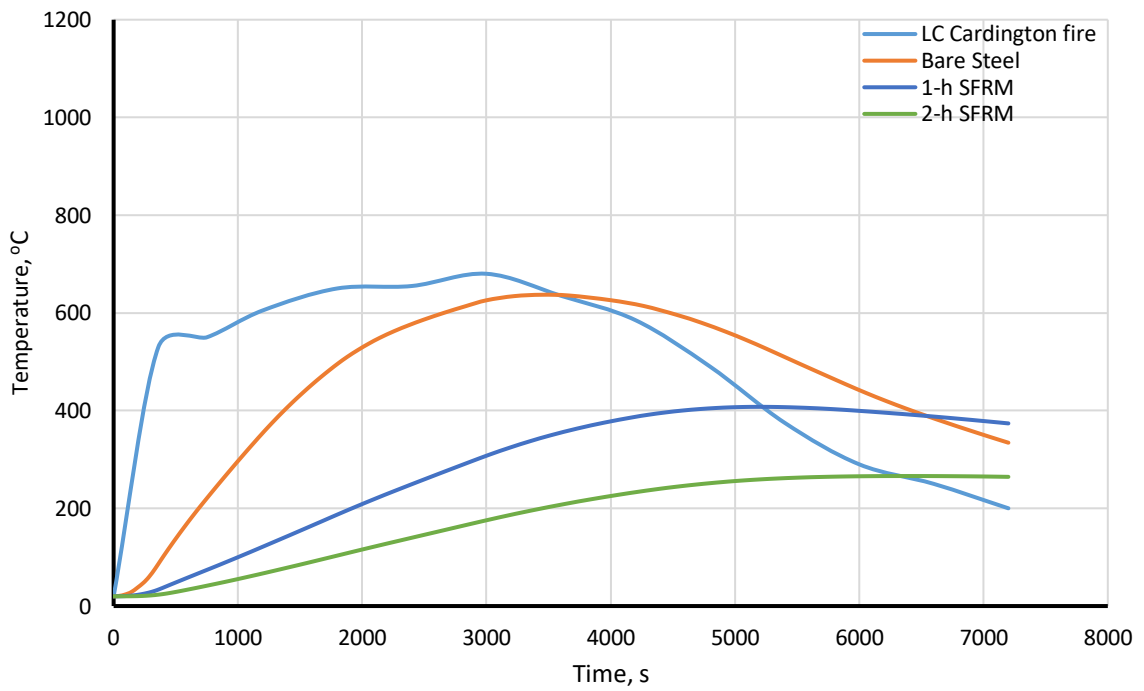


Figure 6-8 Effects of adding SFRM on temperature of 8xx section under the large compartment fire exposure.

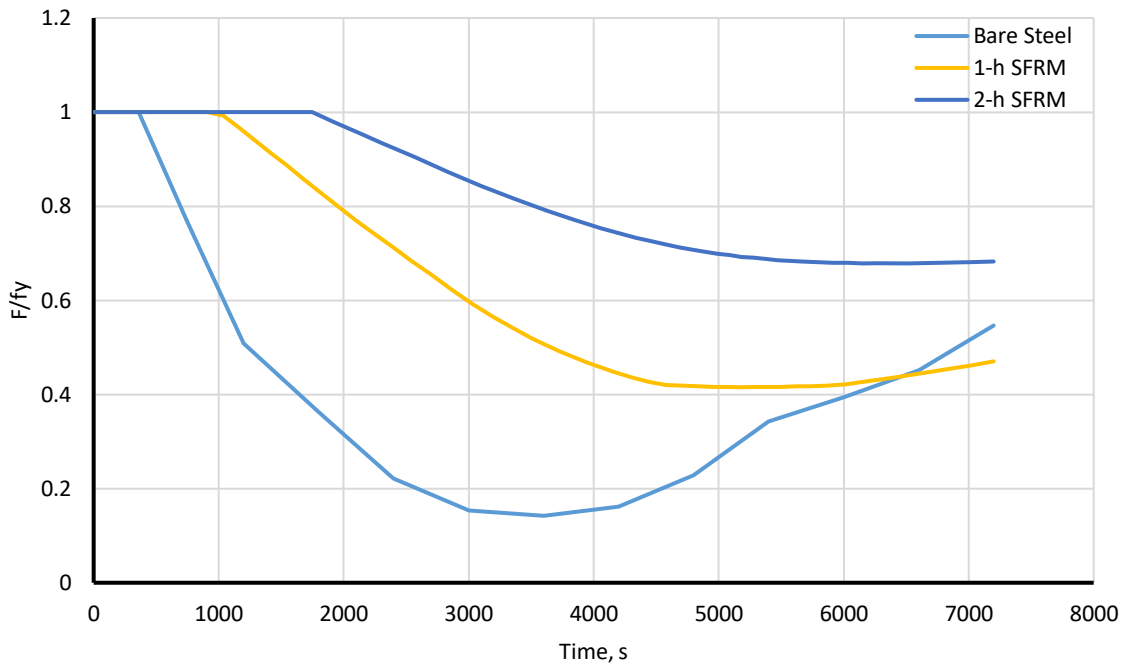


Figure 6-9 Effect of adding SFRM on strength of the section under the large compartment fire exposure.

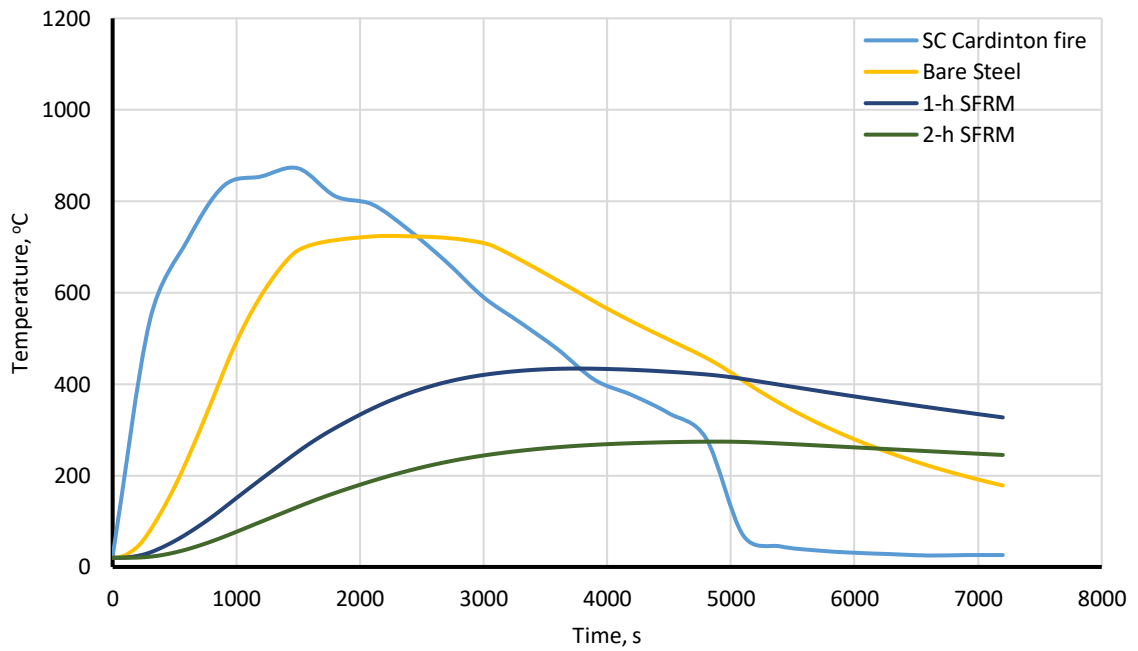


Figure 6-10 Effect of adding SFRM on temperature of 8xx section under the small compartment fire exposure.

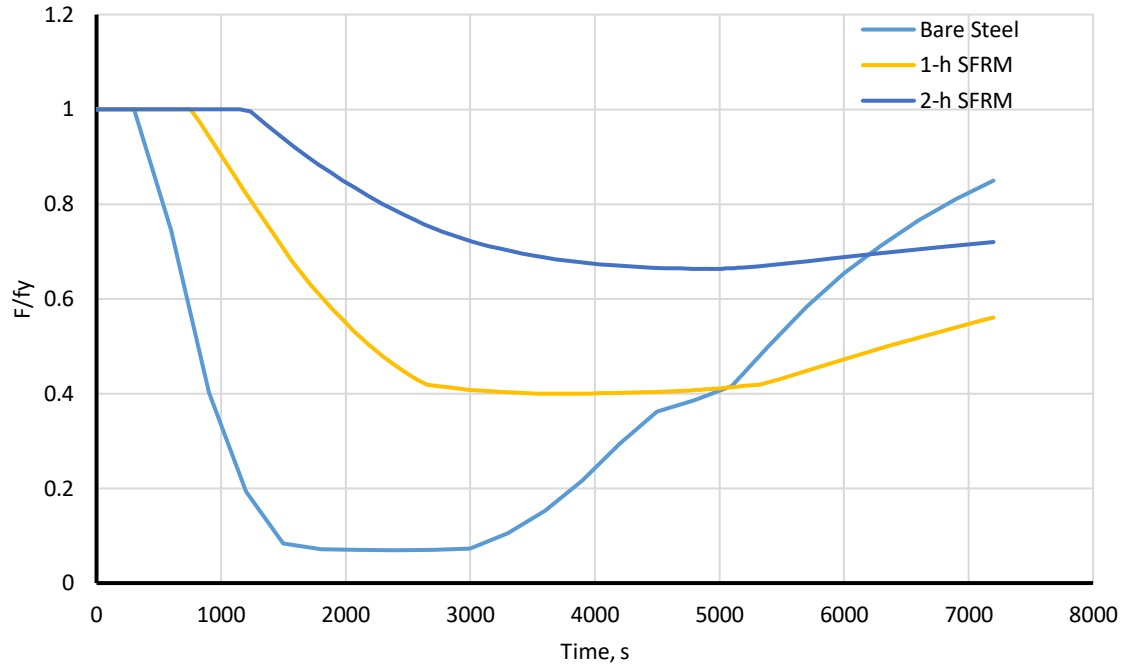


Figure 6-11 Effect of adding SFRM on strength of the section under the small compartment fire exposure.

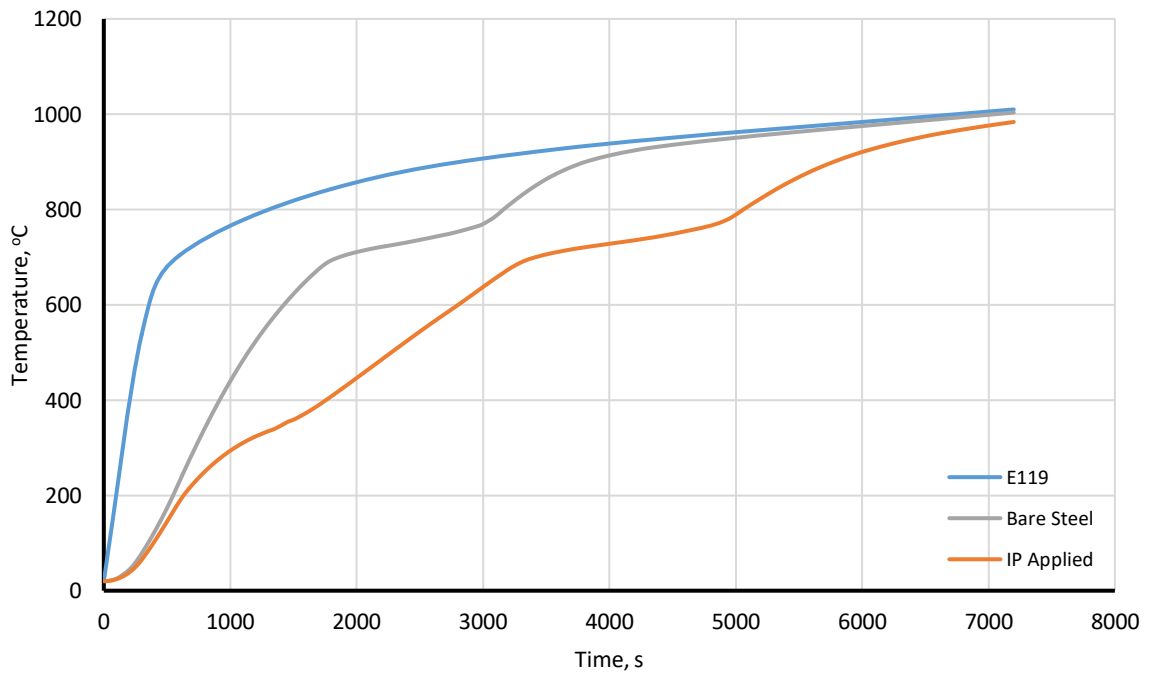


Figure 6-12 Effect of adding intumescent paint to the column surface on temperature of the section under the E119 fire exposure.

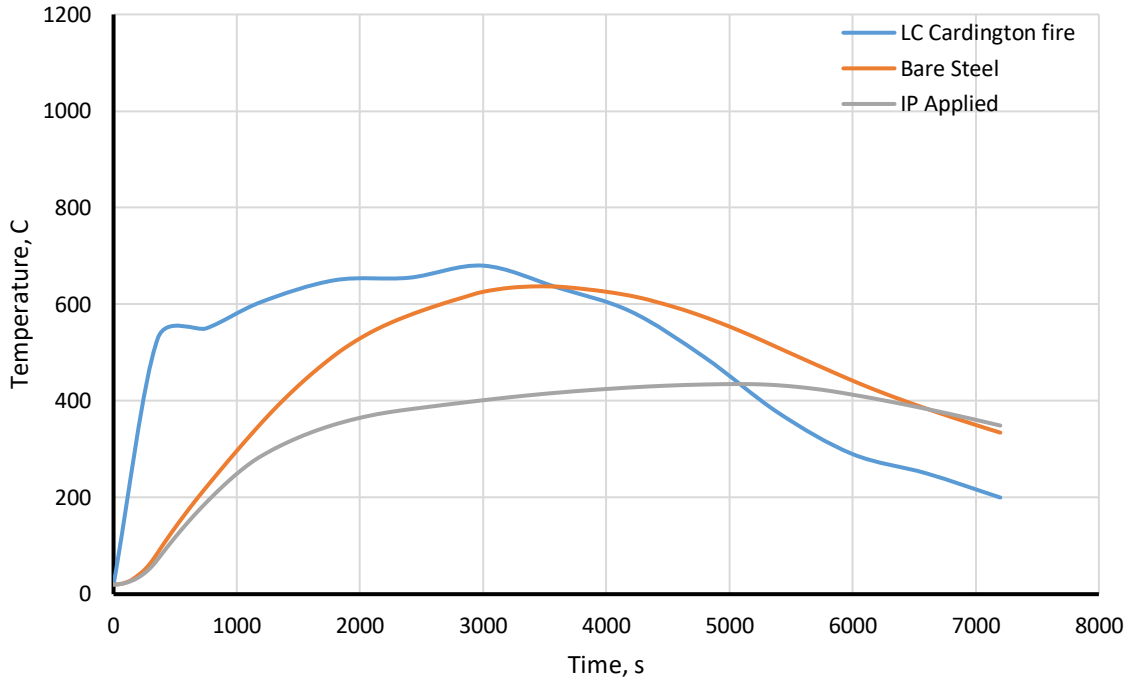


Figure 6-13 Effect of adding intumescent paint to the column surface on temperature of the section under large compartment fire exposure.

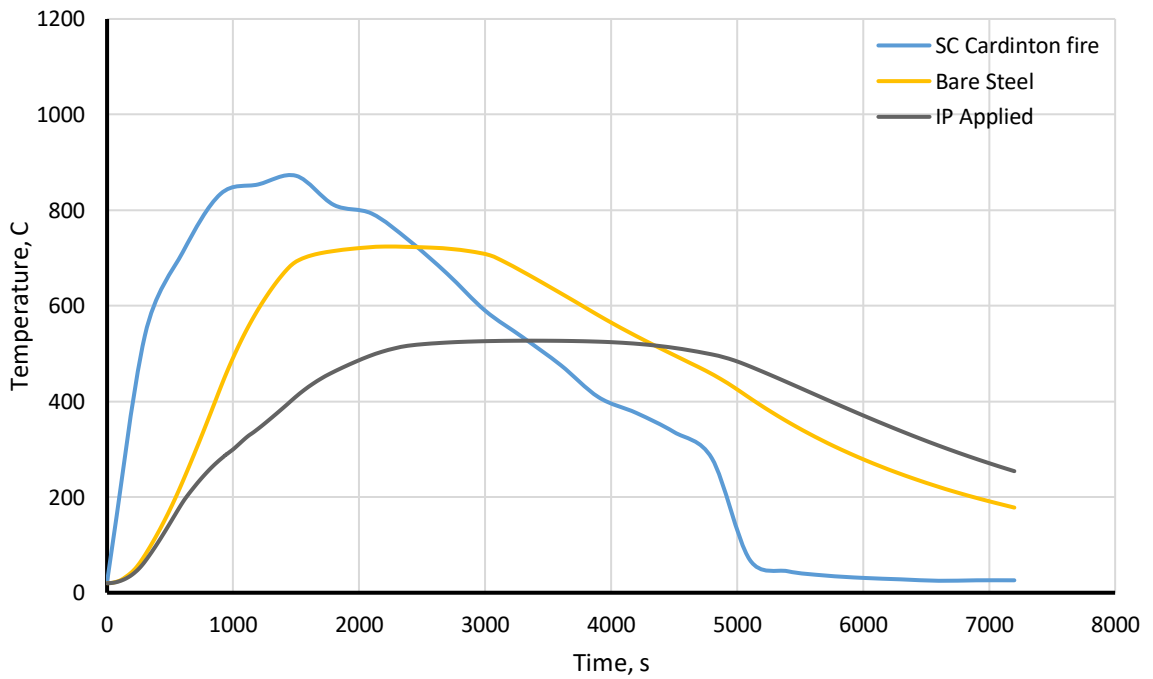


Figure 6-14 Effect of adding intumescent paint to the column surface on temperature of the section under the small compartment fire exposure.

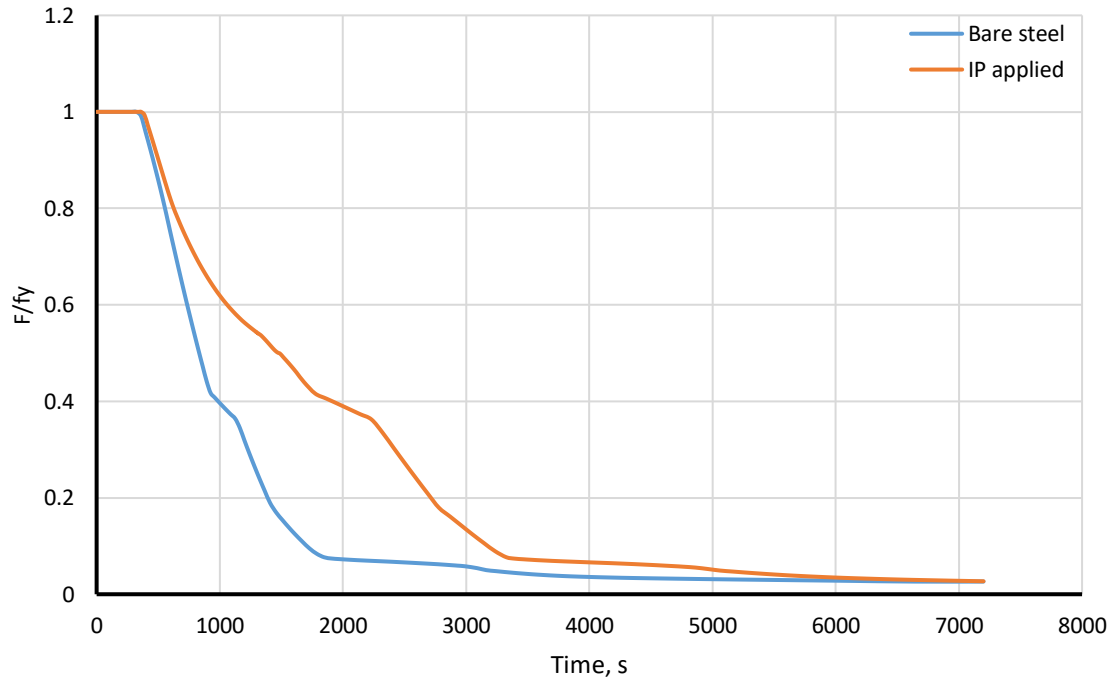


Figure 6-15 Effect of adding intumescent paint to the column surface on strength of the section under the E119 fire exposure.

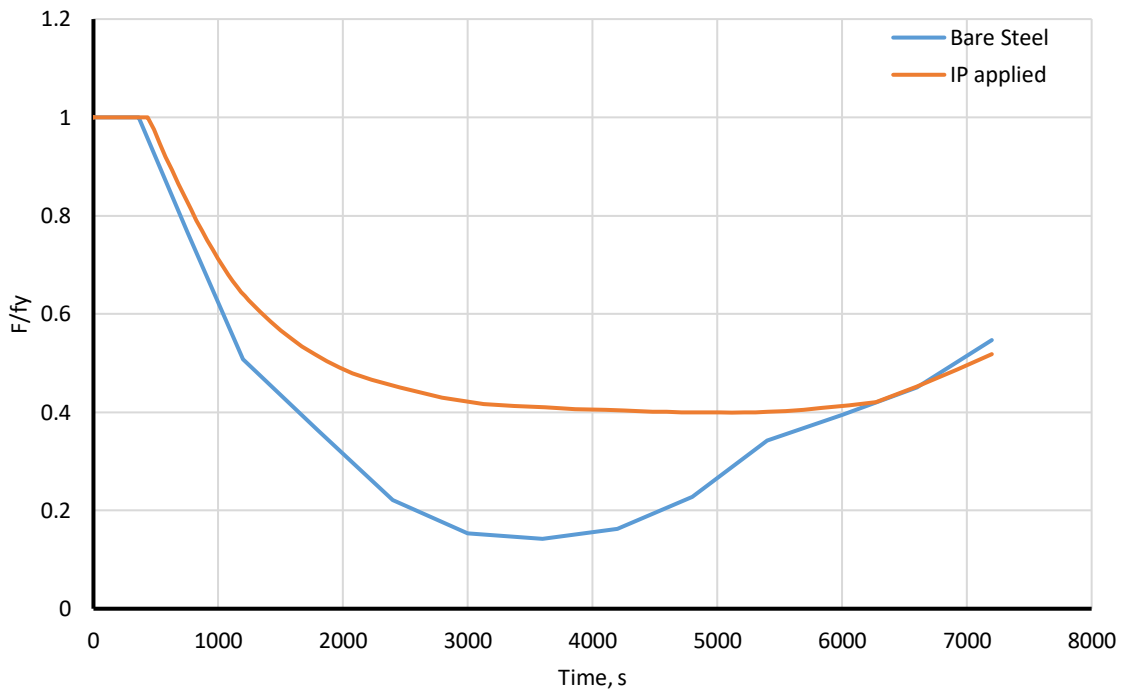


Figure 6-16 Effect of adding intumescent paint to the column surface on strength of the section under the exposure of large compartment fire.

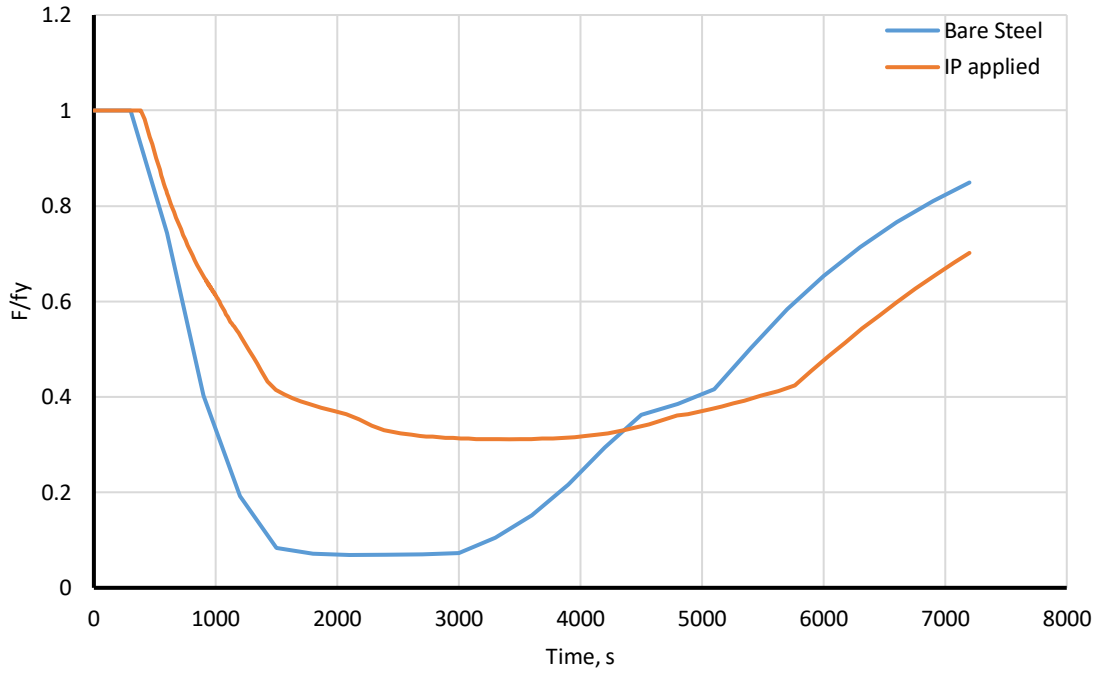


Figure 6-17 Effect of adding intumescent paint to the column surface on temperature of the section under the small compartment fire exposure.

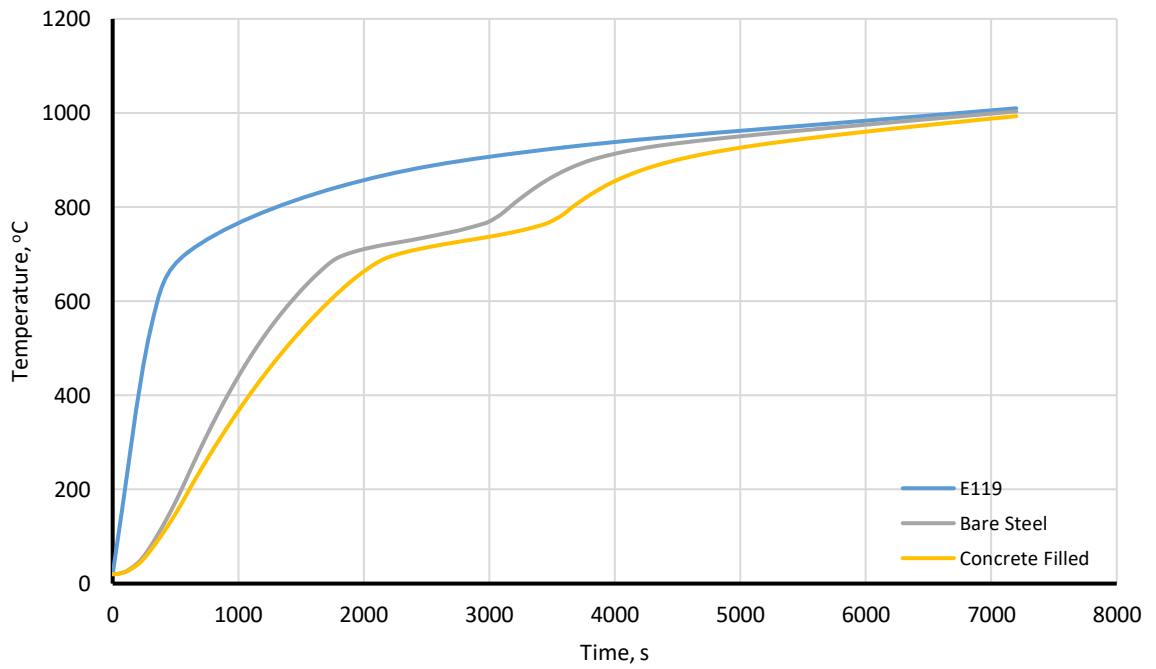


Figure 6-18 Effect of filling the column with concrete on temperature of the section under the E119 fire exposure.

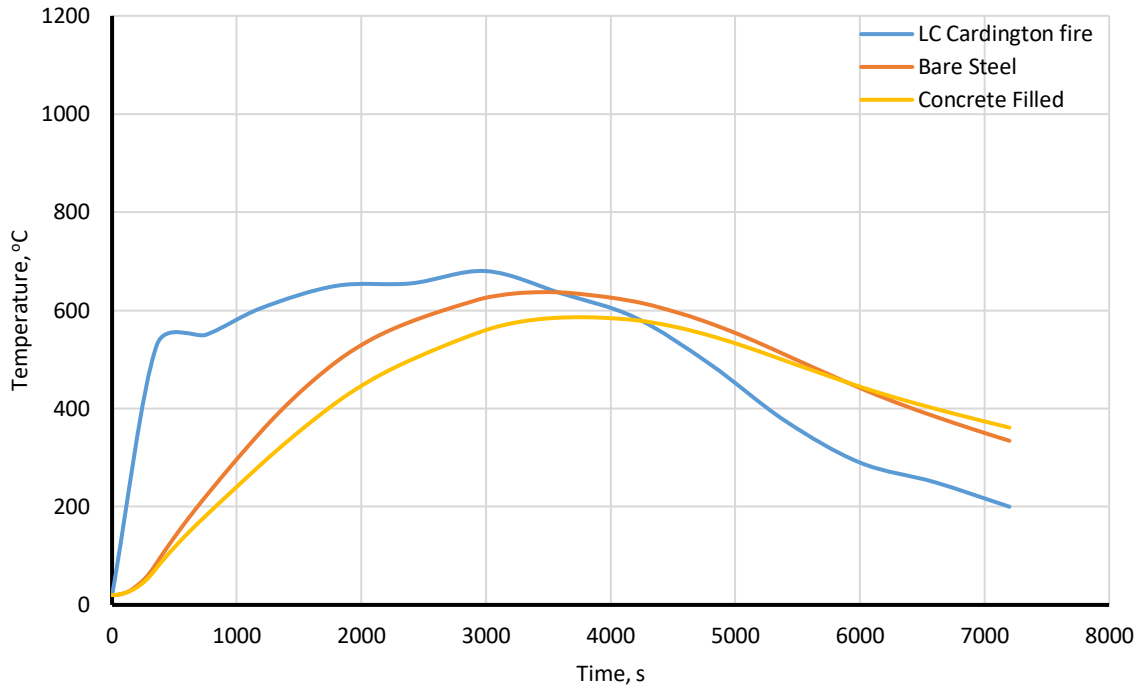


Figure 6-19 Effect of filling the column with concrete on temperature of the section under the large compartment fire exposure.

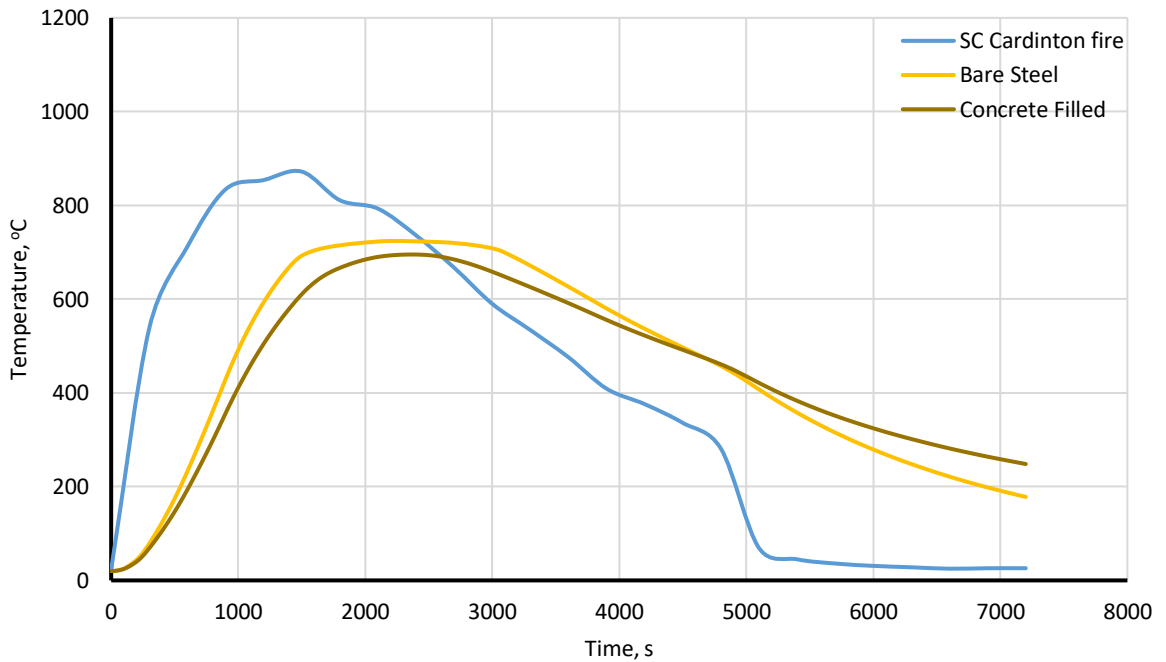


Figure 6-20 Effect of filling the column with concrete on temperature of the section under the small compartment fire exposure.

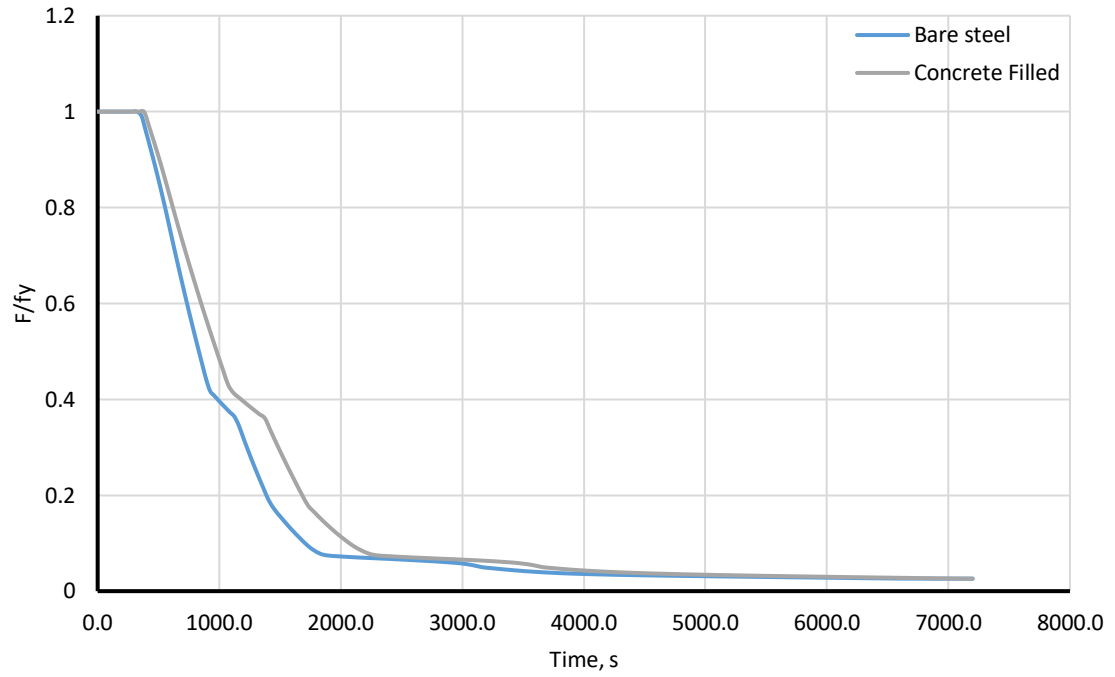


Figure 6-21 Effect of filling the column with concrete on strength of the section under the E119 fire exposure.

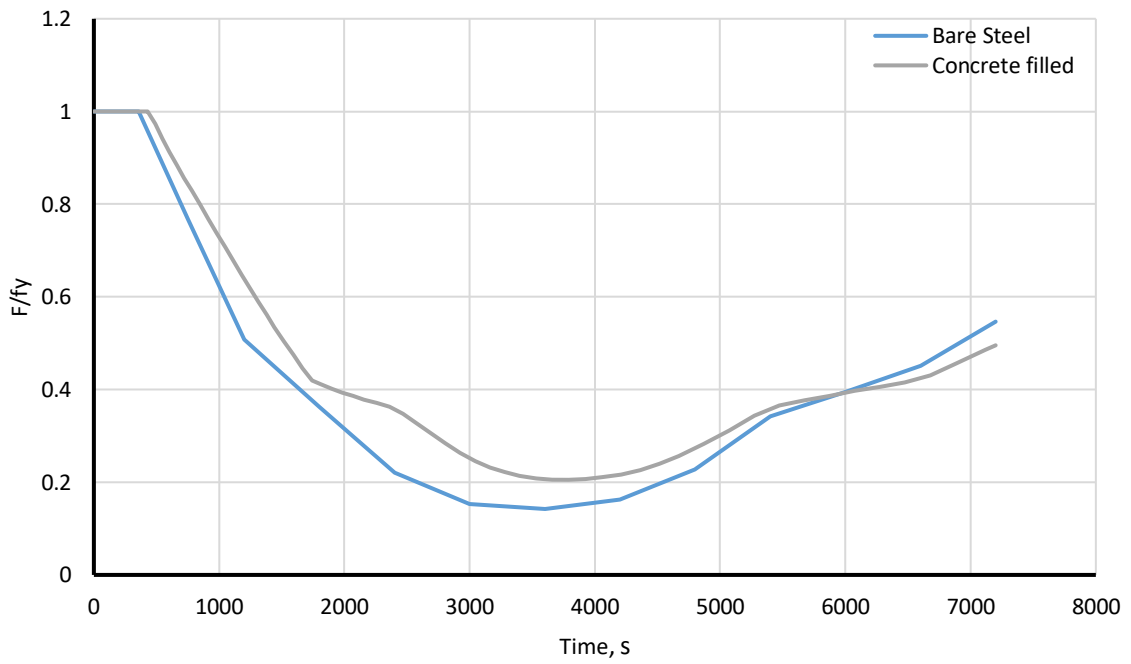


Figure 6-22 Effect of filling the column with concrete on strength of the section under the large compartment fire exposure.

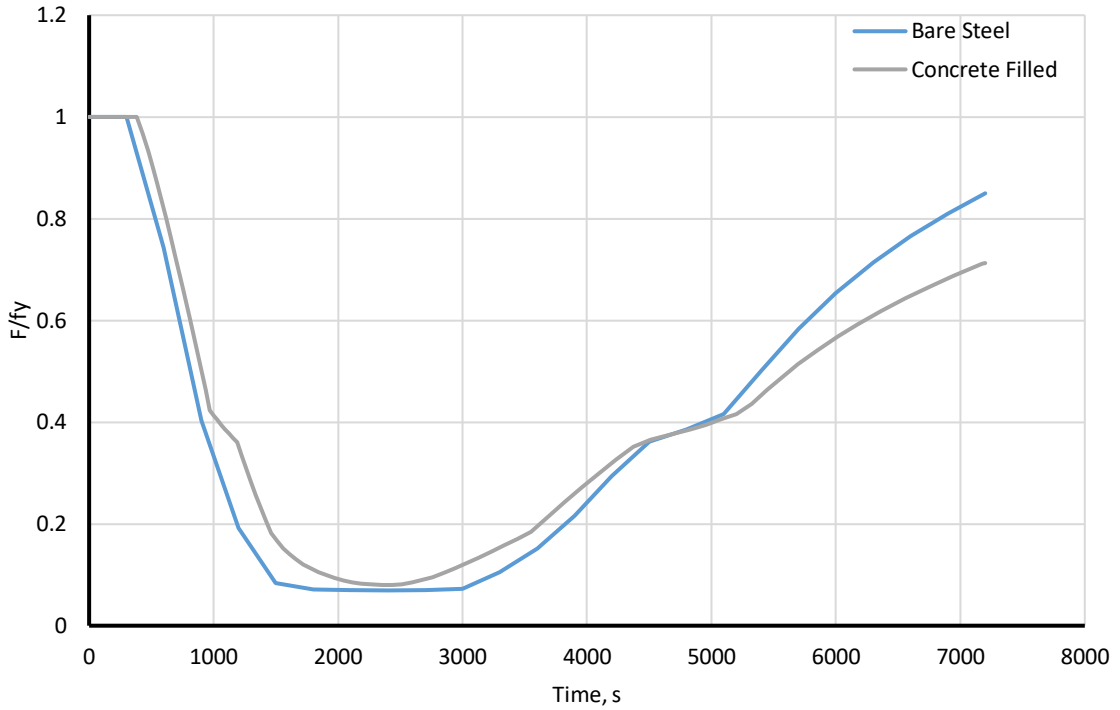


Figure 6-23 Effect of filling the column with concrete on strength of the section under Small compartment fire exposure.

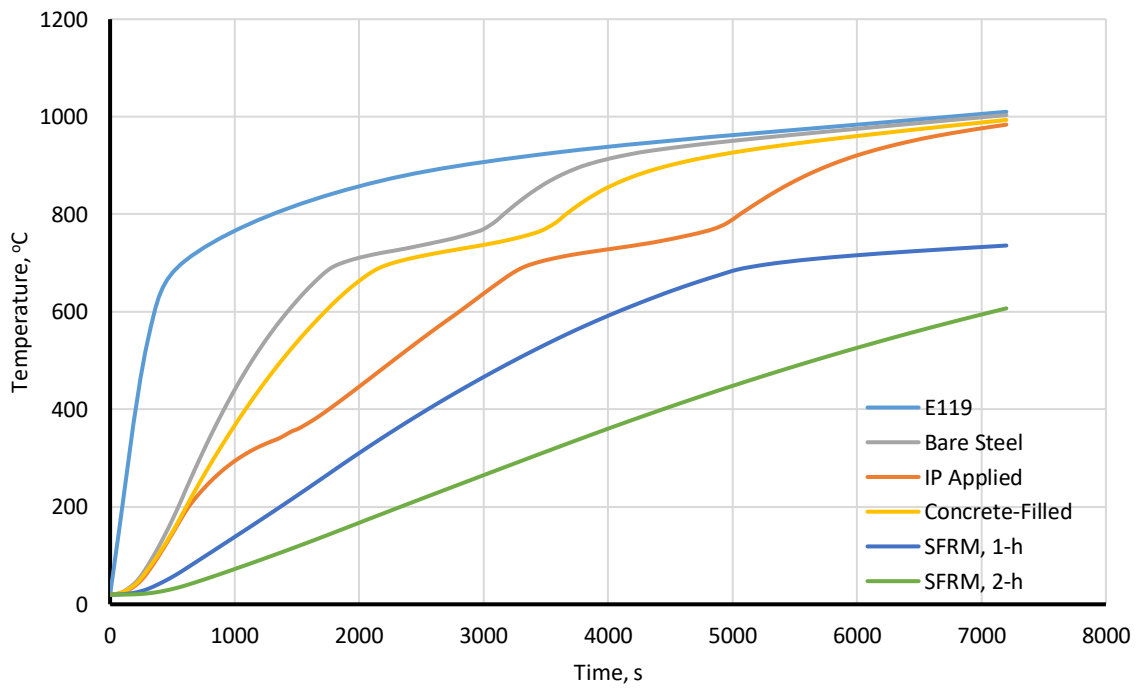


Figure 6-24 Variation of temperature as a function of time with different insulation types for an 8xx steel tube column under E119 fire exposure.

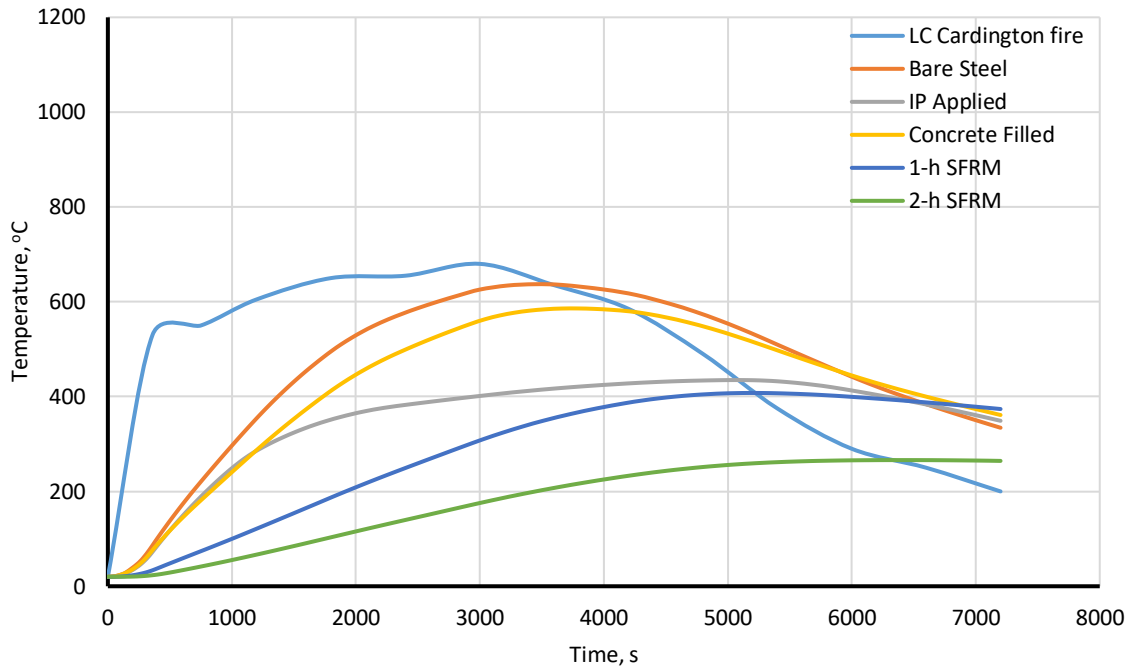


Figure 6-25 Variation of temperature as a function of time for an 8xx steel tube column with different insulation types under large compartment fire exposure.

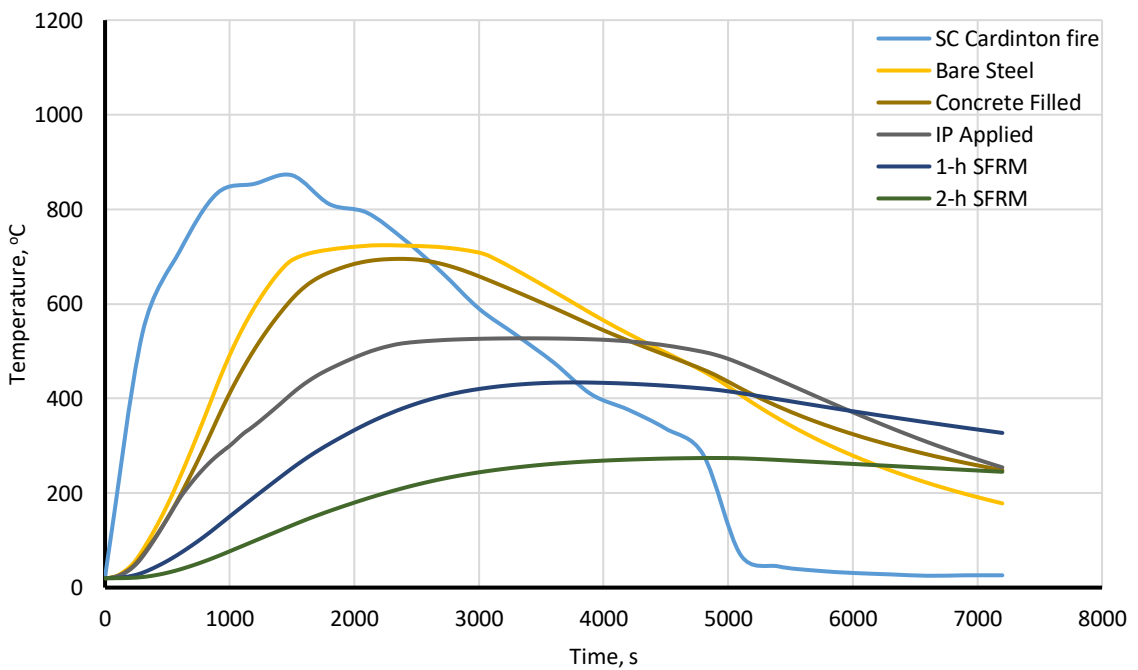


Figure 6-26 Variation of temperature as a function of time for an 8xx steel tube section with different insulation types under small compartment fire exposure.

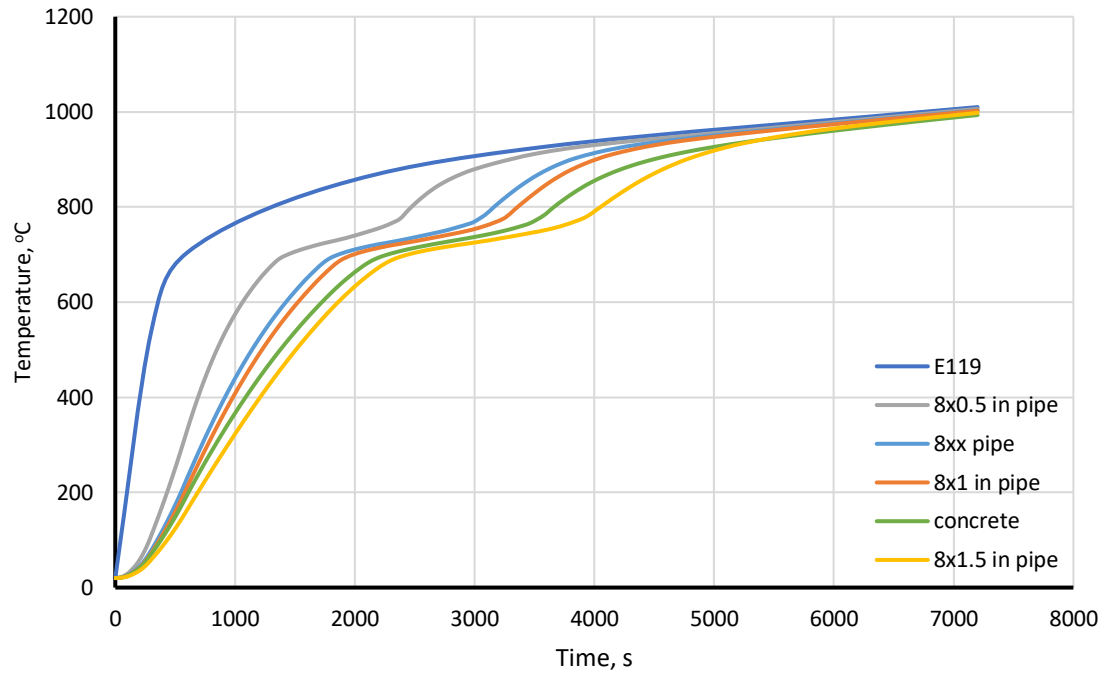


Figure 6-27 Variation of temperature as a function of time for the unprotected 8x1.5, 8x1, 8xx, 8x0.5 and concrete filled 8xx tube sections

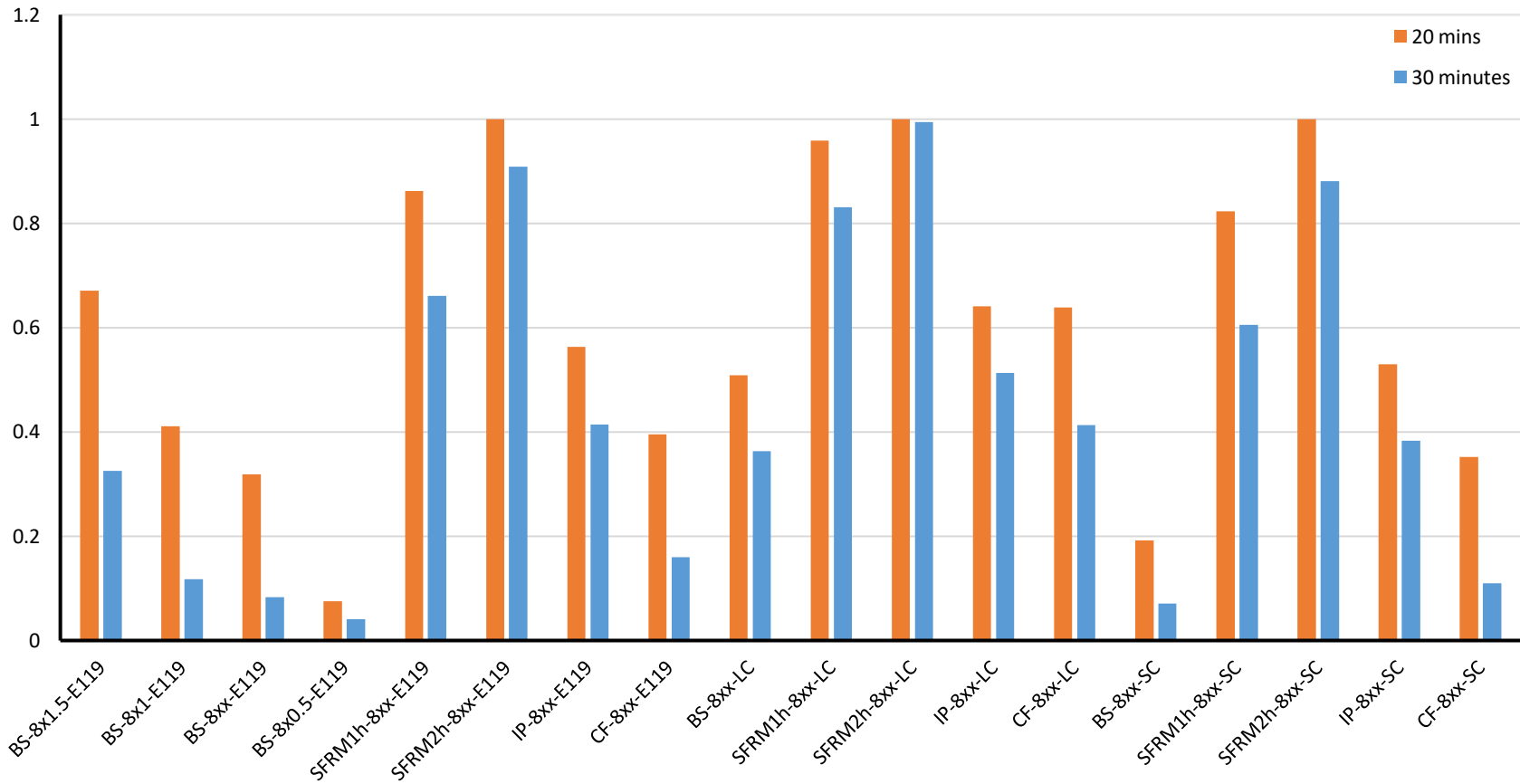


Figure 6-28 Normalized strength of each analyzed model with respect to the strength of unprotected 8xx steel tube section after 20 and 30 minutes of standard and real fire exposures.

CHAPTER 7

SUMMARY, CONCLUSIONS AND FUTURE WORK

7.1 Introduction

The motivation for this study was to investigate the thermal and strength response of the unprotected and fire protected circular hollow steel sections under the standard and real fire exposures. The goal was to use either unprotected or the type of fire protected column sections to preserve the aesthetic appearance of the steel column surface. For the unprotected column sections, the objective was to study the effects of increasing size of the column section on its thermal resistance. Intumescent paint protected and concrete-filled sections are the two types of fire protection methods studied in this research which does not harm the appearance of the steel surface in a column. SFRM-applied sections were the third type of fire insulated sections studied in this report. Using SFRM changes the appearance of steel surface, but provides significant fire resistance to the column.

To attain the objectives of this study, eighteen analytical models were analyzed. Heat transfer analysis of these models is performed in Chapter 4. Based on the obtained heat transfer analysis results, strength of the section for each model is calculated in Chapter 5. The results of chapters 4 and 5 are compared and discussed in Chapter 6. The summary of findings, conclusions and the possible future work on this topic are discussed in this chapter.

7.2 Summary

This section briefly reviews the research tasks and important observations in this study.

7.2.1 Heat Transfer Analysis

Heat transfer analysis was performed on eighteen analytical models with various steel tube section sizes and fire protection (see Section 3.3 and Table 3-1). Four analytical models were created for the unprotected sections under the E119 fire exposure: 8x1.5, 8x1, 8xx and 8x0.5 steel tubes. To investigate effects of compartment fires on unprotected column sections, 8xx tube was exposed to the large and small compartment fires in two separate models (see Table 3-1).

For the fire protected sections, two thickness of SFRM for 1-h and 2-h fire ratings were used. Six analytical models, three for each thickness of SFRM were created. Also, three models for intumescent paint insulated and three models for concrete-filled section were created and analyzed under the standard and real fire exposures (see Table 3-1).

2-dimensional heat transfer finite element analysis was performed with DCD8 elements using Abaqus software for the two hours duration of fire. The temperature data was collected for every 20°C increment in fire temperature at three nodes across the wall of steel tube section. Results of the heat transfer analyses showed that the temperature in unprotected sections increases rapidly and approaches the fire temperature near the end under the exposure to the E119 fire. In real fire exposures, the section's temperature rises to a maximum value and then starts to as the fire temperature begins to decay.

For the SFRM-applied column sections, the temperature was lower than the unprotected columns. The increase in temperature was more gradual with SFRM under E119 fire exposure. In addition, in real fire exposures, SFRM functions as a very efficient mean of fire protection, and significant temperature difference can be observed between the SFRM-protected and unprotected 8xx steel tube columns.

One layer of intumescent paint provided moderate amount of fire protection. Under the E119 fire exposure, temperature of the intumescent paint applied section reached the fire curve near the end (similar to the unprotected sections) due to the reason that intumescent paint material degrades at higher temperatures.

The temperature-time profile obtained for the concrete-filled columns were similar to the unprotected column sections with slightly lower temperatures. Concrete inside the column absorbed small amount of heat energy due to the concrete's low thermal conductivity.

7.2.2 Strength Analysis

The unprotected and fire protected column sections investigated for thermal analysis in Chapter 4 were studied for strength analysis in Chapter 5. The heat transfer results obtained were used to calculate the reduction in yield strength of the column section by utilizing the information presented in Table 2-1. The columns were assumed to be short, so the buckling mechanism was disregarded. Variation in yield strength, modulus of elasticity and section's axial force capacity values are tabulated for every 10 minutes interval of time in Appendix A of this report.

The steel column's strength reduced to its minimum value where the temperature was maximum. For the unprotected column sections, the strength reached their minimum values at the end of the E119 fire exposure (maximum temperature point). In the four unprotected models with varying section sizes analyzed, section's yield strength was delayed at the beginning when the cross-section size was increased, but dropped to the minimum value of 2.5% of their values in normal temperature at the end of E119 fire exposure. Under the real

fire exposures, section's strength dropped to a minimum value then increased back as the column lost heat back to the room (see Table 6-1).

Applying SFRM to the column surface impeded the flow of heat to the column section and therefore, prevented the loss of strength under a fire exposure. In both standard and real fire exposures, section's yield strength followed the temperature trend and was minimum where the temperature was maximum (refer to Table 6-1).

Intumescent paint delayed the reduction in yield strength of the steel section, but reached its minimum value at the end of the E119 fire exposure, similar to the unprotected column sections because intumescent paint degrades at temperatures above 800 °C. In real fires, however, significant contribution were observed because temperature does not increase as high as in the E119 fire.

Strength in concrete-filled sections were closer to the unprotected columns except with slightly increased values due to the lower temperature obtained from its heat transfer analysis. The reason for small change in temperature time profile of concrete filled compared to the unprotected section is the low thermal conductivity of concrete which prevents the flow of heat inside the concrete.

7.2.3 Additional Summary and Remarks

Increase in temperature and reduction in yield strength of unprotected steel columns with various section sizes were similar to each other with a slight change in their values. Enlarging the size of the cross section had small effect on temperature distribution. However, this increase had impact on axial force capacity of the member due to increased section area and was considerable in the first 20 and 30 minutes of fire exposure.

SFRM provides the most effective thermal resistance and its efficiency depends on the thickness sprayed to the column. Intumescent paint insulated columns also showed improved fire resistance, but not as good as SFRM. Concrete-filled sections (where concrete is used solely as heat sink) proved to be the least effective way of fire protection.

7.3 Conclusions

The following are the conclusions drawn from the study in this report.

1. Increase in size of the cross section in unprotected columns has small influence on their temperature-time profile of the section. In all the unprotected sections analyzed under both E119 and compartment fire exposures, the yield strength reduces below 10%. This means that for the sections to remain functional, the factor of safety for the design should be more than 10, which is neither practical nor economical. However, the increase in size of the column cross section can be useful when the fire duration is short and acceptable strength can be achieved in the first 30 minutes of the fire.
2. SFRM provides significant amount of fire protection to the columns. However, this material applied on the outer surface of the column and will change the aesthetic appearance of the steel surface. If architecturally allowed, this material can perform very satisfactory and can provide longer durations of fire protection depending on its thickness.
3. Using intumescent paint coated sections helps postpones the reduction in section's strength at the beginning of the standard E119 fire. After the temperature in E119 fire increases above 800 °C near the end, this material will burn and the column will behave like unprotected section. However, under the exposure of the real fires, since

the temperature does not increase as high, it behaves well and the yield strength does not decrease below 35-40% of their original values.

4. Using concrete inside the column to absorb heat energy from the steel does not provide significant thermal resistance, because the concrete inside the column cannot receive enough heat to store due to the low thermal conductivity of concrete.

7.4 Future Work

The following are recommended future work to further the understanding of this topic:

1. The analysis work conducted in this report was focusing around circular hollow steel sections. Further work can be performed with rectangular hollow sections and other steel shapes commonly used for columns.
2. The strength analysis performed in this study was for the assumed pinned supported short columns. Different boundary condition and different column lengths together with the second order effect and buckling analysis can be included around this topic.
3. Experimental tests of an unprotected circular hollow steel column under E119 fire exposure. Using the experimental test data, the exact heat transfer analysis parameters such emissivity and convection heat transfer coefficient should be quantified.

REFERENCES

- Abaqus v6.10, (2011). *Dassault Systèmes*, Providence, RI. (www.simulia.com).
- AISC Design Guide 19 (2003). *Fire Resistance of Structural Steel Framing*. American Institute of Steel Construction, Chicago, IL.
- ASTM E119-12a: *Standard Test Methods for Fire Tests of Building Construction and Materials*. (2000a). American Society of Testing and Materials (ASTM), West Conshohocken, PA.
- British Steel. (1999). “*The Behavior of Multi-Storey Steel Framed Buildings in Fire*”. STC Technical Report, Swinden Technology Centre, Rotherham, South Yorkshire, UK.
- Buchanan, A. (2002). *Structural Design for Fire Safety*. John Wiley and Sons, New York, NY.
- Bradley, C. and Sizemore, J. (2014). *Experimental study and analytical modeling of intumescent paint coated steel columns*. Lehigh University, Bethlehem PA.
- Bejan, A. (1993). *Heat Transfer*, John Wiley and Sons, New York, NY.
- Brewster, M.Q. (1992). *Thermal Radiative Transfer and Properties*, John Wiley and Sons, New York, NY.
- Chen, C., and Shen, B. (2011). “A Simplified Model for Describing the Effect of Intumescent Coating to Protect Steel under Fire Conditions”. *Advanced Science Letters*, 4(3), 1265-1269.

Drysdale, D. (1998). *An Introduction to Fire Dynamics (2nd Ed.)*. John Wiley and Sons, Chichester, UK.

EC2 (1996), *Design of Concrete Structures – Part 1.2: General Actions – Structural Fire Design*. British Standards Institution, London, UK.

EC3 (2001), *Design of Steel Structures – Part 1.2: General Actions – Structural Fire Design*. British Standards Institution, London, UK.

Holman, J.P. (2010). *Heat Transfer (10th Ed.)*, McGraw Hill, New York, NY.

International Building Code (2006). *International Code Council, Inc.*, Country Club Hills, IL.

Isolatek International Product Manual. (2016). Isolatek International, Stanhope, NJ.

Kirby, B.R. and Wainman, D.E. (1999). “Natural fires in large scale compartments”.

International Journal on Engineering Performance-Based Fire Codes, Volume 1, Number 2, p.43-58.

Keller, W.J. (2012). “Thermomechanical Response of Steel Moment-Frame Beam-Column Connections during Post-Earthquake Fire Exposure”. *PhD Dissertation*, Center for Advanced Technology for Large Structural Systems, Lehigh University, Bethlehem, PA.

Kodur, V. (2014). “Properties of Concrete at Elevated Temperatures”. *Hindawi Publishing Corporation ISRN Civil Engineering, Volume 2014, Article ID 468510.*

Kirby, B.R. and Preston, R.R. (1988). “High temperature properties of hot-rolled, structural steels for use in fire engineering design studies”. *Fire Safety Journal, Volume 13, Issue 1, Pages 27-37.*

- Lee, B. J., Pessiki, S., and Kohno, M. (2006). "Analytical Investigation of Steel Column Fire Tests", *ATLSS Report No. 06-23*, Center for Advanced Technology for Large Structural Systems, Lehigh University, Bethlehem, PA.
- Lamont, S. (2001). "The Behaviour of Multi-Storey Composite Steel Framed Structures in Response to Compartment Fires", *PhD Dissertation*, Department of Civil and Environmental Engineering, University of Edinburgh, Edinburgh, Scotland.
- Lie, T.T. (1992). *Structural Fire Protection - ASCE Manual and Reports on Engineering Practice No. 78*, American Society of Civil Engineers, New York, NY.
- NIST NCSTAR 1-3D (2005). *Mechanical Properties of Structural Steel, Federal Building and Fire Safety Investigation of the World Trade Center Disaster*. National Institute of Standards and Technology, Gaithersburg, MD.
- Siegel, R. and Howell, J.R. (1980). *Thermal Radiation Heat Transfer (2nd Ed.)*, Hemisphere Publishing Co., Washington, D.C.
- Wang, Y.C. (2002). *Steel and Composite Structures: Behavior and Design for Fire Safety*, Spon Press, New York, NY.
- Wang, Y.C. (1998). *An analysis of the global structural behavior of the Cardington steel-framed building during the two BRE fire tests*. The Manchester School of Engineering, University of Manchester, Oxford Road, Manchester M13 9PL, UK.

VITA

Fahim Rustamy was born on Jan12-1991 in a middle class family in Kabul City, Afghanistan. He was raised and did his elementary and high school in his home state Kabul.

He received his B.Sc. degree in Civil Engineering from Kabul University, Kabul, Afghanistan on December 2012. After graduation he started working with a private construction company supporting US Army Corps of Engineers constructing military headquarters for the Afghan National Army (ANA). He started with a position of assistant project manager and then with the position of project manager and eventually management of several ongoing projects. During this time, he received several appreciation letters from both his employer and client for successful completion of projects.

On May 2014 he was awarded the prestigious Fulbright scholarship to pursue his Master's degree studies at Lehigh University. He began his studies in Structural Engineering at Lehigh University on August 2015, and he completed his studies in June 2017.

APPENDIX

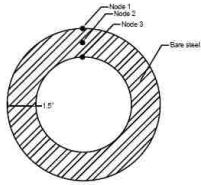
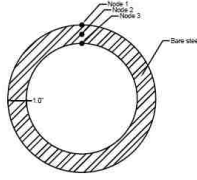
Table A.1 Unprotected 8x1.5 steel tube column under the E119 fire load.				
Time (min)	Mid-section temperature (°C)	F/fy	E/Ey	Section yield capacity (KN)
0	20	1	1	6810
5	59	1	1	6810
10	163	0.878	0.937	5978
20	397	0.422	0.703	2922
30	584	0.197	0.338	1419
40	697	0.076	0.131	534
50	725	0.069	0.120	467
60	752	0.062	0.109	423
70	826	0.047	0.084	320
80	903	0.037	0.067	254
90	941	0.032	0.058	222
100	965	0.029	0.053	200
110	982	0.027	0.049	187
120	998	0.025	0.045	173
Table A.2 Unprotected 8x1 steel tube column under the E119 fire load.				
Time (min)	Mid-section temperature (°C)	F/fy	E/E0	Section yield capacity (KN)
Column with 8-in diameter and 1.0-in thickness				
0	20	1	1	4893
5	73	1	1	4893
10	211	0.786	0.889	3843
20	490	0.366	0.610	1788
30	672	0.104	0.180	512
40	724	0.069	0.121	338
50	754	0.062	0.108	302
60	847	0.044	0.079	214
70	914	0.036	0.064	173
80	941	0.032	0.058	160
90	959	0.030	0.054	147
100	974	0.028	0.051	138
110	988	0.027	0.048	129
120	1002	0.027	0.048	129

Table A.3 Unprotected 8xx steel tube column under the E119 fire load.				
Time (min)	Mid-section temperature (°C)	F/fy	E/E0	Section yield capacity (KN)
0	20	1	1	4355
5	78	1	1	4355
10	230	0.749	0.906	3261
20	523	0.319	0.774	1388
30	693	0.082	0.688	360
40	731	0.067	0.515	294
50	770	0.058	0.232	249
60	877	0.040	0.123	178
70	924	0.035	0.113	151
80	945	0.032	0.100	138
90	961	0.030	0.077	129
100	975	0.028	0.062	125
110	989	0.026	0.054	116
120	1003	0.026	0.048	116

Table A.4 Unprotected 8x0.5 steel tube column under the E119 fire load.				
Time (min)	Mid-section temperature (°C)	F/fy	E/E0	Section yield capacity (KN)
0	20	1	1	2620
5	109	0.976	0.988	2580
10	331	0.544	0.764	1428
20	647	0.126	0.218	329
30	727	0.067	0.117	178
40	781	0.054	0.096	142
50	879	0.040	0.072	107
60	916	0.035	0.064	93
70	936	0.033	0.059	85
80	950	0.031	0.056	80
90	964	0.029	0.053	76
100	978	0.028	0.050	71
110	992	0.024	0.043	62
120	1006	0.024	0.043	62

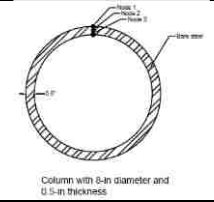
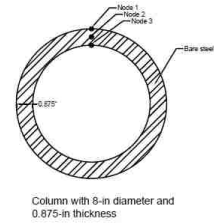


Table A.5 Unprotected 8xx steel tube column under the large compartment fire load.				
Time (min)	Mid-section temperature (°C)	F/fy	E/E0	Section yield capacity (KN)
0	20	1	1	4355
6	86	1	1	4355
12.5	220	0.767	0.880	3341
20	354	0.508	0.746	2215
30	495	0.363	0.605	1579
40	577	0.221	0.376	965
50	625	0.153	0.264	667
60	635	0.142	0.245	618
70	617	0.162	0.279	707
80	573	0.228	0.388	992
90	509	0.343	0.572	1495
100	442	0.395	0.658	1721
110	384	0.451	0.716	1962
120	334	0.547	0.766	2380

Table A.6 Unprotected 8xx steel tube column under the small compartment fire load.				
Time (min)	Mid-section temperature (°C)	F/fy	E/E0	Section yield capacity (KN)
0	20	1	1	4355
5	79	1	1	4355
10	233	0.744	0.867	3238
20	593	0.192	0.330	836
30	715	0.071	0.124	311
40	723	0.069	0.121	302
50	708	0.073	0.127	320
60	626	0.152	0.263	663
70	537	0.294	0.493	1281
80	457	0.386	0.643	1681
90	358	0.501	0.742	2184
100	279	0.653	0.821	2847
110	221	0.765	0.879	3336
120	178	0.849	0.922	3701

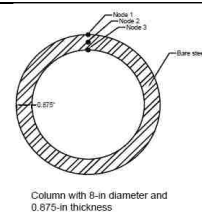
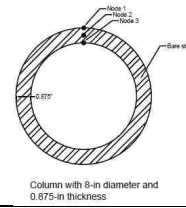


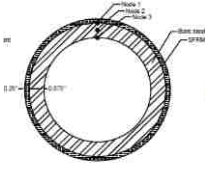
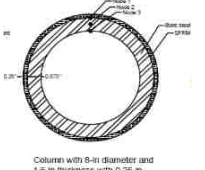
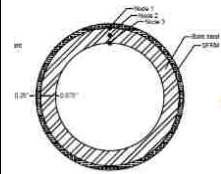
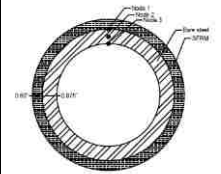
Table A.7 1-h SFRM insulated 8xx steel tube column under the E119 fire load.				
				 <p>Column with 8-in diameter and 1.5-in thickness with 0.25-in SFRM on the outside</p>
Time (min)	Mid-section temperature (°C)	F/fy	E/E0	Section yield capacity (KN)
0	20	1	1	4355
5	31	1	1	4355
10	72	1.000	1.000	4355
20	172	0.862	0.928	3754
30	275	0.661	0.825	2878
40	376	0.466	0.724	2033
50	466	0.380	0.634	1659
60	545	0.278	0.468	1210
70	613	0.167	0.287	725
80	668	0.109	0.188	476
90	701	0.076	0.131	329
100	716	0.071	0.124	311
110	726	0.068	0.119	298
120	736	0.066	0.116	289
Table A.8 1-h SFRM insulated 8xx steel tube column under the large compartment fire load.				
				 <p>Column with 8-in diameter and 1.5-in thickness with 0.25-in SFRM on the outside</p>
Time (min)	Mid-section temperature (°C)	F/fy	E/E0	Section yield capacity (KN)
0	20	1	1	4355
5	29	1	1	4355
10	59	1	1	4355
20	121	0.959	0.979	4177
30	187	0.832	0.913	3621
40	249	0.711	0.851	3096
50	308	0.598	0.792	2607
60	355	0.507	0.745	2211
70	387	0.445	0.713	1935
80	405	0.417	0.695	1819
90	407	0.416	0.693	1810
100	399	0.421	0.701	1833
110	388	0.444	0.712	1931
120	374	0.471	0.726	2051

Table A.9 1-h SFRM insulated 8xx steel tube column under the small compartment fire load.				
Time (min)	Mid-section temperature (°C)	F/fy	E/E0	Section yield capacity (KN)
0	20	1	1	4355
5	31	1	1	4355
10	72	1	1	4355
20	192	0.823	0.908	3585
30	304	0.605	0.796	2638
40	380	0.458	0.720	1997
50	420	0.408	0.680	1779
60	433	0.400	0.667	1744
70	431	0.401	0.669	1748
80	421	0.407	0.679	1775
90	398	0.424	0.702	1850
100	373	0.472	0.727	2055
110	349	0.518	0.751	2255
120	327	0.561	0.773	2442

Table A.10 2-h SFRM insulated 8xx steel tube column under the E119 fire load.				
Time (min)	Mid-section temperature (°C)	F/fy	E/E0	Section yield capacity (KN)
0	20	1	1	4355
5	22	1	1	4355
10	38	1	1	4355
20	90	1	1	4355
30	147	0.909	0.953	3959
40	206	0.794	0.894	3461
50	265	0.681	0.835	2967
60	322	0.570	0.778	2482
70	378	0.462	0.722	2011
80	431	0.401	0.669	1748
90	480	0.372	0.620	1619
100	526	0.313	0.525	1366
110	568	0.237	0.402	1032
120	607	0.173	0.297	752



Column with 8-in diameter and 1.5-in thickness with 0.25-in SFRM on the outside



Column with 8-in diameter and 1.5-in thickness with 0.5-in SFRM on the outside

Table A.11 2-h SFRM insulated 8xx steel tube column under the large compartment fire load.				
Time (min)	Mid-section temperature (°C)	F/fy	E/E0	Section yield capacity (KN)
0	20	1	1	4355
5	22	1	1	4355
10	34	1	1	4355
20	67	1	1	4355
30	103	0.994	0.997	4328
40	140	0.923	0.960	4021
50	175	0.854	0.925	3723
60	207	0.792	0.893	3452
70	233	0.743	0.867	3234
80	251	0.707	0.849	3078
90	262	0.687	0.838	2994
100	266	0.680	0.834	2963
110	266	0.679	0.834	2958
120	264	0.682	0.836	2971

Table A.12 2-h SFRM insulated 8xx steel tube column under the small compartment fire load.				
Time (min)	Mid-section temperature (°C)	F/fy	E/E0	Section yield capacity (KN)
0	20	1	1	4355
5	22	1	1	4355
10	38	1	1	4355
20	99	1	1	4355
30	162	0.881	0.938	3834
40	211	0.786	0.889	3421
50	244	0.722	0.856	3145
60	262	0.687	0.838	2994
70	271	0.670	0.829	2918
80	274	0.663	0.826	2891
90	270	0.671	0.830	2922
100	262	0.688	0.838	2994
110	253	0.704	0.847	3065
120	245	0.720	0.855	3136

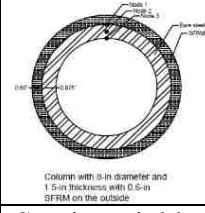
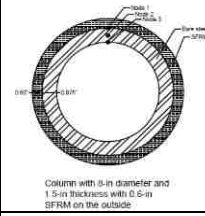


Table A.13 IP insulated 8xx steel tube column under the E119 Fire load.				
Time (min)	Mid-section temperature (°C)	F/fy	E/E0	Section yield capacity (KN)
0	20	1	1	4355
5	65	1	1	4355
10	188	0.819	0.906	3567
20	324	0.563	0.774	2451
30	408	0.413	0.688	1802
40	524	0.307	0.515	1339
50	637	0.134	0.232	587
60	711	0.070	0.123	307
70	736	0.064	0.113	280
80	766	0.056	0.100	245
90	854	0.043	0.077	187
100	920	0.035	0.062	151
110	959	0.030	0.054	129
120	984	0.027	0.048	116

Table A.14 IP insulated 8xx steel tube column under the large compartment fire load.				
Time (min)	Mid-section temperature (°C)	F/fy	E/E0	Section yield capacity (KN)
0	20	1	1	4355
5	54	1	1	4355
10	146	0.908	0.952	3954
20	285	0.640	0.814	2789
30	351	0.514	0.749	2237
40	382	0.454	0.717	1975
50	401	0.419	0.698	1824
60	417	0.410	0.683	1784
70	428	0.403	0.672	1757
80	434	0.400	0.666	1739
90	432	0.401	0.668	1744
100	413	0.412	0.687	1797
110	384	0.452	0.717	1971
120	349	0.518	0.751	2260

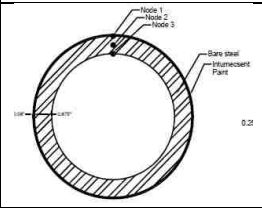
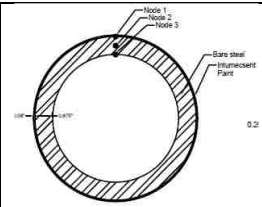


Table A.15 IP insulated 8xx steel tube column under the small compartment Fire load.				
Time (min)	Mid-section temperature (°C)	F/fy	E/E0	Section yield capacity (KN)
0	20	1	1	4355
5	65	1	1	4355
10	189	0.828	0.911	3608
20	343	0.530	0.757	2309
30	462	0.383	0.638	1668
40	517	0.330	0.551	1437
50	526	0.313	0.524	1366
60	527	0.312	0.522	1357
70	521	0.323	0.540	1406
80	498	0.361	0.602	1570
90	440	0.396	0.660	1726
100	371	0.598	0.729	2607
110	308	0.598	0.792	2607
120	254	0.702	0.846	3056

Table A.16 Concrete-Filled 8xx steel tube column under the E119 fire load.				
Time (min)	Mid-section temperature (°C)	F/fy	E/E0	Section yield capacity (KN)
0	20	1	1	4355
5	70	1	1	4355
10	195	0.818	0.905	3563
20	441	0.396	0.659	1721
30	619	0.160	0.276	698
40	709	0.073	0.127	316
50	737	0.066	0.115	285
60	787	0.053	0.095	231
70	877	0.040	0.073	178
80	917	0.035	0.064	156
90	930	0.032	0.058	142
100	977	0.030	0.054	129
110	985	0.028	0.050	120
120	993	0.026	0.046	111

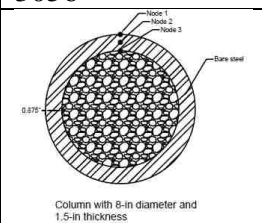
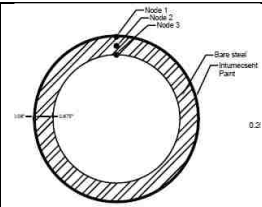


Table A.17 Concrete-Filled 8xx steel tube column under large compartment fire load.				
Time (min)	Mid-section temperature (°C)	F/fy	E/E0	Section yield capacity (KN)
0	20	1	1	4355
5	57	1	1	4355
10	144	0.915	0.956	3986
20	287	0.638	0.813	2780
30	412	0.413	0.688	1797
40	499	0.358	0.596	1557
50	560	0.253	0.427	1099
60	585	0.207	0.353	903
70	580	0.216	0.368	939
80	548	0.273	0.461	1192
90	498	0.357	0.596	1557
100	445	0.393	0.655	1713
110	400	0.424	0.700	1846
120	361	0.495	0.739	2157

Table A.18 Concrete-Filled 8xx steel tube column under small compartment fire load.				
Time (min)	Mid-section temperature (°C)	F/fy	E/E0	Section yield capacity (KN)
0	20	1	1	4355
5	69	1	1	4355
10	194	0.819	0.906	3567
20	504	0.352	0.587	1535
30	667	0.110	0.190	480
40	695	0.080	0.139	351
50	658	0.119	0.205	516
60	591	0.196	0.335	850
70	522	0.320	0.535	1392
80	461	0.383	0.639	1673
90	383	0.452	0.717	1971
100	325	0.566	0.775	2464
110	282	0.649	0.818	2825
120	248	0.713	0.852	3109

